Establishing and Operating a Near East and North Africa Regional Network for Evapotranspiration

(NENA-ETNet)

Output 9: Comprehensive Report

Activity 9.2: Comprehensive Report of Results including Recommendations and Strategies

International Center for Agricultural Research in the Dry Areas (ICARDA
and
Food and Agriculture Organization of the United Nations (UN-FAO)

November 2021

Executive Summary

Establishing and Operating a Regional Network for Field Measurement of Actual Crop Water Consumption (Evapotranspiration)

Actual Evapotranspiration (ETa) is the main component required to understand both hydrological and ecological processes between the land surface and the atmosphere. Reliable spatiotemporal measurements of ET are important for water resources planning, management and monitoring, efficient irrigation scheduling, and climate change mitigation scenarios development. Virtually no existing coordinated measurements and initiatives to validate various estimates of ETa are systematically carried out in the NENA Region although the region is extremely water scarce and vulnerable to climate change. Therefore, the Water Scarcity Initiative (WSI) of FAO for the Near East and North Africa, conceived and promoted the coordination of ETa field measurements as vital in the region with a consistent protocol established through this ET-Network project, which could effectively be used to validate and calibrate the remotely sensed estimations. The overarching objective of this project (named NENA-ETNet) was to establish and operate a NENA Regional Network of specialized institutions, within the countries of reference, to conduct field measurements of actual ET, over selected crops and for at least four seasons, in order to evaluate the accuracy of existing RS-based ET estimates. The idea was to build a common regional understanding on ETa measurements (ETa) in the field and through RS, on accuracy assessments of RS ETa data of different databases and on their analyses and use for agriculture-related applications (e.g., water accounting, water productivity, water management, etc.). Therefore, ICARDA was called upon, in collaboration with FAO and five countries in the region, to establish such a regional ET network to obtain reliable source of ground measurements of ET with the multiple goals of calibrating and validating RS-based ETa retrievals, calibrating and validating crop models and to do regional synthesis using the measured data in a multi-location, multi-season manner, in the context of regional water scarcity. The NENA-ETNet had a special focus on comparing CORDOVA-ET system using other field ETa methods of determination in order to decide if CORDOVA-ET method could be used as a regional standardized validation protocol. The participating countries were Egypt, Jordan, Lebanon, Morocco and Tunisia. The participating countries now have good capacity and facilities for ET measurements using energy balance and micro-meteorological methodologies, lysimeter and gravimetric methods. This report briefly summarizes all the project research results, learnings, challenges, recommendations and strategies on the way forward.

Keywords: Evapotranspiration, ET network, water productivity, water management

Suggested citation:
Govind, A; Biradar, C; Gamal, R; Mazahrih, N; Jomaa, I; Mosad, A; El Meknassi, E; Zitouna, R. Nangia, V. (2021). Comprehensive Report including recommendations and strategies. International Center for Agricultural Research in the Dry Areas (ICARDA), Cairo, Egypt.

Address:
ICARDA, 2 Port Said St, Victoria Square, Ismail El-Shaaer Building, Maadi, Cairo, Egypt

Authors of the Report

Authors:

1. Ajit Govind, Climatologist and CCAFS Contact Point, ICARDA, a.govind@cgiar.org
2. Chandrashekhar Biradar, Head of GIS Unit, ICARDA, c.biradar@cgiar.org
3. Rania Gamal, PhD Research Fellow, ICARDA, r.gamal@cgiar.org
4. Naem Mazahrih, Director General Assistant for Research, National Agricultural Research Center, Jordan. naemmaz@narc.gov.jo
5. Ihab Jomaa, Head of Irrigation Department, LARI, Lebanon, ijomaa@lari.gov.lb
6. Ehssan El Meknassi, Senior Researcher, IAV Rabat, Morocco, ehsan.elmeknassi@gmail.com
7. Alaa Mosad, Assistant Researcher, Soil, Water and Environment Research Institute, ARC, Egypt, alaamosad993@yahoo.com
8. Rim Zitouna, Senior Researcher Institut National de Recherches en Génie Rural, Eaux et Forêts INRGREF, Tunisia, rimzitouna@gmail.com
9. Vinay Nangia, Principal Scientist and Leader – Soil, Water, and Agronomy Research Team, ICARDA, v.nangia@cgiar.org

DISCLAIMER

The views expressed are those of the authors, and not necessarily those of ICARDA or FAO. Where trade names are used, it does not necessarily imply endorsement of, or discrimination against, any product by the Center. Maps are used to illustrate research results, not to show political or administrative boundaries. ICARDA encourages fair use, sharing, and distribution of this information for non-commercial purposes with proper attribution and citation. This document is still in a draft version and under licensing. Unless otherwise noted, you are NOT allowed to copy, duplicate, or reproduce and distribute, display, or transmit any part of this publication or portions thereof without author's permission and to make translations, adaptations, or other derivative works under the following conditions:

ATTRIBUTION. The work still in a draft version and should NOT be attributed, distributed and transformed in any way or form of attribution without permission from the author(s)

Contents

1. Introduction

Reliable spatiotemporal measurements of evapotranspiration (ETa) are important for water resources planning, management and monitoring, efficient irrigation scheduling, and development and monitoring of climate change mitigation scenarios. Due to complex land-plant-atmosphere interactions and natural variability in topography, soil moisture and vegetation type, obtaining accurate information on ET is often challenging, especially in agroecosystems where water is scarce or fluctuates seasonally. There are several conventional field methods used to determine ETa, including: 1) the Eddy covariance/energy balance method; 2) the Bowen-ratio/energy balance method; 3) Weighing lysimeters; 4) Soil-moisture depletion method; and 5) Large Aperture Scintillometer. These methods have their own specific advantages and limitations based on the theory behind and on the instrumentation requirements. However, what they have in common is, among others, the restricted sampling area and the complexity and extremely high costs when attempting to scale-up to larger areas. For large scales (e.g., watershed, sub-national, national and regional), ETa estimation is often established through satellite Remote Sensing (RS), due to progress that has been made in space science in recent years. There are several well-established RS-based algorithms for the determination of ETa, including SEBAL (Surface Energy Balance Algorithm for Land), METRIC (Mapping Evapotranspiration at high Resolution with Internalized Calibration), SEBS (Surface Energy Balance System), ETLook, ETMonitor, etc. Unfortunately, these methods also have their own specific advantages and limitations and are all suffering from a generally limited and scattered field testing. Virtually no testing is systematically carried out in the NENA Region. Therefore, the Water Scarcity Initiative (WSI) of FAO for the Near East and North Africa conceived and promoted the establishment of this ET-Network so that ETa field data could effectively be used to test and calibrate the remote sensing-based estimations.

The overarching objective of this project (named NENA-ETNet) was to establish and operate a NENA Regional Network of specialized institutions, within the countries of reference, to conduct field measurements of ET (ETa), over selected crops and for at least four seasons, in order to evaluate the accuracy of existing RS based ET estimates. To build a common understanding and methodology on ETa estimation methods, in the field and through RS, on accuracy assessments of RS ETa data of different databases and on their analyses and use for agriculture-related applications (e.g., water accounting, water productivity, water management, etc.). To this purpose, the regional network was established by ICARDA and supported by FAO in partnership with 5 countries in the region (Egypt, Jordan, Lebanon, Morocco and Tunisia) with the plan to be further expanded to other countries in the region to have a greater coverage of the NENA region as the network grows. This network includes providing the required technical backstopping from ICARDA to make sure that instrument installation, data sensing, analyses and dissemination are conducted in a scientific and unified way in all participating countries.

There are several online databases as well as algorithms existing to map evapotranspiration (ETa) in time and space. However, these databases and algorithms are based on equations modelling complex land-plant-atmosphere interactions. Before using these databases and algorithms to map ET, there is a strong need to understand the theory on which ETa is mapped. Further, there is a strong need to test the results of these remote sensing derived ETa estimations. Therefore, there is a dire need to build the capacity of the local institutions who are end user of these products. If they are not able to map the ETa, at least they should understand the basis of these maps. Further, the local institutions should have not only physical

infrastructure to test the remote sensing derived ETa products but also fully understand how ETa is properly determined from these instruments.

The CORDOVA-ET station is a cost-effective ET determination device developed by the University of Cordoba in Spain. The CORDOVA-ET station senses meteorological parameters (solar radiation, air temperature, humidity, rainfall, wind speed), together with the canopy temperature using an infrared thermometer. The combination of these variables allows the determination of the sensible heat [H] (Maes and Steppe, 2012). The net radiation [Rn] can be estimated using models based on the meteorological observations (Berni et al., 2009). At daily intervals, the ground heat flux [G] is assumed zero. It estimates the grass reference ET (ETo) using the meteorological data in the standard modified Penman-Monteith equation. It estimates ET based on an energy balance approach by determining the components of the energy balance equation. The system is built using low-cost commercial off-the-shelf sensors and parts, complemented with 3D printed components and do-it-yourself electronics. The total cost of the node is less than 500€. All the main components are equipped with solar panels as well as Internet of Thing (IoT) technology for automatic wireless communication. The nodes transfer data through LoRaWAN network to the gateway inside the base station. The gateway and the weather station upload data in real time to the internet using the Wi-Fi through a 3G/4G router. Deploying several nodes at a time permits obtaining data from different areas within a plot and from different plots to obtain robust estimates of ET that can be compared with other methods. The CORDOVA-ET stations are deployed to all the five countries along with the ongoing in-house ET measuring approach with the overall technical and theoretical backstopping from ICARDA. A detailed description of CORDOVA-ET is provided in the Annexure-2.

Therefore, ICARDA in collaboration with FAO and five countries in the region has established a regional ETa network to establish a reliable source of ground estimation of ETa with the multiple goals of calibrating and testing RS-based ETa retrievals and calibrating and testing crop models with the ETa and related datasets. In addition to testing model estimates (RS and crop models), this database also serves as an invaluable database to perform multi locational and multi crop observational data based regional synthesis in the context of regional water scarcity. The NENA-ETNet will have a special focus on calibrating CORDOVA-ET system using other field ET methods of determination in order to decide if the CORDOVA-ET method can be used as a regional standardized protocol.

2. Field Sites and Reporting of ET and Related Meteorological Data

There are several sensing and measurement methods to determine ET. Typically, only one is considered a 'direct' measurement method: (i) the water budget, which includes the weighing lysimeter and the soil water balance methodology. Sensing of water vapor transfer in the atmosphere above the crop and soil surfaces, which includes the eddy covariance and the Bowen ratio, are indirect methods because: 1) They involve sensing, not direct measurement, of state variables that are dependent on ET but are not themselves ET; and 2) They are subject to advection and divergence, lack of buoyant eddies under stable conditions common in arid and semi-arid irrigated environments, and other factors that render the data obtained indirectly related to the evapotranspiration even though they may be strongly correlated with ET. The four methods that the NENA-ETNet utilized for field ET estimation in the second season (Summer 2020) were: 1) Eddy covariance; 2) Weighing Lysimeters; 3) Soil moisture depletion; and 4) Surface Energy Balance. Each station in all selected five countries had more than one ET determination facility. Figure 1 and Tables 1,2 present the sites and their coordinators, and information on ET instrumentation used and crops grown. There were several issues associated with the repair and maintenance of the ET equipment. Complete knowledge on the functionality of the instruments was of paramount importance in helping to

address repair and maintenance issues during the first season and to keep the equipment in good shape to have a full crop cycle measurement in the following seasons and to ensure quality data among all countries. These sites also had the CORDOVA-ET Stations deployed. The field measurement in the NENA-ETNet network began in the winter season 2019/2020 using the existing ET facilities. This report is targeted to elaborate the obtained results from four seasons in the five countries of the network.

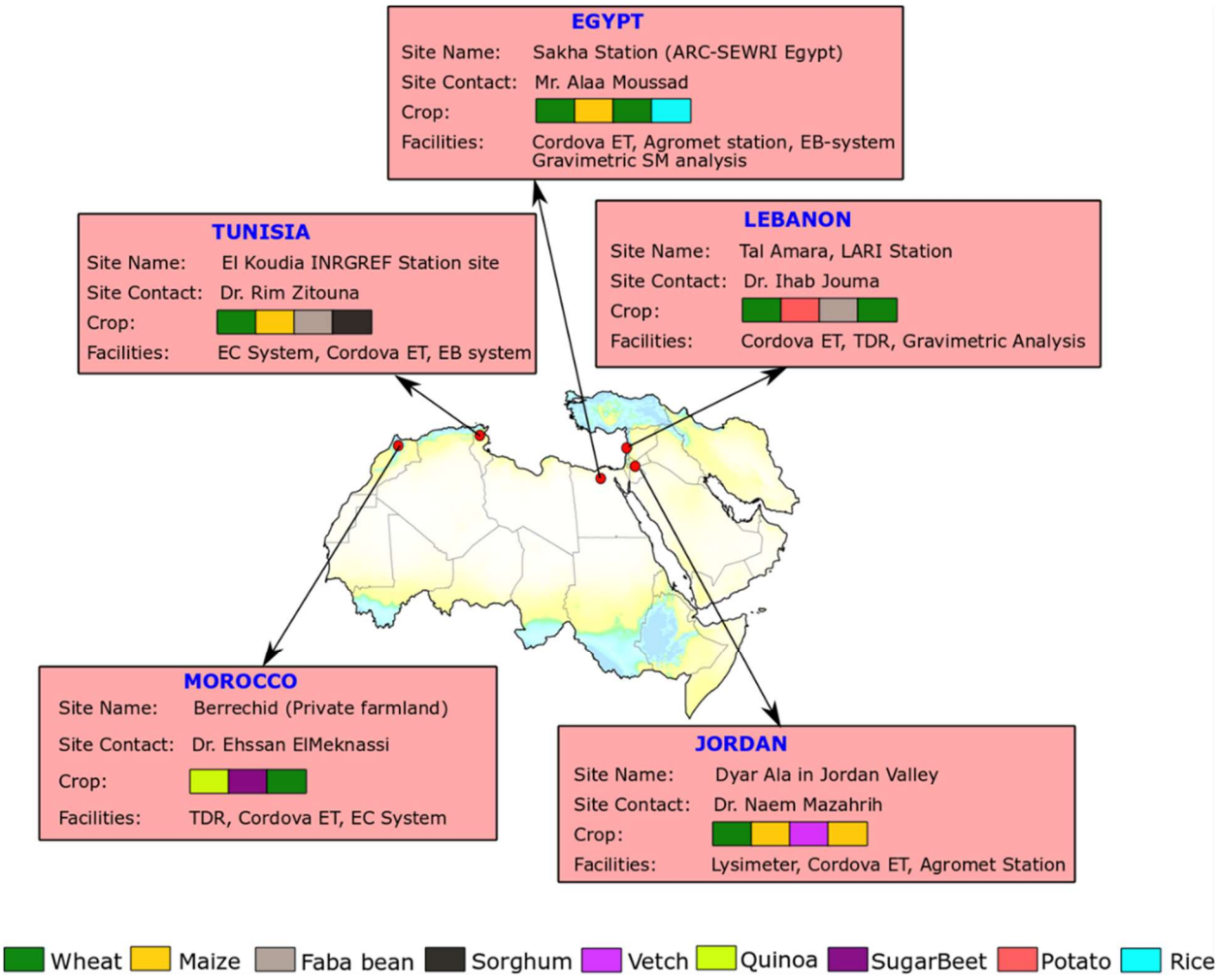

Fig 1 Countries, organizations and the sites that participated in the NENA-ETNet of the WSI. The site level details such as the available instrumentation and the sequence of crops in the four seasons are also shown.

Table 1 Countries, organizations, the sites and the methods of ET measurement used.

Country	Field Station & Institution	Latitude/Longitude	ET Methods available
Egypt	Sakha, Nile Delta (ARC)	31°15'52.00'N 30°46'06.00''E	1. Surface Energy Balance (using Eddy Covariance for sensible heat flux - H) 2. Surface Energy balance (CORDOVA-ET)
Jordan	Dyar Ala, Jordan Valley (NARC)	32°19'00.00'N 35°34'43.00''E	3. Weighing lysimeter 4. Surface Energy balance (CORDOVA-ET)
Lebanon	Tal Amara (LARI)	33°51'51.00'N 35°59'05.00''E	5. Soil moisture depletion 6. Surface Energy balance (CORDOVA-ET)
Morocco	Birched, Casablanca (private farm)	33°34'12.00'N 7°37'13.00''E	7. Soil moisture depletion 8. Eddy Covariance for latent heat flux (λE) 9. Surface Energy balance (CORDOVA-ET)
Tunisia	Gendouba (INGC-INRGREF)	36°32'47.83'N 9°00'50.00''E	10. Eddy covariance for latent heat flux (λE) 11. Surface Energy Balance (using Eddy Covariance for sensible heat flux - H) 12. Surface Energy balance (CORDOVA-ET)

Table 2 Countries and the crops on which ET monitoring was undertaken for the different seasons.

Country	Season-1	Season-2	Season-3	Season-4
Egypt	Winter Wheat *(Dec 1,2019 – May 13, 2020)*	Summer Maize *(July 20, 2020 – Oct 21, 2020)*	Winter Wheat *(Nov. 25, 2020 – April 30,2021)*	Summer Rice *(June 16, 2021 – Oct. 20, 2021)*
Jordan	Winter Wheat *(Dec 25, 2019 – May 5, 2020)*	Summer Maize *(July 15, 2020 – Oct. 20, 2020)*	Fodder Vetch *(Jan. 13, 2021 – April 30, 2021)*	Maize *(June 14, 2021 – Sep. 9, 2021)*
Lebanon	Wheat *(Dec 7, 2019 – July 2, 2020)*	Potato- Fallow *(March 1, 2020 – July 31, 2020)*	Faba bean *(Dec. 3, 2020 – May 6, 2021)*	Maize *(June 17, 2021 – Oct. 8, 2021)*
Morocco	Maize *(Feb 23,2020 – July 3, 2020*	Beetroot *(Aug. 27, 2020 – Nov. 11, 2020)*	Durum Wheat *(Jan 11, 2021 – May 31, 2021)*	NA
Tunisia	Wheat *(Dec 3, 2019 – June 23, 2020)*	Maize *(July 19,2020 – Nov 3, 2020)*	Faba bean *(Dec. 19, 2020 – May 26, 2021)*	Sorghum *(Aug. 9, 2021 – Nov. 2, 2021)*

In this project, a clear protocol was designed to collect, report and archive the data collected systematically across the network. Depending on the level of processing, temporal resolution and units of the reported variables, three levels of files are designed and are routinely prepared and archived. These are the L-type files. Unlike the RAW files, L-type files are aggregate files that combine various information obtained from various sources (RAW files) but put together on a monthly basis. There are clear definitions on the characteristic features of the L-type files. If any of the variables are not monitored at a site, it is reported as NaN, and if it is missing it gets reported as -9999. The characteristic features of L-type files are reported in Table 3.

Table 3 Characteristic features of the three levels of reporting files.

Feature	**L1 File**	**L2 File**	**L3 File**
Temporal Resolution	Half hourly	Half Hourly	Daily
Data Gaps (-9999)	Possible	Not possible	Not possible
Time Stamp	1200, 1230…..2400	1200, 1230…..2400	NA
Day Stamp	1, 2,..365	1, 2,..365	1, 2,..365
Unavailable Data (NaN)	Possible	Possible	Possible
Gap Filling	Not Mandatory	Mandatory	Mandatory
Units	Original	Original	See Table 2
Auxiliary Data (LAI, NDVI)	NA	NA	If available, reported
Reporting to ICARDA	Mandatory	Optional	Mandatory
Attestation requirement	Country manager	Country manager	Country manager
File Naming convention	*COUNTRY_SiteName_Year_Month _L1.csv*	*COUNTRY_SiteName_Year_Month _L2.csv*	*COUNTRY_SiteName_Year_Month _L3.csv*

The temporal resolution of L1 and L2 file is half hour. The difference between L1 and L2 is that L1 files will NOT have gap filled. Hence missing values will have -9999 and unavailable values will be depicted as NaN. L1 files are subjected to rigorous quality checks and then gap filled, leading to the L2 level of processing. The type of gap filling method and the date of processing and details of processing should be explained in the L2 file (e.g., regression based, or interpolation based). Thus, in the ideal case in L2 there are NO -9999 values. Often, we can do gap-filling only if the gaps are small. If we have continuous gaps for more than 3 hours (6 HH) during a 24 h period, that gap is reported as -8888 in the L2 file. However, NaN values may still exist if that site does not measure a variable. Typically, L1 and L2 files are created for each month of a year. The L3 files are gap filled (i.e., no -9999 values) and are at daily time step. A typical L3 file is a monthly file with daily values reported. However, for L3 files, daily values (average or sum, depending on the variable, of 48 half hourly values, which includes both daytime and nighttime) need to be reported and be consistent with the units used. Some biometric variables such as LAI or NDVI if collected at the site can also be included in this file that may be useful for data interpretation and further synthesis. In order

to create L3 files, it is mandatory to create L2 files to do the averaging (or summing) correctly. L3 files generated from L2 files that have -8888 values (days with large gaps) will take a value of -8888. Typical variables recorded in L-type files are reported in Table 4.

Table 4. Description of Common Variables Used to Report L1, L2 and L3 files along with their acronyms and units

Description of Variable	Variable Short name	Unit used
Year	YEAR	YYYY
Month	MONTH	MM
Julian Day of the Year	DOY	DDD
Local Time (2400hr format)	TIME	2330
Potential ET measured by CORDOVA method	ETo_COR	mm/day
Potential ET measured by SELF approach	ETo_COR	mm/day
ET measured by CORDOVA method	ETa_COR	mm/day
ET measured with Lysimeter	ETa_Lysi	mm/day
ET measured with EB Method	ETa_EB	mm/day
ET measured with EC Method	ETa_EC	mm/day
ET measured with SM Depletion	ETa_SMD	mm/day
Sensible Heat Flux	H	W/m^2
Ground Heat Flux	G	W/m^2
Latent Heat Flux	LE	W/m^2
Air Temperature	A_Temp	^oC
Soil Temperature at 10cm	S_Temp	^oC
Plant Canopy Temperature	Canopy_Temp	^oC
Incoming SW Radiation Flux	SW_In	W/m^2
Outgoing SW Radiation Flux	SW_Out	W/m2
Incoming LW Radiation Flux	LW_In	W/m^2
Outgoing SW Radiation Flux	LW_Out	W/m^2
Net Radiation Flux	NetRad	W/m^2
Relative Humidity	RH	%
Volumetric Soil Water Content	VSMC	fraction
Wind Speed at 2m	WS	m/sec
Air Pressure	Pressure	mbar
Leaf Area Index	LAI	m^2/m^2
Irrigated Water (mass flux units)	Irrigation	mm/day
Method used for Gap Filling	Gap_Method	Regression
Person who prepared the file	PreparedBy	Initials of Technician
Date of this dataset preparation	Date of Prep	dd/mm/yyyy
Attested By	CountryManager	Initials of CM

Templates of these L1, L2, L3 files are provided to the country managers by ICARDA (filled with dummy values) with clear guidelines. The red items are essential variables that must be reported even if other variables are reported as NaN. If the sites have data on the other parameters, they are encouraged to

report them too without altering the excel sheet format. If these datasets are not available, the variables should be reported as NaN without changing the structure of the file. It is also important to report the variables in the appropriate units as described in Table 4.

The L3 data product will be used for inter-comparison between different instruments (e.g., Eddy covariance and CORDOVA-ET) and between different estimates (e.g., ETa_EC and ETa_Lysi). This L3 product is used for calibration of remote sensing algorithms and testing of various products that are generated based on those algorithms. Assuming that the L3 product proves to be sufficiently accurate and unbiased, it might also be used to calibrate and test crop simulation models such as APSIM, CropSyst or AquaCrop with the whole set of useful data along with the metadata reported from each site for each crop and season. L2 datasets may be used to calibrate and validate crop models that operate at sub-daily time steps.

The data processing and archiving procedure is briefly presented in figure 2. There is a rigorous process of peer-review and iterative improvement of the initially submitted L1, L2 and L3 data, before the Network arrives at a finalized set of datasets for a given season. The submitted data are heavily scrutinized and peer-reviewed in terms of data gaps, magnitudes, trends and reporting style accuracy. The spurious data that are acquired due to methodological and sensor errors are kept as-is so that it helps us to analyze the accuracy and efficacy of the methods of data acquisition (e.g. - ET values obtained by a given method or system). This finalized data set is what is archived for data analysis and synthesis.

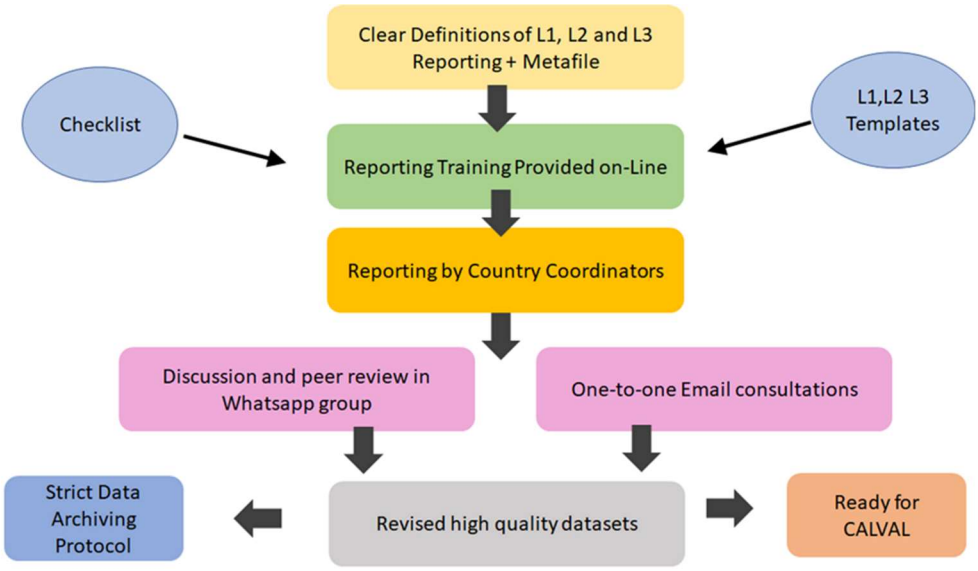

Figure 2 Sequential flow of the processing sequence of quality-controlled data in the NENA-ETNet (CALVAL: calibration and validation)

3. EGYPT, Sahka Site

3.1. Location Details

Sakha City, Kafr el Sheikh Governorate, North Nile Delta Region, with an elevation of about 6 meters above mean sea level. Sakha Agricultural Research Station, of the Agricultural Research Center (ARC), is located in Kafr El-Sheikh Governorate, at 31° 07'N latitude, 30° 57'E longitude (figure 3). The field size of the site is 2.5 hectares. The eddy covariance flux tower and Cordova-ET station were installed in the middle of the field at about 150 m from the edges. At this site, the main ET determination approaches historically have been eddy covariance and energy balance. Although, the eddy covariance was deployed many years ago, the calibration was not conducted for the last three years because the seasonal calibration kit was missing, and the gas analyzer was obsolete. In addition to the eddy covariance system, the station also includes Energy Balance (EB) sensors, which are well maintained and calibrated so that all the components of the energy balance equation are measured, except latent heat flux (LE). Table 5 lists the team of Sakha site.

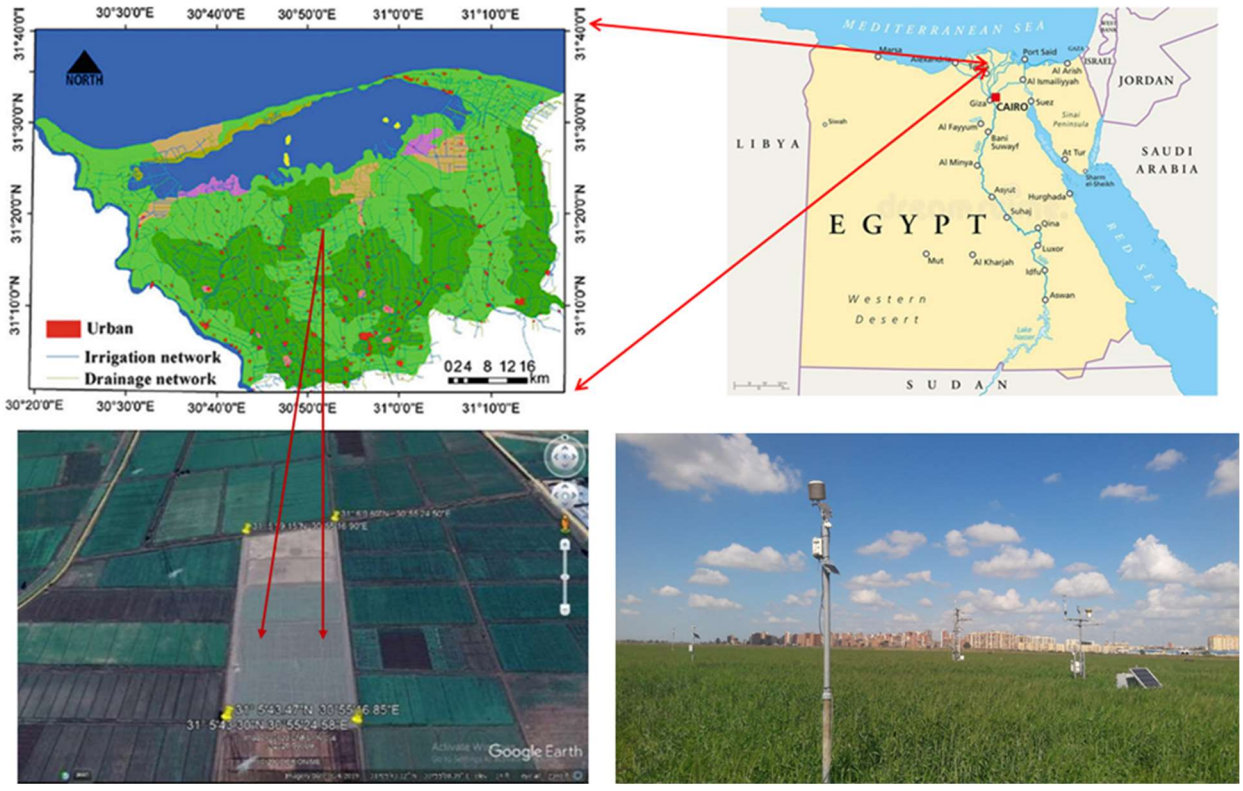

Figure 3. Location of the field site in Sakha Agricultural Research Station, Egypt (aerial photograph). Location of the field experiment.

3.1.1. People involved

Table 5 People involved at the Sakha site in Egypt

Name of Participant	Institution	Responsibilities
Prof. Dr. Mohamad Ismail	ARC-SWERI	Coordinator and Responsible of the Sakha Station in this Project
Alaa Mosad	ARC-SWERI	1. Contact Point and Researcher 2. Field operations, Collecting Data 3. And Reporting the Data. 4. Writing Report
Mohamad Saad	ARC-SWERI	Maintenance of CORDOVA-ET Station
Rania Gamal	ICARDA	CORDOVA-ET Station Quality Control
ARC: Agriculture Research Center, Egypt SWERI: Soils, Water, Environment Research Institute		

3.1.2 Soil characteristics

The soil of the site has a heavy clay texture, and its structure tends to be granular. It is a heavy clay soil with more than 49% clay fraction. In the surface layer (0-20 cm), on mass basis, saturation percent is about 59%, Field Capacity (FC) approaches 46.5% and Permanent Wilting Point (PWP) is 25%. The bulk density (BD) ranges from 1.07-1.29 g/cm^3 along the soil profile. Chemically, electrical conductivity (EC) ranges from 2.5-3.2 dS/m, pH is in the range of 7.8-8.3, dominant cations are sodium, calcium, magnesium and potassium, whereas chloride, bicarbonate and sulphate are main anions (Table 7). Such soils are classified as Entisols (Vertic Torrifluvents). Soil samples were collected at depths of 0-15, 15-30, 30-45 and 45-60cm to determine physical properties (Table 6), according to James (1988). Bulk density and particle size distribution were estimated using methods of Klute (1986). Chemical analysis of the soil was obtained using the methodology outlined by Jackson (1973).

Table 6 Physical properties of the soil at the Sakha site in Egypt (BD=bulk density; FC=field capacity; PWP=permanent wilting point)

Soil depth (cm)	BD (g cm^{-3})	Porosity (m^3 m^{-3})	FC (%)	PWP (%)	Sand (%)	Silt (%)	Clay (%)	Textural Class
0 – 15	1.07	0.596	46.61	25.33	19.70	29.2	50.10	Clay
15 – 30	1.13	0.574	45.20	24.56	19.62	30.73	49.65	Clay
30 – 45	1.20	0.547	43.70	23.75	24.43	23.27	52.30	Clay

45- 60	1.29	0.513	42.30	23.10	24.71	26.94	48.35	Clay

Table 7 Chemical properties of the soil at the Sakha site in Egypt (EC=electrical conductivity)

Soil depth cm	EC dSm^{-1} *Paste extract*	P^H (1:2.5) *Soil-water suspen.*	Soluble Ions, meq/L							
			Cations				Anions			
			Ca^{2+}	**Mg^{2+}**	**Na^{+}**	**K^{+}**	**CO_3^{2-}**	**HCO_3^{-}**	**Cl^{-}**	$SO4^{2-}$
0-15	2.60	8.05	9.92	4.62	11.25	0.23	0.00	6.82	12.50	6.70
15-30	2.59	8.11	10.04	5.60	10.10	0.19	0.00	4.40	9.40	12.13
30-45	2.68	8.13	11.17	5.97	10.52	0.18	0.00	4.20	8.30	14.34
45-60	3.14	7.94	12.00	6.78	12.50	0.17	0.00	4.10	1.20	19.85
Mean	2.75		11.03	5.74	11.09	0.19		4.88	7.85	13.25

3.1.3 Water Characteristics

The irrigation system here is predominantly surface flooding type and depends mainly on fresh Nile River water. Irrigation Water (IW) of fresh Nile River water EC ranges from 0.40-0.55 dS/m and pH 8.00-8.40, however, average EC values for the drainage water (DW) and groundwater (WT) are 0.85 and 1.37 dS/m, respectively. Sodium Adsorption Ratio (SAR) values are 1.14, 1.72 and 2.39 for IW, DW & WT, respectively. The drainage system involves both tile and open drains. Typical water characteristics of Sakha station are reported in Table 8.

Table 8. Physico-chemical properties of irrigation water at the Sakha site in Egypt

Type of Water	pH	EC (ds/m)	Ca^{2+}	Mg^{2+}	Na^{+}	K^{+}	$CO3^{2-}$	HCO_3^{-}	Cl^{-}	SO_4^{2-}	SAR
			Meq/L								
Irrigation	8.39	0.56	2.82	1.04	1.58	0.22	0.00	2.25	1.88	1.53	1.14
Drainage	8.31	0.85	3.45	1.96	2.83	0.23	0.00	3.23	2.30	2.97	1.72
Water table	8.06	1.37	5.63	2.97	4.96	0.14	0.00	4.80	3.98	4.92	2.39

3.2. Crop cultivation and agronomic practices

There is no clear typical crop rotation in Egypt, especially in north Nile delta region, due to agricultural area fragmentation to as low as about 0.14 feddan per capita. The site essentially has two seasons, summer and winter while spring and fall are quite short. Major summer crops are rice, maize and cotton; winter crops involve wheat, sugar beet, faba bean, clover and barley. At the Sakha Research Station, a wheat crop was cultivated in Season 1, a maize crop was cultivated in Season 2, a wheat crop was cultivated in season 3 and a rice crop was cultivated in season 4. The field agronomic practices during the four seasons are described in Tables 9, 10 ,11 and 12.

Table 9 Summary of agronomic practices during the winter season 2019 (season 1) in Sakha, Egypt

Operation	Date	Notes
Land preparation	Nov 7, 2019	Ploughing
	Nov 16, 2019	Land levelling
Planting (Wheat)	Nov 27, 2019	Traditional flat planting method was used 50 kg seeds/acre Two bread wheat varieties were cultivated (Sakha 95 and Giza 171)
Fertilizer application	Nov. 30, 2019	Recommended doses; 75-unit nitrogen, 25-unit phosphorus and 20-unit potassium Half of recommended nitrogen doses were added through sowing irrigation event, and the rest was added with the second irrigation event. Phosphorus and potassium fertilizers were added before planting.
Weed control	Jan. 1, 2020	Application of herbicides (Tribenuron-methyl) to control the dicotyledonous weeds.
	Jan. 25, 2020	Application of herbicides (Clodinafop – Propargyl + Pinoxaden) to control the monocotyledonous weeds.
	Mar. 8, 2020	Mechanical control.
Controlling yellow rust (Most aggressive fungal disease)	Mar. 3 & Mar. 11, 2020	Using Propiconazole, Wheat varieties of Sakha 95 and Giza 171 are highly tolerant to such fungal diseases; however, we repeated the control treatment twice.
Irrigation events	1/12/2019	Sowing irrigation event with about 225 m^3 /ha It was followed by a good germination
	15/2/2020	Second irrigation event (204 m^3/ha) It was during flowering stage
	30/03/2020	Third irrigation event (200 m^3/ha) It was during mid-season stage(grain-filling)
	18/4/2020	Fourth irrigation event (165 m^3/ha) It was during maturity stage- same as above

Operation	Date	Notes
		These long intervals were due to the rainfall in the 2019/2020-wheat season (about 145 mm), as well as the high contribution of shallow groundwater (1-1.1 m). Irrigation method was surface flood, with fresh water; EC ranges from 0.45-0.55 dS/m; pH sits at 7.9-8.12. Drainage system involves both open and tile drains.

Table 10 Summary of agronomic practices during the summer 2020 (season 2) in Sakha, Egypt

Operation	Date	Notes
Land preparation	Jul 5	Land ploughing by chisel and disc
	Jul 15	Land levelling
Planting (maize)	Jul 18	Planting by planter machine Triple white hybrid 324 cultivar
Fertilizer application	Aug 10	Application of nitrogen fertilizers (recommended is 120 N unit/Fed). Added half of the recommended dose (60 N unit)
	Sept 23	Adding the other half dose of N fertilizer
Weed control	Jul 20	Application of herbicides after planting and before irrigation, that combat both mono & di-cotyledons weeds
	Aug 17	Application of herbicides after emergence growth stage
Fungicide and Insecticide Applications	Aug 28	Application of fungicides and insecticides
Irrigation events	Jul 20	1st irrigation event (359.45 m^3 of applied water per Fed)
	Aug 11	2nd irrigation event (320 m^3 applied water/Fed)
	Sept 4	3rd irrigation event (350 m^3/ Fed)
	Sept 24	4th irrigation event (340 m^3/ Fed)
Harvesting	Nov 1	Harvest

Table 11 Summary of agronomic practices during the winter 2021 (season 3) in Sakha, Egypt

Operation	Date	Notes
Land preparation	Nov 12, 2020	Land ploughing by chisel and disc
	Nov 18, 2020	Land levelling
Phosphorous and potassium fertilizers	Nov 22, 2020	25-unit phosphorus and 20-unit potassium Phosphorus and potassium fertilizers were totally added before planting
Planting (Wheat)	Nov 24, 2020	Traditional flat planting method was used 50 kg seeds/feddan Wheat variety: Ceds 14
Nitrogen Fertilizer	Jan 25, 2021	Recommended doses; 75-unit nitrogen, 1/3 the recommended dose was added directly before the first irrigation event (Sowing).
	Feb 5, 2021	2/3 the recommended dose has been added through the second irrigation event.
Weed control	Dec 15, 2020	Application of herbicides (Tribenuron-methyl) to control the dicotyledonous weeds.
	Dec 30, 2020	Application of herbicides (Clodinafop – Propargyl + Pinoxaden) to control the monocotyledonous weeds.
	Mar 20, 2021	Mechanical control.
Controlling yellow rust	Feb 25, 2021 Mar 10, 2021	Using Propiconazole, twice.
Irrigation events (Flood Irrigation)	Nov 25, 2020	1st irrigation event (550 m^3 / Fed) at planting
	Feb 6, 2021	2nd irrigation event (350 m^3 / Fed)
Harvesting	April 30, 2021	Grain Yield 2.48 t/Fed

Table 12 Summary of agronomic practices during the summer 2021 (season 4) in Sakha, Egypt

Operation	Date	Notes
-Application of phosphorous fertilizers	June 5	30 unit of P_2O_5/feddan
Land plowing	June 7	By chisel and disc, twice orthogonal
Land leveling	June 13	Laser technology
Application of potassium fertilizers	June 14	25 unit from K_2O/feddan
Sowing rice grains	Jul 15	60 kg/feddan
1st time Irrigation event	June 16	(355 m3 of applied water per Fed)
Application of herbicides Planting date	June 29	against narrow and broad leaves of weeds
Application of nitrogen fertilizers	June 30	(total recommended dose is 70 N unit/Fed) Here we have added just 20 unit of the recommended dose
Application of herbicides	July 20	(second time), as soil site is very weedy
Application of second dose of nitrogen fertilizer,	July 21	30 N unit
Application of third dose of nitrogen fertilizer	Aug 4	20 N unit
Application of fungicides and insecticides	Late Aug	To control insects and diseases
Application of potassium	Sept 25	as foliar spray
Harvesting	Oct 22	Yield is 2.13 ton/feddan
Irrigation		18- Applying 5 -7 cm of irrigation water every 7-10 days along the season. Soil almost times was saturated. Irrigation has been prevented 20 days before harvesting date.

3.3. Equipment and Associated Instrumentation

At this site, the main approaches included Energy Balance (EB) sensors in conjunction with eddy covariance for the determination of the sensible heat flux (H), which are well maintained and calibrated, so that all the components of the energy balance equation are measured, except latent heat flux (LE) (figure 4).

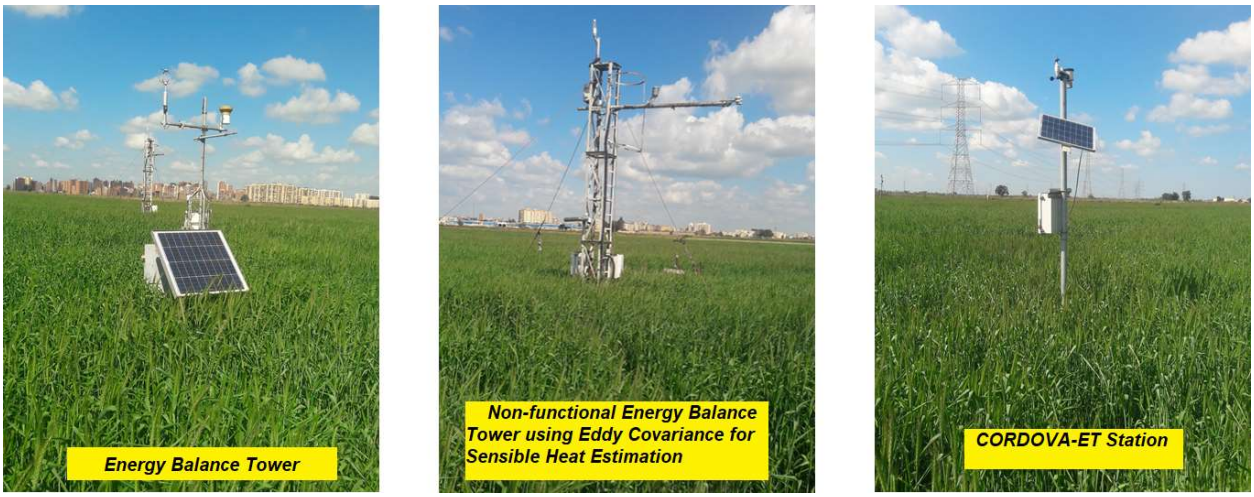

Figure 4 The availability of various ET measuring facilities at the Sakha site, Egypt.

3.3.1. Energy Balance Tower

The flux tower has various meteorological instruments that sense various components of the surface EB. Sensible Heat (H) estimation is done using the EC method. For the calculation of H, the datalogger records high frequency (10Hz) data for wind 3D vector components (Ux, Uy, Uz) and sonic temperature Ts (81000VRE, Young USA), and then computes the corrected sensible heat from the covariance of vertical wind (w') and sonic temperature (Ts'). Low frequency (1 Hz) data for net solar radiation (NRLite2, Kipp&Zonen) and Soil Heat Flux (HFP01, HukseFlux, Inc.) were used to obtain 30 min net radiation (Rn) and soil heat flux (G). Soil temperature gradient (TCAV, Campbell Scientific, Inc.) and soil moisture (CS655, Campbell Scientific, Inc.) were sensed to calculate Heat Storage (S) in the soil surface layer while S canopy was not measured (assumed negligible for crops). The EC method was used to calculate sensible heat (H) only.

Other data recorded from sensors placed in the flux tower are: wind direction (81000VRE, Young, Inc., USA); air temperature and relative humidity (HS2s3, Rotronic, Inc. USA); and rainfall (TE525MM, Texas Electronics, Inc.). The sensors were mounted to an adjustable height instrumentation tower to facilitate the maintenance of the equipment and adapt to different crops and crop heights, making sure that all the sensors covered the area of interest. An onsite datalogger (CR3000, Campbell Scientific, Inc.) computed continuously corrected fluxes every 30 minutes for net radiation (Rn), soil heat flux (G), and sensible heat flux (H). Latent heat flux (LE) was then calculated using the surface energy balance equation, LE= Rn - G – H. To obtain 30-min ET, LE over the 30 minutes was divided by the latent heat of vaporization. In order to maintain good quality ET data, a new energy balance flux tower (EB) was installed in the site to double-check with the eddy covariance flux tower. The EB tower sensed Rn using net radiometer, H using sonic anemometer and G using soil heat flux plates and soil temperature thermocouple.

3.3.2. CORDOVA-ET Station

The CORDOVA-ET station was installed in Sakha on Feb 17, 2020. Data were retrieved through the data Grafana collection platform and the Base station was installed since first season. The system was active from the start of 2020 summer season (July) to mid-September. Issues of nighttime power cuts were periodically encountered. Only nodes 5 and 8 were active, while nodes 6 and 7 were not functional from 15th July 2020. Data were not available during the winter 2021 season due to the instrumentation failure of the system. University of Cordova has been informed of the recent status of the station and the nodes, spare and faulty parts have been requested since this time, but the replacement parts have not arrived to this date. There is a consistent problem in radiation sensors everywhere across the network. The current status of the CORDOVA-ET station is summarized in Table 13. For Season 3 onwards CORDOVA-ET at this site was not functional.

Table 13 Summary of the current status of CORDOVA-ET Station installed at Sakha, Egypt

Item	Installation date	Current Status (**Non-Functional)
CORDOVA-ET Station	12 Feb 2020	There were no ET data available for this season for Sakha site (calculated by the UCO team).
Frogitt weather station	12 Feb 2020	Frogitt weather station was working well, its performance was more than 90% of the crop duration.
CORDOVA-ET Station	July 2020	From 20 July 2020 to 31 Oct. 2020, there were nighttime power cuts. Air temp. sensors not working anywhere since installation. On 26th Sept, there was a visit by FAO team to raise CORDOVA sensors above the canopy, from about 70 cm to 1 m.
Node 5	July 2020	Canopy temperature too high, it gave negative ETa
Node 6	July 2020	Stopped/didn't recharge since 15 July On 22nd of Sept 2020, there has been a visit by a team from FAO and MIWR for troubleshooting and fixing issues.
Node7	July 2020	Stopped working since 15 July On 22nd of Sept 2020, there has been a visit by a team from FAO and MIWR for troubleshooting and fixing issues.
Node 8	July 2020	Nonfunctional

3.4. Data results, analysis and reporting

In general, the data reported from the Sakha site for the 4 seasons reflects the fact that predominantly the only method of ETa determination available at this site was the energy balance tower, except for the first two seasons when CORDOVA-ET estimates were available for some of the time. There were few data gaps from the energy balance tower and all the 4 seasons were well covered by this method. The CORDOVA-ET station was not functional most of the time and hence, none of the ET estimates (ETa) were recorded using the CORDOVA-ET station, although ETo was adequately determined in season 1 and season 2. The following detailed analysis is performed for the Sakha site with respect to the different meteorological variables. For the ease of analyses and discussion across various sites in a consistent manner, the measured variables were grouped into clusters and discussed as shown below. Although this site has performed gravimetric analysis for soil samples in the previous season, the found out that ET_SMD estimated from it was erroneous owing to the fact that the soil moisture changed quite rapidly between the sampling phase and the laboratory estimates. Thus ETa_SMD was discontinued at this site.

3.4.1. Potential Evapotranspiration (ETo)

It was observed that there is good agreement between the ETo estimated by the CORDOVA-ET Station (ETo_COR) and by the on-site weather station (ETo_SELF). The increasing trend of ETo from Winter to Spring to Summer and decline from Summer to Winter seasons for both 2020 and 2021 were well captured Meteorological data from the on-site agromet-station was used to estimate ETo_SELF (using the modified Penman Monteith equation (FAO56 approximation (fig 5). Analyzing the trend of ETo_SELF during the crop phase (Winter to Spring to Summer), as expected, the declining ETo showed realistic trends with an increasing atmospheric demand for evaporative flux from the land surface. This is primarily because of increasing net radiation and the increase of vapor pressure deficit of the atmosphere. ETo is computed based on a combination of a set of meteorological variables and assumption of a standard canopy, using the modified-Penman Monteith equation (which is the FAO56 approach or the ASCE approach). Because it is based on a combination of measured meteorological variables (which vary negligible among different approaches). The comparison between the two ETo estimates indicate that the divergence between the two estimates increase towards end of the Fall in 2020. ETo_COR is pretty much stable with very less day-to-day variations as opposed to ETo_SELF. This reflects the differences in the way the instruments at this site (Agromet station vs the CORDOBA-ET Station) estimates the values of various meteorological variables. This calls for a serious cross-validation of meteorological variables using various approaches at this site and ensure the sensors/ instruments are cross-calibrated (for example, air temperature measured by various approaches, radiation measured by various sensors etc.). Details of the sensors that measure meteorological variables that are used to compute ETo_SELF are provided in the Annexure-I.

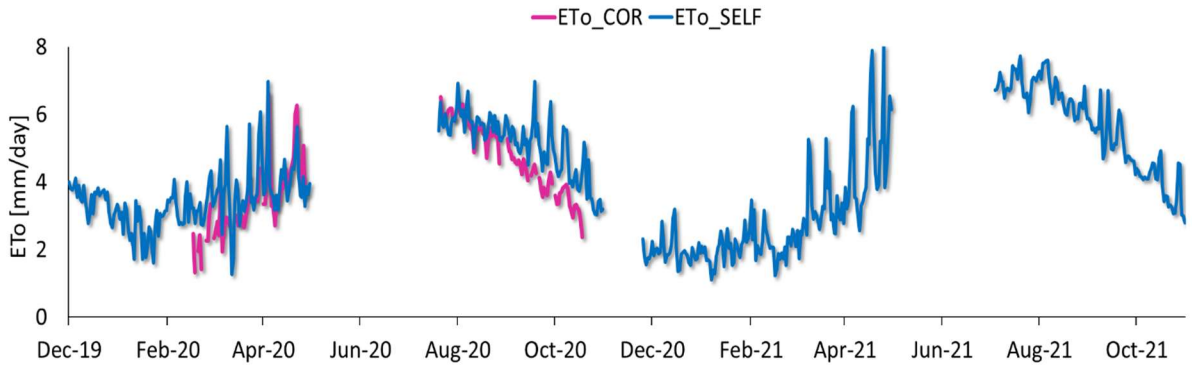

Figure 5 ETo measured at the Sakha Site, Egypt by on-site meteo-station (ETo_SELF)

3.4.2. Actual Evapotranspiration (ETa)

The comparison of the ET retrievals based on the two approaches (figs. 6a and 6b) imply relatively lower congruencies between the CORDOVA-ET Station (ETa_COR) and the in-house Energy Balance Tower based (ETa_EB) estimates. While ETa_EB shows reasonably good patterns of the seasonal ET for all the 4 crops, ETa_COR suffers from lot of spurious patterns. The sudden decreases in the ETa estimates in ETa_COR is a common thing we have observed across the sites and hence we believe that there is some serious fault in the way some variables are sensed by the CORDOVA-ET Station that is reflected in the ET estimates. The analysis of ETa retrieval based on the Energy Balance approach (ETa_EB) shows reasonable trends. The notable fact was that there were ET data available for 100% of the crop duration making this a complete dataset for comparing with satellite retrievals. The ~100% L3 ETa reflects the fact that all the components of the energy balance (H, G and LE) were properly recorded without any gaps even with the high-quality control criteria we consider in the data analysis while upscaling L2 to L3.

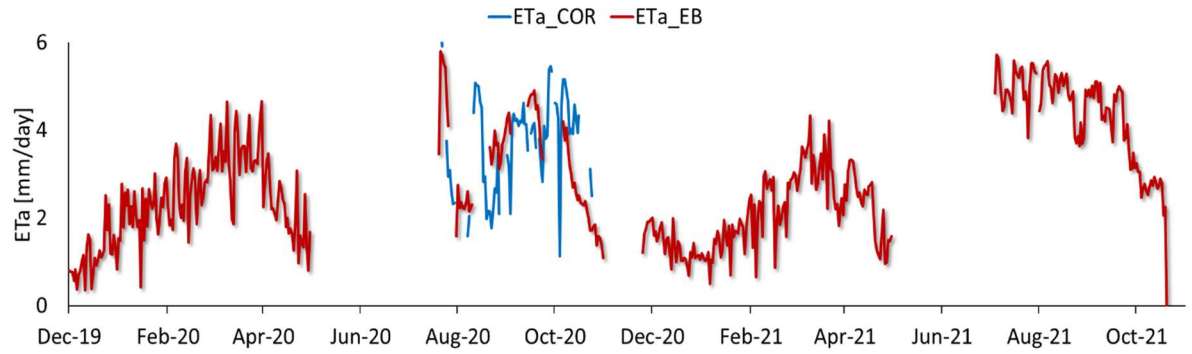

Figure 6a ETa measured at the Sakha Site, Egypt, by the on-site approach of Energy Balance (ETa_EB).

It can be noted that the ETa (ETa_EB) follows the pattern of crop growth (unlike ETo) peaking around 6th March in 2020 and 10 march in 2021 when the vegetation abundance is the highest (when the ETa is around 4.3 mm/day). We need to note that at this site, during the 4 winter seasons, the crop was bread wheat, and the only source of water was the sparse winter rainfall and the 2 irrigations.

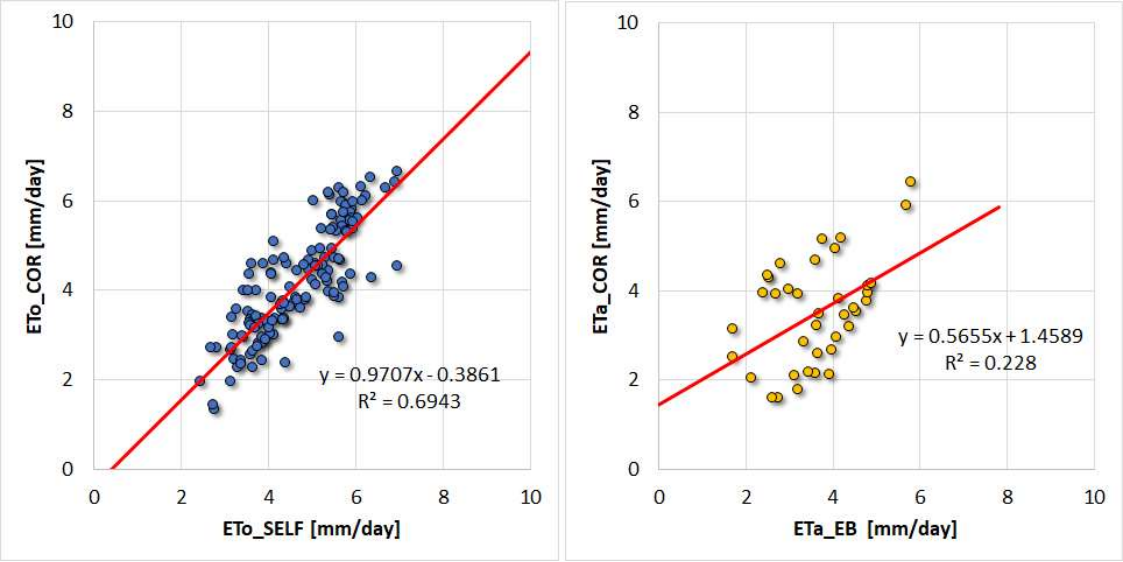

Figure 6b Statistical comparisons between the different estimates of ETo and ETa, respectively. A linear regression ($y=\beta_1 x+\beta_0$) was evaluated. R^2 explains the percentage of the variance in the dependent variable that the independent variables explain collectively.

3.4.3. Energy Balance Components

Analysis of surface energy balance at the Sakha site is quite important because this approach is the primary method of ETa retrieval at this site. Analysis of the various surface energy balance components measured at the site reflects the fact that the net radiation (Rn) is predominantly converted to latent heat flux (LE) rather than sensible heat flux (H) in the Sakha site. It can be noted that the energy balance components were not available for season 1. The site has some days when there are gaps in the LE data. The trend of LE is similar to the ETa_EB data (as expected) where similar data gaps can be seen because ETa_EB is derived from LE. The gap-free data measurements of various components of the energy balance in seasons 2 through 4 is quite encouraging and gives a higher confidence in ET_EB. As the crop season progressed from Winter-Spring-Summer-Autumn to Winter, the seasonal Rn, and LE, components also changed because of the increased crop growth that increased evapotranspiration from the crop growth and also because of irrigation events that occurred during the cropping season. It is clear from the data that whenever the LE increased (due to higher ET), there were days when the latent heat flux was as large as ~120-135 W/m2. The sensible heat at the Sakha site remained relatively smaller (25-35 W/m^2) reflecting the fact that the plot was humid enough that the crop surface was relatively cool. However, towards the end of the crop H started to increase dramatically while the LE fluxes declined fig. 7). The G also shows small but significant amount of energy flux (0-15 W/m^2). This is true on the days that overlapped with the irrigation events. This demonstrates that the assumption of G=0 is not fully correct in the daily surface energy balance as adopted by CORDOVA-ET. Station.

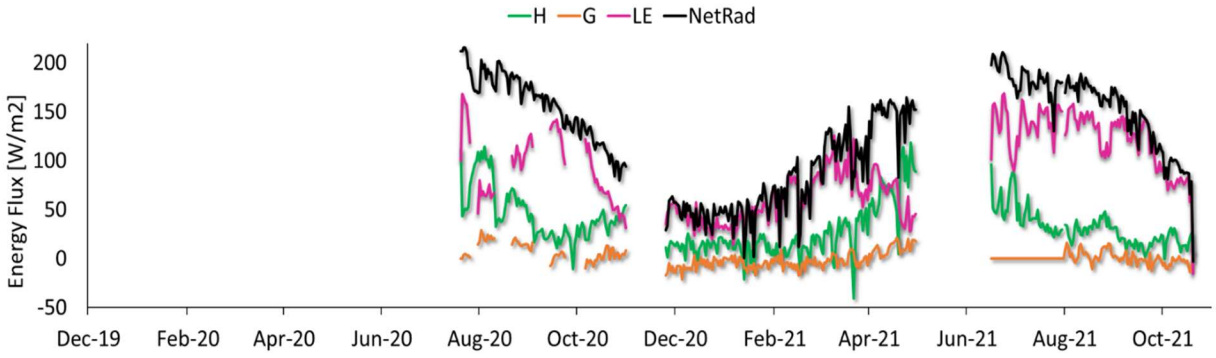

Figure 7 Components of the Surface Energy Fluxes (H- Sensible Heat Flux, LE Latent Heat Flux, G- Ground Heat Flux along with Net Radiation Flux) at the Sakha Site, Egypt.

3.4.4. Temperature Components

Theoretically, the temperature of various components of the land surface should be different owing to the differences in the thermal properties. It can be observed from the data (fig. 8) that all the reported temperature components tend to decline from summer to fall during the course of crop growth. At this site in Sakha, in general, the soil temperature was less than air temperature on most of the days in the crop growing phase. The soil temperature was larger in the initial phase when it was winter and early spring, and the ground was less covered with vegetation. However, as the vegetation abundance increased, it was noted that soil temperature was 1-2 degrees less than the air temperature, except for the last few days towards the end of the crop. Because there were canopy temperature measurements, we could see the difference between air temperature, canopy temperature and soil temperature. Temperature is an important biophysical variable that influences the long wave radiation emission from a given surface based on the surface specific emissivities based on the Stefan Boltzmann law and hence forms an integral part of the surface energy balance and hence the ET mechanism.

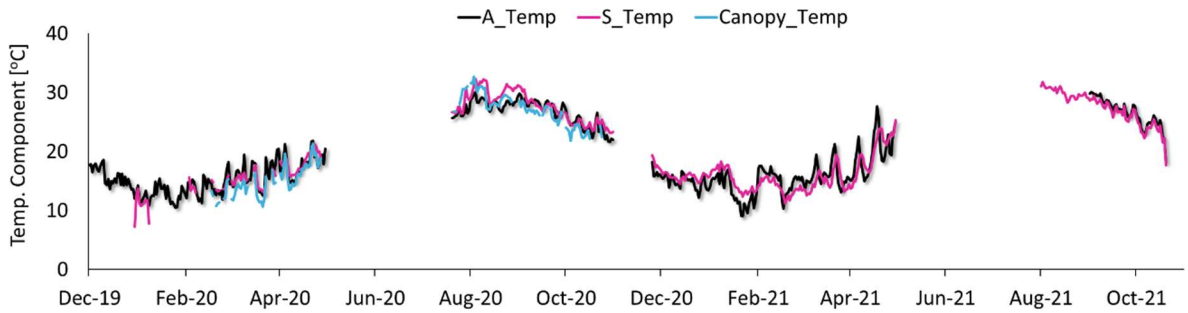

Figure 8 Various Temperature components at the Sakha Site, Egypt.

3.4.5. Hydrometeorological Components

The hydrometeorological variables of various types collected at the Sakha site were plotted together and analyzed for all the four seasons continuously (fig. 9). It can be observed that the RH at this site is quite fluctuating on a day-to-day basis and the RH showed a slightly declining trend from summer to fall.

Nevertheless, we see from the data that in the wintertime often the daily average RH was measured close to 90% which is a rare phenomenon in this arid climate is recommended that the hygrometer at this site be checked in detail. This has a minor influence on the measured sensible heat (H) in the energy balance equation that is used to get LE via its influence on the density of air measured. The climate is classified as arid due to the small annual precipitation; but the humidity is strongly influenced by the nearby Mediterranean Sea and seasonal wind patterns as well as the fact that the rainy season, such as it is, is in the wintertime. It is entirely plausible that humidity would increase and often be near 90% in wintertime when air temperature is cooler and relative humidity increases due to that. Although Sakha is an arid agroecosystem, we also have to keep in mind that the site was irrigated twice with large amounts of water using the Nile River water in the form of surface flooding method which may increase the local humidity to some extent. This has an implication on the ETa probably via the decreased atmospheric demand for water, which reduces the ETa reduces.

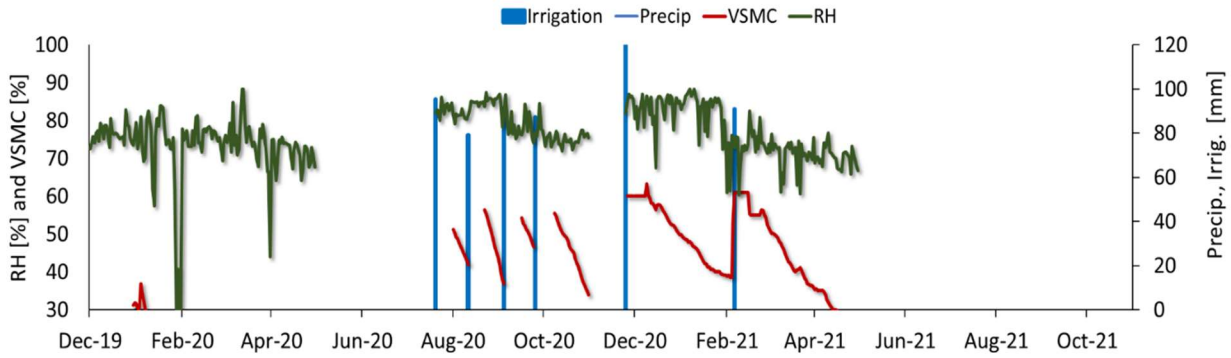

Figure 9: Measured Hydrometeorological variables at the Sakha Site, Egypt.

The plot also shows no rainfall events (as the region is lying in an arid region). Comparing the ET trends with RH and irrigation events reflects the fact that ET happened mostly when the crop growth was highest vegetation stage, when the RH was lowest and when the soil moisture was relatively available due to the irrigation events. Unfortunately, soil volumetric water content values were greater than possible (in excess of 60%) given the soil air filled porosity that was at maximum 59.6%. This indicated that the soil water sensors may have been out of calibration and should be calibrated for the soil at this location. Also, the lack of soil water content data after the first four irrigations was problematic in terms of having a complete record.

3.4.6. Pressure-Windspeed Components

The atmospheric pressure pattern seemed to fluctuate rapidly as the season changed to the summer from winter. This is reflected in the daily wind speed patterns observed in the data (fig. 10). Had there been a barometer, we could have compared this with the surface pressure dynamics. As of now, no conclusion can be made other than the fact that the wind speed fluctuation is highly random, and it has a slight influence on the ETa mechanism via the aerodynamic resistance of the biosphere and the atmosphere and the turbulent nature of the boundary layer.

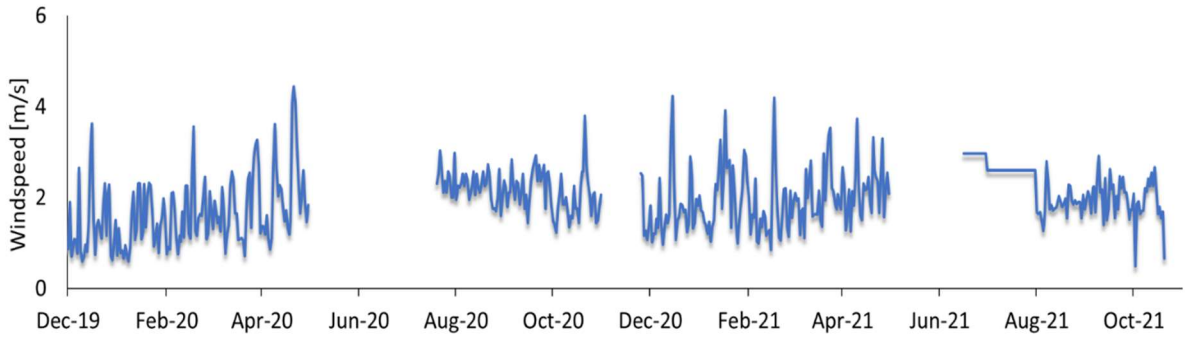

Figure 10: Pressure-Wind dynamics (no pressure data available) at the Sakha Site.

3.5. Brief data results discussion

1. ETo was realistically captured by the in-house method.
2. The ETa was realistically captured by Energy Balance but there weren't other methods to compare.
3. The ETa_SMD method was terminated at this site due to the tedious nature of gravimetric procedure and the shallow depth of VSMC observation by TDR.
4. The sites need to have a barometer as pressure is not monitored. It is recommended to seek from a nearby agrometeorological station.
5. The data gaps need to be reduced by frequent checking of sensors in a proactive manner to avoid malfunctioning.
6. The CORDOVA-ET Station needs to be urgently repaired and made functional at this site.
7. The observed data can be readily used for RS calibration and validation with ETa_EB as the standard.

4. JORDAN, Dyar Ala Site

4.1. Location Details.

The site is located at the National Agricultural Research Center (NARC)/Dyar Ala Station in the central Jordan Valley (32°11'26"N, 35°37'06" E) with an elevation of 224 meters below sea level, as shown in fig. 11. This location receives 270 mm rainfall annually and offers unique meteorological conditions. It is a hub-location for irrigated agriculture in the Jordan valley, focusing mainly on cultivating vegetables and cereals. The central Jordan Valley is considered one of the main semi-arid areas in Jordan with low precipitation (250-350 mm/y), almost completely occurring during the winter season, and high evaporative demand. Main water resources are represented by the fresh water coming from the Yarmouk River and then mixed with the King Talal dam water, which is already mixed with treated wastewater that comes from Kherbet El Samra treatment plan. Water is mainly used for irrigation in the central Jordan Valley. Site selection for the lysimeter occurred in 2007 during visits by NARC and USDA-ARS personnel to several locations. The site is on a well-established NARC agricultural research station (fig. 11). An agricultural micrometeorological weather station is located there. A relatively large (100 × 200 m, 2 ha) field was available, providing adequate fetch in the prevailing E-W wind direction (up and down slope between the valley sides and the Jordan River). The Jordan Valley Authority's main water distribution canal is adjacent to the station, and a reservoir and drip irrigation system exists to irrigate the field (water EC is 1.5-1.7 dS m^{-1}). The location and soil are typical of irrigated areas in the Jordan Valley. The site is approximately midway between the less saline irrigated areas to the north and the more saline irrigated areas to the south and is near the center of the most densely irrigated part of the valley. Electrical power is accessible. A CORDOVA-ET station was installed in the maize field on 9th Feb 2020.

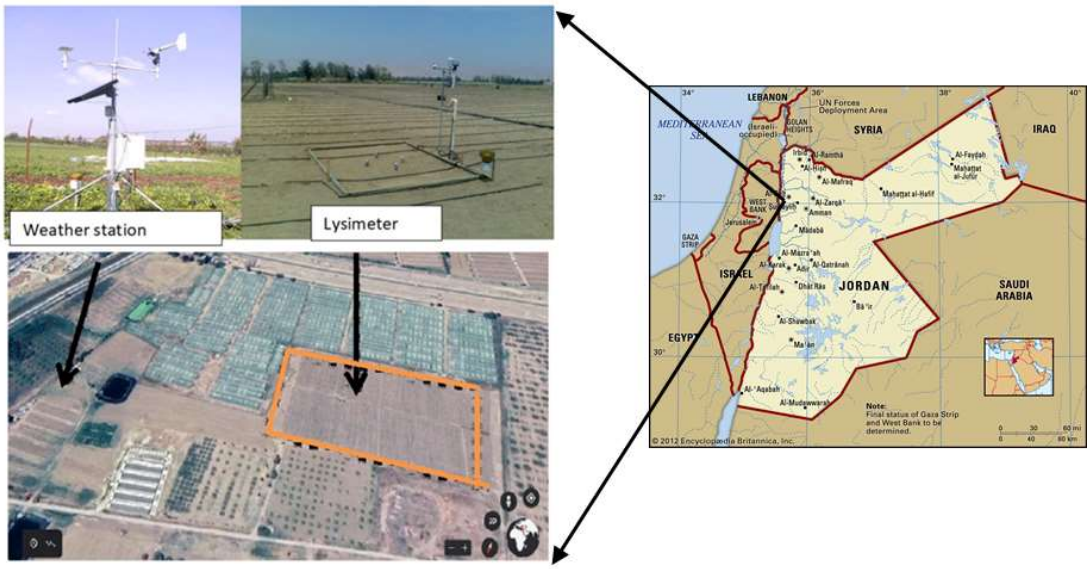

Figure 11 The location of the Dyr Ala Site in Jordan Valley in the NARC facility

4.1.2. People Involved

Table 14 People involved at the Dyar Ala site in Jordan

Person	Position / Organization	Role in the project
Dr. Naem Mazahrih	National Agricultural Research Center (NARC)	Coordinator / irrigation expert
Eng. Shehab Aldlqamoni	National Agricultural Research Center (NARC)	Horticulture and crop science (Researcher)
Eng. Ahmad Alwan	National Agricultural Research Center (NARC)	Crop science (Researcher)
Eng. Osamah Owaneh	National Agricultural Research Center (NARC)	Soil and environment (Researcher)
Eng Iyad Al Zoubi	National Agricultural Research Center (NARC)	Soil and environment (Researcher)
Eng. Osama Amarat	National Agricultural Research Center (NARC)	Plant protection (Researcher)
Eng. Mira Haddad	ICARDA	Senior Research Assistant

4.1.3. Soil characteristics

Soil and water characteristics include both the physical and chemical properties of the soil. The quality of irrigation water affects the field water balance to a certain extent and hence the ET_a. At this site, the soil is predominantly a heavy clay soil with 55% clay fraction. This has a major influence on the plant water availability in terms of both the soil-water property dynamics, as well as plot-scale hydrology, due to the cracking and swelling characteristics. Tables 15 and 16 show the salient features of soil hydraulic properties and chemical properties, respectively, at the Dyar Alla research station.

Table 15 Physical soil properties of at Dyar Ala Research Station in the Jordan Valley (BD=bulk density; FC=field capacity; PWP=permanent wilting point)

Soil depth	BD ($g.cm^{-3}$)	FC (%)	PWP (%)	Sand (%)	Silt (%)	Clay (%)	Textural class
0 - 15	1.33	31.00	19.95	13.9	31.9	54.2	Clay
15-30	1.35	32.50	21.59	10.3	33.7	56.0	Clay
30-45	1.32	33.00	21.95	13.7	28.4	58.9	Clay
45-60	1.45	34.50	22.90	8.2	32.0	59.8	Clay
60-75	1.46	34.80	22.95	11.6	32.1	56.3	Clay
75-90	1.50	35.69	23.00	14.9	32.2	52.9	Clay

Table 16 Chemical properties of soil at Dyar Ala Research Station in the Jordan Valley

Soil depth	N%	P (ppm)	K (ppm)	pH	EC (dS/m)
0-15	0.112	67	812	7.8	3.2
15-30	0.089	62	696	7.7	2.2
30-45	0.056	70	627	7.7	2.4

4.1.4. Water characteristics

Table 17 Physico-chemical properties of irrigation water at Dyar Ala Research Station, Jordan

EC	pH	HCO3	K	Ca	Mg	SAR	HCO3
dS/m	-	ppm	ppm	ppm	ppm	ppm	ppm
1.92	8.44	271.49	28.50	83.50	44.29	5.34	272.00

4.2. Crop cultivation and agronomic practices

The conventional crop pattern at the research station includes mainly winter vegetables grown in the open fields and inside large plastic greenhouses. The main vegetables grown in green houses are tomato, cucumber and sweet pepper. In the open fields, eggplants cabbage, cauliflower, onion, etc. The cereal crops that are grown are mostly wheat and maize. Vetch is also grown as a forage legume. For season 1, a winter wheat crop was grown (Dec 25, 2019-May 5, 2020); for season 2 summer maize was grown (July 15, 2020 – Oct. 20, 2020); for season 3 a fodder vetch was grown (Jan. 13, 2021 – April 30, 2021); and for season 4 a summer maize was grown (June 14, 2021 – Sep. 9, 2021). The full set of field agronomic practices during the four seasons in 2020 and 2021 are detailed in Tables 18-21 below.

Table 18 Agronomic practices for the Wheat crop during Winter 2020 at Dayr Alla research station.

Operation	Date	Notes
Land preparation	1. Dec 2019	land preparation using disc plough
	21 Dec 2019	collect soil samples from 4 location in the experimental site
Planting (winter wheat)	25 Dec 2019	Rate of 100 kg seeds /ha. Ammon Variety was cultivated. Sowing wheat (Ammon cultivar) with a density of 10 cm, row spacing 20 cm
Fertilizers application	25 Dec 2019 5 Marc 2020	DAP was applied 100kg/ha and Urea 100kg/ha. 100kg/ha and Urea was applied.
Irrigation event (Drip Irrigation)	19 Feb 2020	Irrigation of the transplanted wheat with 4 mm.
	22 March 2020	30 mm of irrigation water was applied (milk stage)
	4 April 2020	40 mm of irrigation water was applied (filling stage)

Operation	Date	Notes
	14 April 2020	40 mm of irrigation water was applied (filling stage)
Harvest event	5 May 2020	Taken the harvested wheat samples from the lysimeter (7.2 m^2) location and 6 crop samples (1 m^2) from different locations in the field and calculate the biomass and yield s.

Table 19 Agronomic practices for the Maize crop during Summer 2020 at Dayr Ala research station.

Operation	Date	Notes
Land preparation	3 June	land preparation using disc plough
	8 June	Installation of irrigation system
	18 June	Installation black mulch
Planting (Maize)	18 July	Sowing maize *Ranger* variety (with a density of 40 cm, row spacing 75 cm Rate of 20 kg seeds/ha. Irrigation 33 mm
Fertilizer	25 July	weeding
	4 August	Applying 100kg (20 N: 20P2O5: 20K2O) Weeding
		Applying 80L humic acid
	9 August	Applying of 10-liter fungicide added with irrigation water TACHIGAZOLE (SLHYMEXAZOL)
Insecticide		
	11 August	Application of micronutrient fertilizer.
	19 August	Insecticides sprayed 2L
	20 August	150kg ammonium sulphate added + 3kg chelated iron
	22 August	Spray insecticide
	24 August	Applying micronutrients
	27 August	insecticides sprayed
Weeding	31 August	The beginning of the flowering stage
	2 September	The beginning of the flowering stage
	3 September	60 L Humic acid + potassium fertilizer added
	13 September	+canopy temperature sensors height adjustment
	22 September	and insecticides sprayed liquid sulfur fertilizer added insecticides sprayed, lysimeter load cell adjusted

Operation	Date	Notes
Harvest event	20 October 2020	Take the harvested maize samples from the lysimeter (7.2 m^2) location and 6 crop samples (1 m^2) from different locations in the field and calculate the biological & seed yield weight
Irrigation Events by Sprinkler irrigation	18-Jul 15mm 21-Jul 10mm 22-Jul 11mm 25-Jul 18mm 29-Jul 17mm 2-Aug 06mm 4-Aug 15mm 5-Aug 09mm 9-Aug 02mm 10-Aug 08mm 12-Aug 08mm 13-Aug 08mm 15-Aug 04mm 17-Aug 10mm 18-Aug 04mm 19-Aug 27mm 22-Aug 16mm 24-Aug 24mm	25-Aug 1mm 27-Aug 18mm 29-Aug 18mm 31-Aug 7mm 5-Sep 14mm 6-Sep 22mm 7-Sep 15mm 9-Sep 18mm 11-Sep 11mm 13-Sep 36mm 15-Sep 42mm 21-Sep 44mm 26-Sep 52mm 27-Sep 5mm 30-Sep 21mm 3-Oct 13mm 7-Oct 21mm 13-Oct 42mm

Table 20 Agronomic practices for the Fetch crop during Winter 2021 at Dayr Alla research station.

Operation	Date	Notes
Land preparation	22 December 2020	land preparation using disc plough Installation of the Irrigation System
Sowing /Planting	1 January 2021	Sowing seeds (150 kg seeds /ha)
Fertilizer Insecticide Weeding / herbicides	1 January 2021 9 February 2021 17 February 2021 18 March 2021	100 kg of urea ($CO(NH_2)_2$) Weeding 100 kg of urea ($CO(NH_2)_2$) 100 kg of urea ($CO(NH_2)_2$)
Irrigation Events	9 January 2021 10 January 2021 11 January 2021 12 January 2021 3 February 2021 24 arch 2021 3 April 2021 3 April 2021 9 April 2021	9 mm (Drip irrigation) 15 mm (Drip irrigation) 5 mm (Drip irrigation) 3.5 mm (Drip irrigation) 33 mm (Drip irrigation) 20 mm (Drip irrigation) 20 mm (Drip irrigation) 16 mm (Drip irrigation) 33 mm (Drip irrigation)

Harvest and Yield	22 April 2021	Take the harvesting vetch samples from the lysimeter (7.2 m2) location and 4 crop samples (1 m2) from different locations in the field and calculate the biological & seed yield weight.

Table 21 Agronomic practices for the Maize crop during Summer 2021 at Dayr Alla research station.

Process	Date	Notes
Land preparation	5 June	land preparation using disc plough
	10June 14 June	Installation of irrigation system
Planting (Maize)	14 June	Sowing maize *Ranger* variety (with a density of 40 cm, row spacing 75 cm Rate of 20 kg seeds/ha.

Date	drip (mm)	Date	drip (mm)	Date	drip (mm)	Date	drip (mm)	Date	drip (mm)
19-Jun	*65.5*	1-Jul	*17.3*	15-Jul	*14.2*	14-Aug	*6.7*	29-Aug	*13.9*
21-Jun	*10.1*	4-Jul	*16.6*	17-Jul	*11.3*	17-Aug	*9.3*	30-Aug	*5.5*
23-Jun	*11.8*	7-Jul	*4.8*	18-Jul	*14*	19-Aug	*10.3*	3-Sep	*4.7*
25-Jun	*2.0*	10-Jul	*13.4*	31-Jul	*8.3*	21-Aug	*14*	5-Sep	*4.2*
26-Jun	*34.7*	11-Jul	*7.7*	5-Aug	*6.9*	23-Aug	*6.4*		
28-Jun	*13.7*	13-Jul	*12.8*	9-Aug	*9.1*	25-Aug	*2.2*		
29-Jun	*17.6*	14-Jul	*12*	12-Aug	*11.5*	26-Aug	*7.2*		

4.3. ET Measurement Equipment and Allied Instrumentation

4.3.1. Lysimeter

The main available ETa measurement method was a weighing Lysimeter (fig. 12) with dimensions of 2.4 m x 3 m x 2.5 m deep installed in an open field of two hectares surrounding the lysimeter (Evett et al., 2009). The soil is composed of clay loam. The main irrigation method is drip irrigation. The ET data were measured at half-hourly intervals with an accuracy of 0.1 mm. The lysimeter has been recently improved as we replaced the load cell and data logger as well as connected to internet with a modem-based data transmission facility so that diurnal variation of ETa is being recorded automatically with high accuracy and confidence.

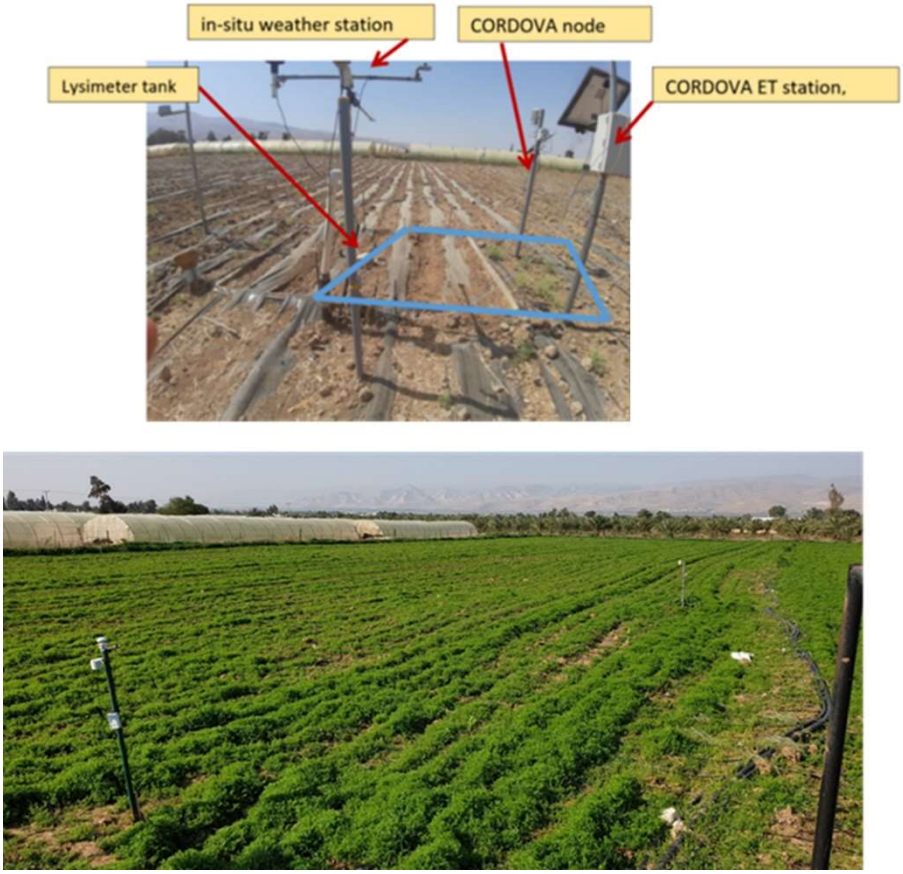

Figure 12 Location of the Lysimeter and the CORDOVA-ET Station at Dyr Ala, Jordan.

4.3.2. CORDOVA-ET Station

A Cordova base station with 4 nodes was installed in Jordan on 11/2/2020 inside 2 hectares field next to the lysimeter as shown in figure 12, and it seems to be working satisfactorily (Table 21) except sometimes when there is an electricity outage or communication network errors. For the weather station, two nodes lost the communication (node 3 since 27/10/2020 and node 4 since 8/11/2021). For tall canopies such as maize, the recorded data seem to have some errors for wind speed and canopy temperature sensors, when the maize height reached above 2 m.

Table 21 Current status of CORDOVA-ET Station installed at Dyar Alla, Jordan.

item	Installation date	Remarks /Condition
Weather station	11/2/2020	Works well with all the sensors, except between 5-10th Feb 2021, and from 15-16th Feb 2021.

item	Installation date	Remarks /Condition
Node 1	11/2/2020	Soil sensor works well, air temperature and humidity disconnected since 26/1/2021, canopy temperature lost the connection since 2/2/2021 until it was replaced on 27/4/2021.
Node 2	11/2/2020	canopy temperature works well, air temperature and humidity disconnected since 26/1/2021, Soil sensor worked well except some odd reading due to sensor wire not well connected with the base board.
Node 3	11/2/2020	Soil sensor worked well, air temperature and humidity disconnected since 26/1/2021, canopy temperature lost not worked since 2/2/2021.
Node 4	11/2/2020	Soil sensor worked well, air temperature and humidity disconnected since 26/1/2021, canopy temperature lost not worked since 2/2/2021.

4.4. Data results, analysis and reporting

In general, the data reported from the Dyar Ala site tells that all the four seasons had reasonable numbers of data. This implies that the occurrence of large gaps in the L3 data was smaller than the other sites. On the other hand, with respect to the Lysimeter approach, which is the primary ETa measurement approach, 85% of the 4 seasons had good measurements. The following detailed analysis was performed for the Dyar Ala site with respect to the different meteorological variables. For the ease of analysis, the ETa and the allied variables were grouped into clusters for analysis and discussion. While quantitative statistical comparisons were performed for ET variables, qualitative interpretations were given for other data clusters.

4.4.1. Potential Evapotranspiration (ETo)

There was poor agreement between the ETo estimated by the CORDOVA-ET Station (ETo_COR) compared with the in-house estimates obtained using meteorological measurements obtained at the Agromet station (ETo_SELF) in all the three seasons (fig. 13). It can be seen that there are abrupt and sudden low values of ETo_COR on DOY 230, 240 and 260 for example in the figure below. It reflects the fact that there is a serious technical problem in the sensors used in the CORDOVA-ET Station and the malfunctioning of those sensors. Only for the season 3 was there was reasonable agreement between the ETo estimated by the CORDOVA-ET Station (ETo_COR) and the on-site estimates obtained using meteorological measurements (fig. 13) obtained at the Agromet station (ETo_SELF). Details of the sensors mounted on the Agromet Station and the sensed variables that were used to compute ETo_SELF are provided in the Annexure-I. It can be seen that the daily variability in ETo is somewhat congruent in both the approaches. It reflects the fact that the sensors used in the CORDOVA-ET Station are sensing meteorological variables quite similar to those used in the on-site weather station. Again, it has to be understood that ETo is purely

a biophysical indicator representing the atmospheric demand, computed based on a combination of various meteorological variables alone. As it is purely based on meteorological variables, a less-consistent agreement between various ETo estimates necessarily implies the inconsistency in various meteorological measurements made by sensors. This is hence a litmus test of the efficacy of the CORDOVA-ET station to sense the of various meteorological variables at the site.

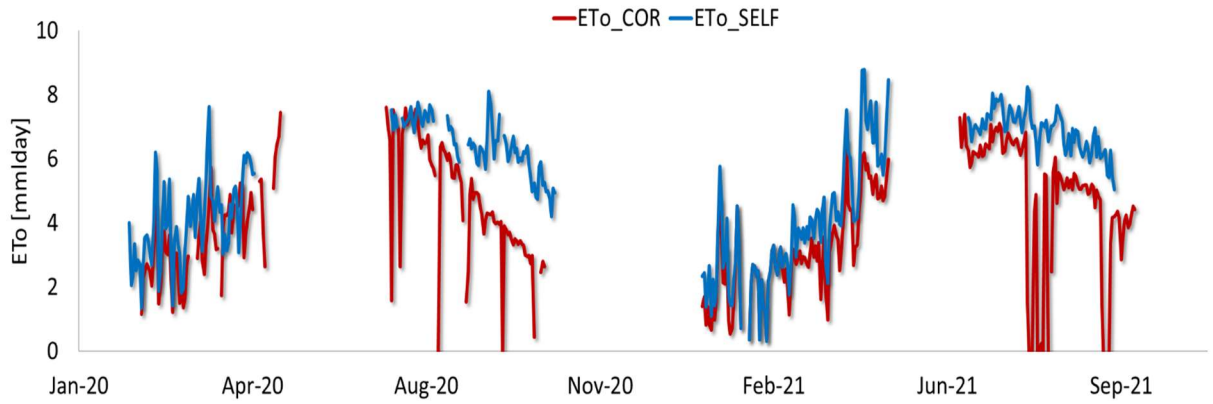

Figure 13 ETo measured at the Dyar Ala Site, Jordan by CORDOVA-ET Station (ETo_COR) and inhouse approach (ETo_SELF).

4.4.2. Actual Evapotranspiration (ETa)

The comparison of the ETa retrievals at Dyar Ala, based on the two approaches imply relatively less congruence between the CORDOVA-ET Station (ETa_COR) and the in-house Lysimeter (ETa_Lysi) estimates (figs. 14a and 14b). The agreements are reasonable in the winter seasons (2020 and 2021), while the divergences are greater in the summer seasons (2020 and 2021). While ETa_Lysi shows reasonably good patterns of the seasonal ETa of a typical well irrigated crop in arid regions, ETa_COR suffers from spurious patterns, including ET less than zero. The sudden decreases in the ET_COR estimates ETa_COR are a common thing we have observed across the sites and hence we believe that there is some serious fault in the manner in which some variables are sensed by the CORDOVA-ET Station that is reflected in the ETa estimates. In the initial phase of the crop (between DOY 200-235), ETa_COR values were negative. At daily time step, ETa, however, cannot be negative. This is theoretically impossible, and we can never get negative ET at a daily time step.

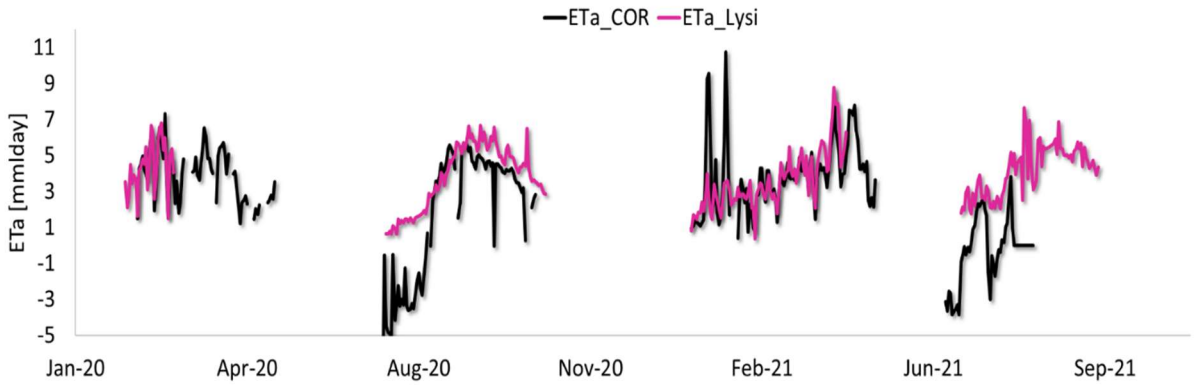

Figure 14a ETa determined at the Dyar Ala Site, Jordan, by CORDOVA-ET Station (ETa_COR) and in-house approach, which was a weighing lysimeter (EaT_Lysi).

Slight negative ETa is possible at some daily time steps when the air is very humid, and the land surface is colder than the near surface air above. This is manifested by the process of surface condensation and dew formation. At daily time step, ETa however can never be negative. This implies a technical issue with the CORDOVA-ET Station. In the winter seasons, the comparison of the ETa suggests that there is a larger congruency (fig. 14) between the CORDOVA-ET Station (ETa_COR) and the on-site Lysimeter (ETa_Lysi) estimates. ETa_COR suffers from some spurious patterns especially in the initial stages when the vegetation is sparse (e.g., very high values in Winter 2021). During the sparse vegetation stage, on the days the ETo is larger, ETa is estimated unrealistically large by ETa_COR. A critical analysis of the time series at this site says that the phenological pattern of vegetation is not captured by both these estimates adequately (see the season 3 where we don't see a sinusoidal pattern) although the congruency between the estimates is good and the data gaps are minimal.

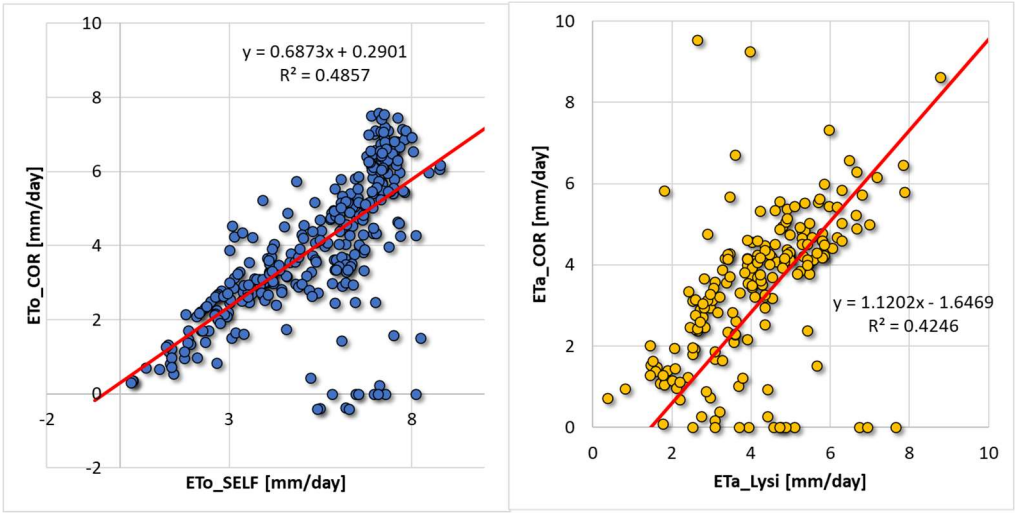

Figure 14b Statistical comparisons between the different estimates of ETo and ETa, respectively. A linear regression ($y=\beta_1 x+\beta_0$) was evaluated. R^2 explains the percentage of the variance in the dependent variable that the independent variables explain collectively.

4.4.3. Temperature Components

Theoretically, the temperature of various components of the land surface should be different owing to the differences in the thermal properties. It can be observed from the data (fig. 15) that all the reported temperature components tend to increase from winter to summer during the course of the vetch crop growth. At this site in Dyar Ala, in general, the soil temperature, canopy temperature and air temperature cyclically changed in intensities. What can be generalized is that the soil temperature remained fairly stable relative to canopy and air temperature (which were fluctuating more rapidly). On days with high air temperature, soil temperature remained less than the canopy temperature implying thick vegetative density and sparse exposed ground surface. In the initial stages, in the wintertime, soil temperature was slightly larger than the air temperature. There were some gaps in the measurement of the temperature components. It was noted that, as the crop reached maturity, the soil temperature declined substantially relative to the air temperature. The reason for this could be due to the higher soil moisture on the land surface and most of the energy partitioned to change the phase of water via latent heat flux (ET) and also shaded ground surface. As this site does not measure the various surface energy balance components, we are not in a position to corroborate these trends with surface energy partitioning.

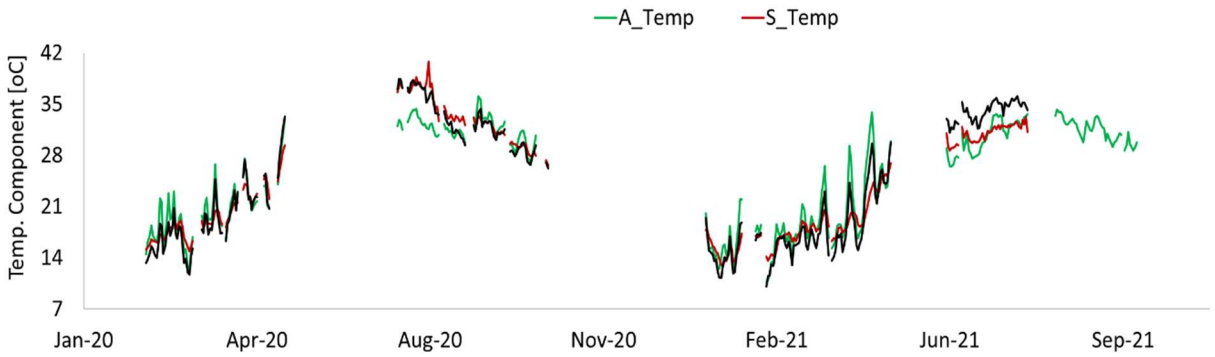

Figure 15 Various Temperature components at the Dyr Ala Site, Jordan.

4.4.4. Hydrometeorological Components

Various hydrometeorological indicators measured at the Dyar Ala site during the four seasons are plotted in fig. 16. The datasets plotted here came from diverse sources but are put together under one category. The crop received some precipitation at this arid site most of which occurred in the winter. Precipitation was measured by the automatic weather station. Drip irrigation was also provided (see the blue bars in the fig. 16). The plot however shows the precipitation and irrigation events combined did not create the corresponding rapid dynamics of soil moisture (VSMC). There was a TDR system installed separately to monitor the VSMC in the field. The data reveal that the VSMC is not very sensitive to inputs of water in the form of irrigation events and outflux of water as ET fluxes. Thus, it is advised to check the functioning of TDR at this site. This raises the question regarding the depth at which the TDRs are buried, and in what position relative to the drip lines? Deeper sensors would be less responsive to irrigation evens, par1ticularly from drip irrigation. And sensors not close to an emitter might not respond at all the irrigation events. The RH pattens reveal that in this below sea level location the RH is quite dynamic and ranged from 40-80% which declined as the summer approached.

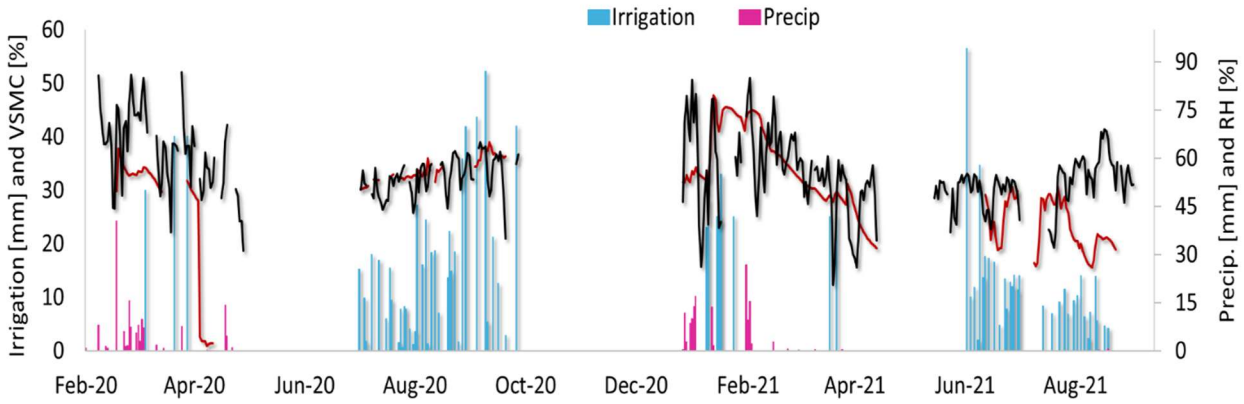

Figure 16 Hydrometeorological variables at the Dyar Ala, Jordan.

4.4.5. Pressure-Windspeed Components

The atmospheric pressure did not show any temporal pattern and what can be generalized is a slight declining trend as the summer approaches and a slight increase as the winter approaches (fig. 17). The windspeed variability shows that there were days in the winter (early stage of the crop) when windspeeds were larger (with a corresponding signal in the atmospheric pressure pattern). However, it became calmer with random windspeed as the crop matured. Regional wind patterns as a function of surface pressure heterogeneities are, however, large-scale phenomena. Nevertheless, we see slight indicators of pressure-wind relationships from the data collected from the CORDOVA-ET Frogitt weather station. It is important to note that Dyar Alaa is a site below the mean sea-level (224 below msl) which already has a big impact on the atmospheric pressure. The seasonal change in atmospheric pressure which affects several biometeorological processes has a significant role in governing the physics of boundary layer meteorological phenomena and thus this site is quite interesting. It is suggested that a careful look into the barometer (pressure sensor) of the CORDOVA-ET station performance be done along with onsite weather station.

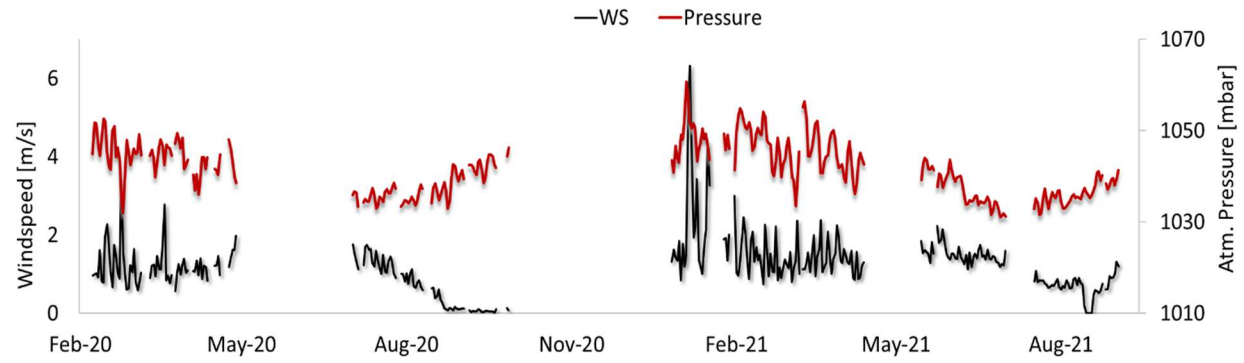

Figure 17 Pressure-Wind dynamics at the Dyr Ala, Jordan.

4.5. Brief data results

1. ETo was realistically captured by on-site agromet station but not consistently by the CORDOVA-ET Station.
2. The agreement between methods for ETa was good in winter and extremely bad in the summer seasons. Main issues included drastic underestimation of ET_COR during summer, and significant overestimation of ETa_COR during less vegetated stages, implying excessive sensitivities of microsensors or some problem with CORDOVA-ET station algorithms.
3. Often it was observed that the magnitudes of the ETa were not significantly lower than ETo even if the irrigation was limited, implying some unique characteristics of the vegetation (very high plant density may be one of the reasons). The negative value of ETa estimated by CORDOVA-ET reflects some serious issues with the instrumentation.
4. The temporal pattern of VSMC is not very clearly visible with irrigation and rain events, which may be due to depth of sensors and placement of sensors relative to the drip emitters.
5. This site has the unique feature of a well-functioning Lysimeter, and elevation below mean sea level, so it has to be augmented, if possible, with other methods.

5. LEBANON, the Tal Amara Site.

5.1. Location Details of Tal Amara Site in Bekka Valley.

In Lebanon, the ET field measurement and experimental site is located at Tal Amara Research Station premises of LARI (Lebanese Agriculture Research Institute), situated about 70 km northeast of the capital Beirut city (35.987927ºE, 33.860117 ºN, Fig. 18). The general climate of the area (Bekaa Valley) is typically Mediterranean, but it is affected by the presence of two elevated mountain ranges, at the two sides of the Bekaa and Baalbeck-Hermel Governorates. The area is characterized by hot dry summer and relatively cold-rainy winter. Precipitation is concentrated between October and April with trace rainfall in May and September. The average annual rainfall is about 600 mm with 95% of the rain occurring between November and March. The rainiest month is January with an average of about 150 mm. Summer is completely dry with zero rain. The rain ceases in mid-May and rarely starts in mid-September. Recalling ten years back, the rainy season 2013-2014 was the driest with rainfall of 280 mm while the wettest rainy winter reached a maximum 1,250 mm (rainy season of 2017-2018). Temperature changes drastically over the year, with summer temperatures averaging about 25°C and winter temperatures near averaging about 6°C. The average yearly temperature is about 15°C. Temperature might reach to as high as 40°C in July and August and it could freeze in some winter days. The Department of Irrigation and Agrometeorology (DIAM) of LARI manages over 50 automated Agrometeorological Weather Stations (AWS) across the country including in the Bekaa Valley. Yearly reference evapotranspiration ETo is observed through the AWS network. It reaches a yearly total ETo of about 1300 mm. The yearly gaps between average rainfall and average reference evapotranspiration comes to about 600 mm/year.

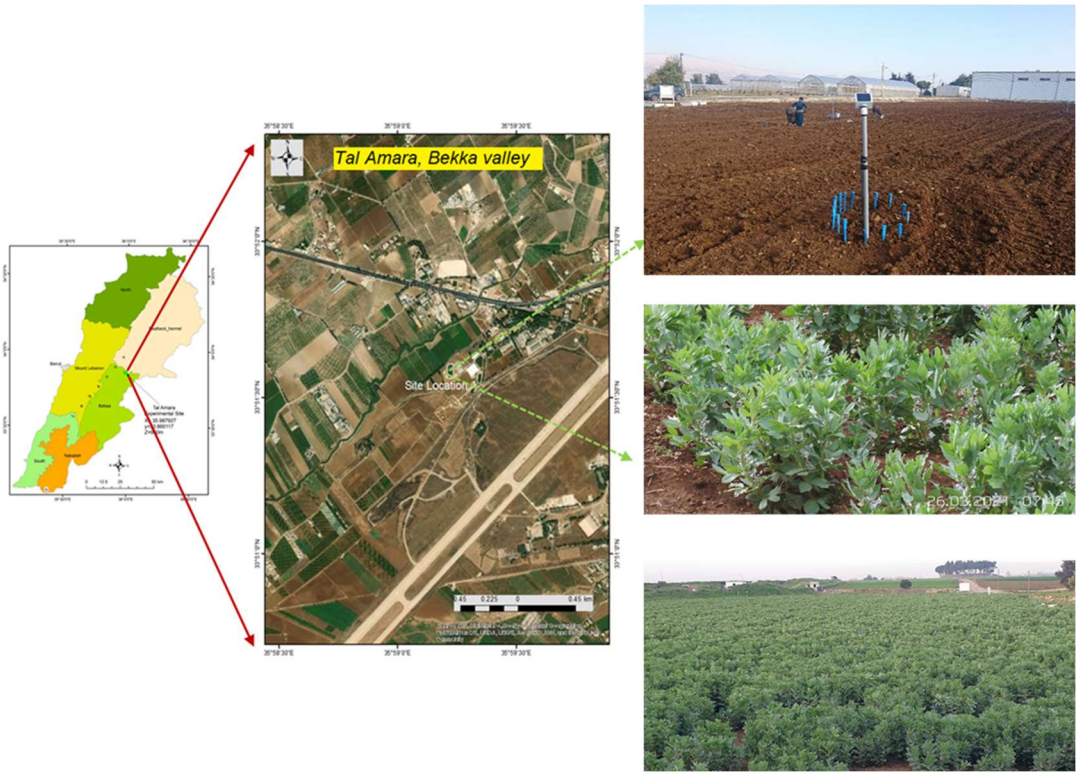

Figure 18 Location of the Tal Amara Site in Lebanon in the LARI Bekka Valley campus

5.1.1. People involved

Table 22 People associated with the Tal Amara site in Lebanon.

Person	Organization	Role in this Project
Ihab Jomaa	Researcher Department of Irrigation & Agrometeorology (DIAM) at LARI	Coordination ET Cordova Station Maintenance Reporting Data, preparing reports Weather Station maintenance
Sleiman Skaff	Technician, LARI	Field data collection
Ibrahim Mortada	Labor	Field data collection

5.1.2. Soil characteristics

Soils of the ET experimental site are deep where the root zone might extend more than 2 m. It is a fairly well drained soil with a slope gradient of less than 1%. The soil texture is clayey with 28% sand, 28% silt and 44% clay with a medium level of Organic Matter (1.47%). The soil has a homogeneous characteristic to about a meter depth (Table 23). The soil is mostly alkaline with pH value of 7.8. Salinity is very low with EC of 0.13 dS/m. The soil bulk density is about 1.4 g/cm^3. The field capacity and the wilting point reach about 0.38 and 0.20 on volumetric basis, respectively. The hydraulic conductivity is about 40 mm/day. The soil is poor in total nitrogen with 0.15% but rich in potassium (626 ppm K_2O) (Table 24).

Table 23 Physical properties of the soil at the Tal Amara site in Lebanon (BD=bulk density; FC=field capacity; PWP=permanent wilting point).

Soil depth	BD g/cm^3	FC m^3 m^{-3}	PWP m^3 m^{-3}	Sand %	Silt %	Clay %	Textural class
0 - 20	1.4	0.38	0.2	28	28	44	Clay
20-40	1.3	0.36	0.2	26	28	46	Clay
40-60	1.3	0.35	0.2	25	27	48	Clay
40-80	1.27	0.35	0.2	23	27	50	Clay

Table 24 Chemical properties of the soil at the Tal Amara site in Lebanon (EC=electrical conductivity).

Soil depth (cm)	pH	EC (ds/m)	$CaCO_3$ Total (%)	$CaCO_3$ Active (%)	P_2O_5 (ppm)	K^2O (ppm)	Na (ppm)	MgO (ppm)	CaO (ppm)
0-30	7.9	0.13	16	4	166	626	129	432	1026

5.1.3. Water characteristics

Irrigation water is collected in open water cement tank of about 3000 m^3 in size. The water source is groundwater pumped from 60 m depth borehole-well. Water is alkaline with low electrical conductivity (Table 25).

Table 25 Physico-chemical properties of irrigation water at the Tal Amara site in Lebanon (EC=electrical conductivity).

EC (dS/m)	pH	Ca^{2+} (mg/l)	$HCO3^-$ (mg/l)	Mg^{2+} (mg/l)	Na^+ (mg/l)	Cl^- (mg/l)	NO_3^- (mg/l)	SO_4^{2-} (mg/l)	Fe (mg/l)
0.52	7.9	112	45.2	1.7	8.5	5.68	41.5	6	0.02

5.2. Crop cultivation and agronomic practices

The cultivated land surface area was about 9000 square meters. Ploughing and land leveling is a routine practice and an intensive first weed control is the norm. About 20 days before sowing in each season, the land soil was wetted, using sprinkler irrigation for 10 hours. For the season 1, a winter wheat crop was grown (Dec 7, 2019 – July 2, 2020); for season 2 spring potato was grown followed by a summer fallow (March 1, 2020-July 31, 2020); for season 3 a faba bean crop was grown (Dec. 3, 2020 – May 6, 2021); and for the season 4 a summer maize was grown (June 17, 2021 – Oct. 8, 2021). Tables 26-29 provides details on the agronomic practices followed for each crop at this site.

Table 26. Agronomic practices for the Wheat crop in Winter 2020 at Tal Amara site.

Operation	Date	Notes
Land preparation	Oct 25, 2020	Watering land before ploughing and as first control measure for weeds
	Nov 15, 2019	Land Preparation (Ploughing)
	Nov 16, 2019	Land levelling
Planting Durum Wheat (ICARASHA)	Dec 7, 2019	Sowing using ICARDA's planting machine 23 kg seeds/1000 sqm Durum wheat variety ICARASHA
Fertilizer application	Feb 6, 2020	50 Kg/1000sqm of Ammonium Sulphate (21 NH_4 and 21 SO_4)
Weed control	April 20, 2020	Application of herbicides Metalaxy11+Azoxystrobin28: 750 ml/1000 L of water) to control the dicotyledonous weeds.

Operation	Date	Notes
	April 30, 2020	Application of herbicides Metalaxy11+Azoxystrobin28:750 ml/1000 L of water) to control the dicotyledonous weeds.
Pesticide	May 1, 2020	Application of insecticide
Irrigation event	None	None (Completely Rainfed)

Table 27 Agronomic practices for the Potato Spring 2020 at Tal Amara site.

Operation	Date	DAS	Notes
150 kg Fertilizer	24 March 2020	-	15N-15P_2O_5-15K_2O
Sowing	25 March 2020	0	Potato (cv. Spunta), using seeder, Sowing rate 70 cm x 30 cm
Weeding	26 March 2020	1	Herbicide: SENCOR (Metribuzin)
Weeding	13 May 2020	50	Hand weeding at 50 DAS
50 Kg Ammonium sulfate	15 May 2020	52	21% N at 52 DAS
Pesticide application	25 May 2020	62	Cymoxanil 5% and Mancozeb 68% At 62 DAS
Harvesting	24 July 2020	122	46 ton/ha Biomass 58 ton/ha At 122 DAS

Table 28 Agronomic practices for the faba bean crop in Winter 2021 at Tal Amara site.

Operation	Date	Notes
Land preparation	14 Nov and 1 Dec 2020	Land was wetted on 14 Nov and then ploughed/prepared for sowing on 1 Dec
Sowing /Planting	3 Dec 2020	Using special planting machine for large faba bean Seeds
Fertilizers Insecticide	21 Mar 2021 5 March 2021	100 Kg Urea 150 kg of soluble 20-20-20 on

Operation	Date	Notes
Weeding / herbicides		
Irrigation Events		No irrigation events
Harvest and Yield	5 May 2021	the yield was 1674 g pods per plant

Table 29 Agronomic practices for the maize crop in Summer 2021 at Tal Amara site.

Operation	Date	Notes
Land preparation	7 June 2021 and 12 June 2021	Land was deeply ploughed to about 60 cm and then leveled
Seeding/sowing	17 June 2021	Using sowing machine for maize seed
Plant spacing at sowing	17 June 2021	70 cm between rows and 40 cm between plants inline
Fertilizers Insecticide Weeding / herbicides	75 Kg Urea 20 DAS and 150 kg of soluble 12-16-10 on 56 DAS	Weeding using herbicide Tribuneron on 20 DAS and manually on 70 DAS
Irrigation Events	20 irrigation events	Irrigation soil depth or rooting depth was considered 40 cm all through. Total ETc = 511 mm, Total irrigated water = 525 mm
Harvest and Yield	8 October 2021	Kernels 20 t/ha and grain yield 15 t/ha

5.3. ET Measurement Equipment and Associated Instrumentation

The main tool of ET measurement at Tal Amara was originally planned to be with the already installed weighing lysimeter. Throughout the wheat growing season the weighing lysimeter was malfunctioning causing DIAM research to rely on monitoring soil moisture content, using gravimetric sampling. The site is equipped with a weighing Lysimeter with surface dimensions of 3 by 3 m and 3 m depth. The Lysimeter is connected to a counter-reader and laptop installed in a shed at 100 m distance. The recording software is DAQ Master that may register momentarily the weighing balance of the Lysimeter. The DIAM team is working together with ICARDA experts to maintain the weighting lysimeter and put it back into function. However, under the current circumstances of travel limitations and region-wide lockdowns, lysimeter maintenance took longer than expected; we are still working on this mission. The experimental site is equipped, in addition to the weighing lysimeter, with an Automatic Weather Station (AWS), soil moisture sensors of Frequency Domain Reflectometry (FDR) type and labs for volumetric soil moisture content. Currently, this lysimeter is under repair.

Tal Amara ET Network experimental site is equipped with four nodes and base weather station of CORDOVA-ET station. Each node has soil moisture, air temperature, relative humidity, and canopy temperature sensors. The base weather station is equipped with a solar radiation sensor, anemometer, rain gauge, atmospheric pressure, air temperature and relative humidity. The nodes and base weather

station communicate to a data logger through a LoRa radio network, and the base station sends data to the CORDOVA-ET server, using a GPRS system. Nodes of CORDOVA-ET were causing troubles of discontinuity. Nodes 1 and 2 were more robust than the other two (Table 30) and kept functioning throughout the four seasons. The base Cordoba weather station stopped communicating to the datalogger. However, it was possible to be downloaded and uploaded manually to the Cordoba server.

A separate system for soil water content monitoring was installed using a node and gateway system (Acclima, Inc., Meridian, Idaho USA). This system was equipped with Acclima True-TDR soil water sensors. Nonetheless, the Acclima system did not function correctly because the data SIM card of the reading website (Hologram) does not cover Lebanon. The TDR sensors have worked for a long period, but they have never accepted change of date and time. It kept bouncing back to default setting, because as was explained before, this issue is related to communication on the Hologram and data SIM card. It was supposed that the communication with the Hologram website goes smoothly but it appeared that Lebanon is not covered by Hologram countries (https://www.hologram.io/pricing/coverage). Thus, the TDR gateway and nodes have never communicated to Hologram and the date and time keep bounces back to default. This problem can be remedied by new firmware for the nodes and gateway that will allow the system to operate without using the Hologram server and SIM.

Figure 19 Location of the Tal Amara farm where the gravimetric soil moisture measurements were taken.

5.3.1. CORDOVA-ET Station

A CORDOVA-ET station was installed in November 2019. The setup in Lebanon had four nodes in parallel with the weather station. The four nodes started functioning in November 2019 together with the CORDOVA-ET weather station. However, the nodes and the CORDOVA-ET weather station routinely pause and stop sending data until they are reset again. These interruptions have happened many times throughout the last year (Table 30). The Cordoba-ET weather station (Frogitt type. https://www.froggit.de/Weather-Station/). HS Group GmbH & Co. KG, Escherstr. 31 50733 Köln, Germany) seemed to have some configuration issues that changed communication settings or interrupted it by the GPRS. Since then, the Frogitt CORDOVA-ET weather station was not able to send data through GPRS. Instead, the data were downloaded and sent for re-uploading with the help of the UCO team. Note that the radiation sensor keeps making errors in reading from time to time.

Table 30 Current status of CORDOVA-ET Station deployed at the Tal Amara site in Lebanon.

item	Installation date	Remarks /Condition
Weather station	November 2019	Stopped communicating to the main datalogger late 2020. The data is downloaded manually and uploaded to the Cordoba data server
Node 1	November 2019	Functions well
Node 2	November 2019	Functions well
Node 3	November 2019	Stops for long periods
Node 4	November 2019	Occasionally stops

5.3.2. Soil Moisture Depletion Method

Recently, the station was equipped also with soil moisture sensors of Frequency Domain Reflectometry (FDR) made by Decagon (type 10HS that measure large range of soil moisture content). The sensors are connected to a data logger from Hobo Technology, Inc., USA. The sensors that measure the dielectric constant estimate the soil moisture content. Once the soil water content varies, the FDR sensors detect these variabilities and register the VWC (Volumetric Water Content) in the data logger. The data is downloaded manually using a laptop through Hobo's software facility.

5.4. Data results, analysis and reporting

The data reported from the Tal Amara site for season 3 showed that less than 14.44% of season 3 had either no measurements or days when there were significant gaps in the L3 data with respect to CORDOVA-ET station as well as the ET components by the Soil Moisture Depletion approach. It is worthwhile to note that both CORDOVA-ET and the soil moisture depletion method operated at the same time without any gaps when they were operational. These approaches stopped measurements from DOY 125 while other meteorological measurements continued until the faba bean crop harvest. Thus, the data gap is not a gap that arose due to instrumental failure or systemic problem. The following detailed analysis is performed for the Tal Amara site with respect to the different meteorological variables. For ease of analysis, the ET and the associated variables were grouped into clusters for analysis and discussion. While quantitative statistical comparisons were performed for ET variables, qualitative interpretations are given for other data clusters.

5.4.1. Potential Evapotranspiration (ETo)

There was good agreement between the ETo estimated by the CORDOVA-ET Station (ETo_COR) and by the on-site station (ETo_SELF). The increasing trend of ETo from Winter to Spring to Summer was captured by both the estimates in both the years 2020 and 2021. In general, it can be observed that ETo_COR was slightly smaller than ETo_SELF, which again implies systemic bias in some of the micro sensors that sense the meteorological variables and the inherent systemic bias. This calls for an instrumental cross

calibration. The relatively good agreement between the two estimates of ETo which necessarily implies that the various meteorological variables observed by sensors based on different systems are relatively consistent (compared to other sites) and cross-calibrations are not urgently needed at this site. Again, the main biases if any are noted when the vegetation is sparse (early stages of crop or later stages of crop).

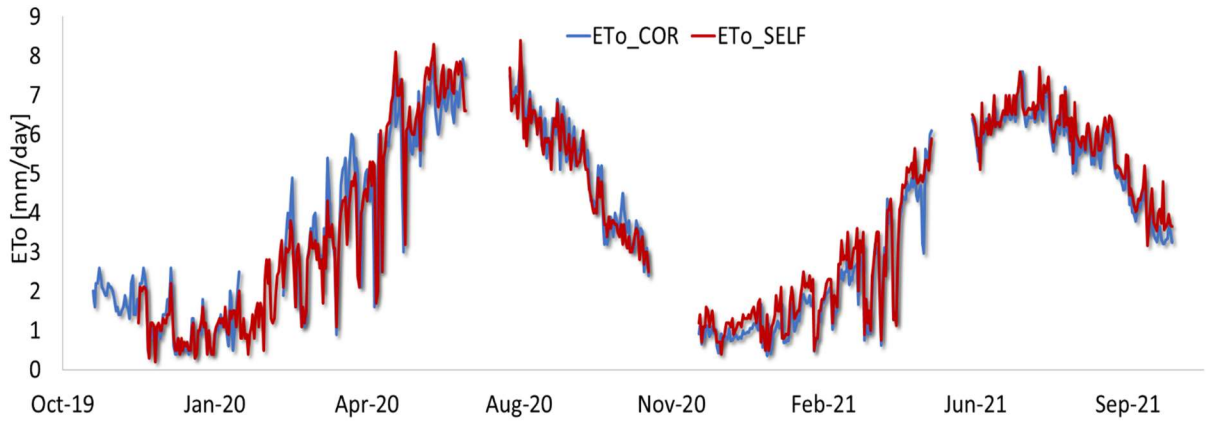

Figure 20 ETo measured at the Tal Amaara Site, Lebanon.

5.4.2. Actual Evapotranspiration (ETa)

At the Tal Amaara Site, ETa was primarily estimated using the Soil Moisture Depletion technique (ETa_SMD). The logic behind this method is that a change in soil moisture (VSMC) integrated over the rootzone is assumed to be basically used as ETa and any change in the depth integrated VSMC will give us an estimate of ETa. The caveats of this method include the scale differences of TDR footprint vs. the footprint of other methods when we do intercomparison of methods. The analysis of the VSMC derived ETa_SMD shows that ETa was captured rather robustly. The temporal patterns of ETa_SMD followed the expected patterns of ETa for a healthy vegetation. The magnitudes of ETa estimates are also reasonable. The comparison of the two ETa estimates (ETa_SMD with ETa_COR) reflects the fact that ETa_COR suffers from some spurious overshoots (see fig. 21, 9th Jan 2021, 21 February 2021, etc.). This rapid over estimation of ETa could be an inherent problem in the energy balance method where the sensors of CORDOVA-ET may be overestimating Rn or underestimating H creating very high LE flux estimates.

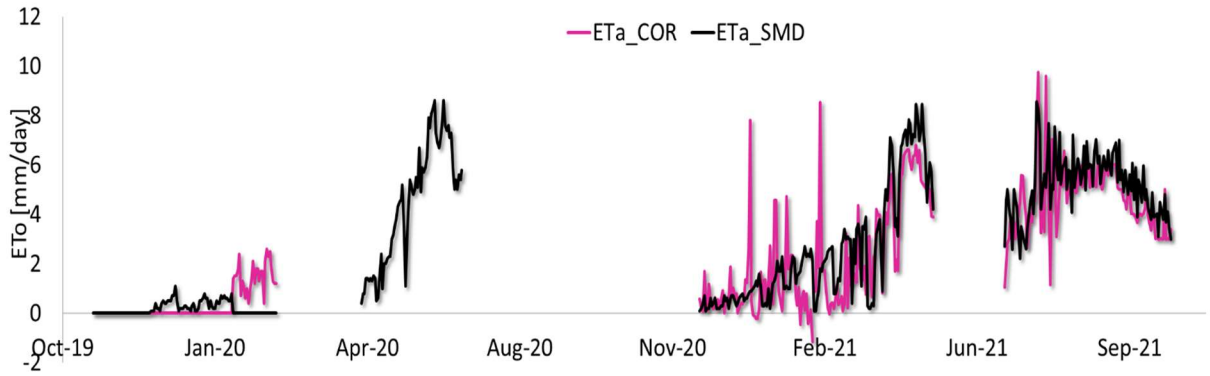

Figure 21 ET measured at the Tal Amara Site, Lebanon.

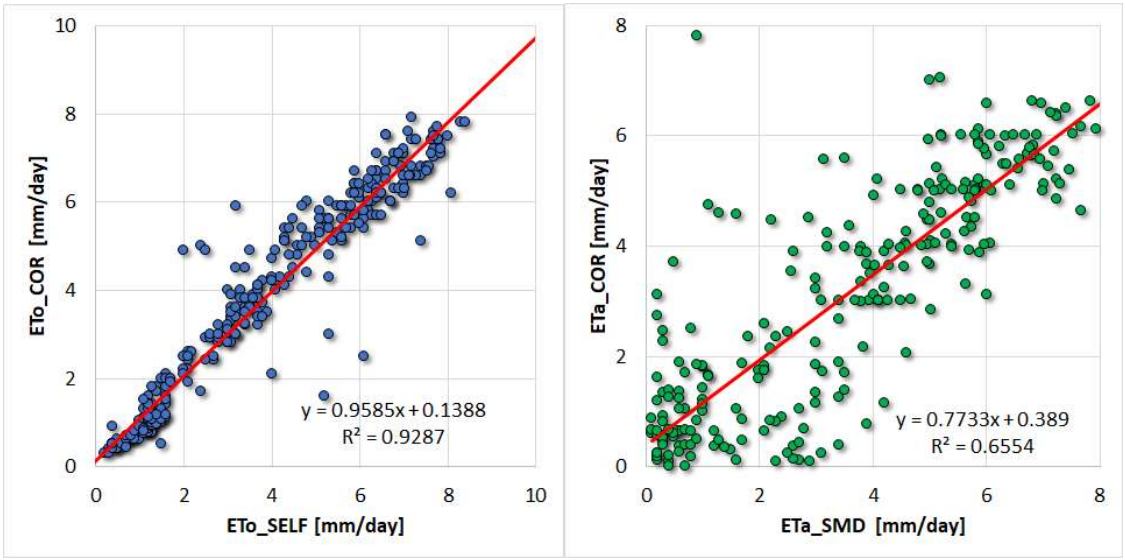

Figure 21b Statistical comparisons between the different estimates of ETo and ETa, respectively. A linear regression ($y=\beta_1 x+\beta_0$) was evaluated. R^2 explains the percentage of the variance in the dependent variable that the independent variables explain collectively.

5.4.3. Temperature Components

Theoretically, the temperature of various components of the land surface (near surface air, soil and vegetation) should be different owing to the differences in their inherent thermal properties. It can be observed from the data collected at the Tal Amara (fig. 22) that all the reported temperature components tended to slightly and then increase from Dec to April during the crop growth phase. At this site the soil temperature was larger than canopy temperature when there were no crops in the summer fallow (2020) situation. However, when spring potato was on the ground the soil temperature was less than air and canopy temperature. However, as the potato crop reached harvest it was seen from the data that the temperature of the crop was 6 to 7 degrees warmer than soil temperature which is surprising. The reason for this could be due to the larger signal sensed by the infra-red camera and the nature of brightness to

temperature algorithm used. The strong differences between the soil and canopy temperature warrants that the canopy temperature sensor used by the CORDOVA-ET Station needs to be closely examined. Tal Amara is at a relatively higher elevation and the rapidity of change in season is captured well within the temperature signals. From winter to summer, February seems to be the coldest month with occasional snowfall, although at lower intensities. At this site, in general, the soil temperature remained less than canopy and air temperature when there was little vegetation on the ground. Subsequently, soil temperature gradually increased while the canopy and air temperature remained smaller. A detailed analysis of the accuracy of canopy temperature is necessary as it forms the basis of CORDOVA-ET method to calculate certain influential variables (e.g., sensible heat flux) used in the Energy Balance-based ET retrieval.

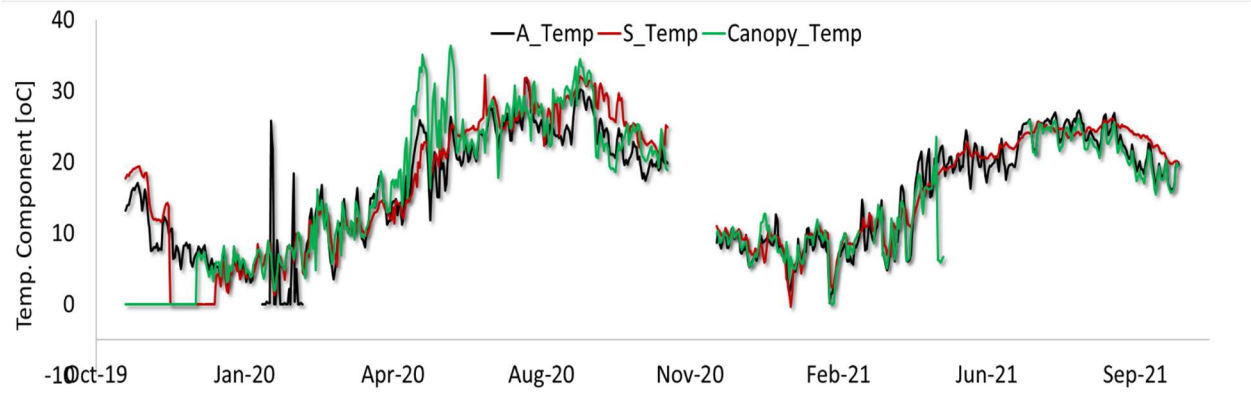

Figure 22 Various Temperature components at the Tal Amara, Lebanon

5.4.5. Hydrometeorological Components

From the analysis of hydrometeorological variables from winter to summer continuously, it can be observed that the RH at this site fluctuated on a day-to-day basis, with often the RH reaching 80% when the precipitation events occurred. This is very realistic, and the measurements are adequately captured. It can be seen that the RH shows a declining trend as the season changed from winter to spring to summer to autumn. This has an implication on the ET probably via the enhanced atmospheric demand (higher vapor pressure deficit) for biospheric water to the atmosphere via ET. The plot also shows the rainfall events and the nature of its distribution during the winter seasons (wheat and faba bean crops in 2020 and 2021 respectively). It is well distributed, and the maximum intensity was recorded on 15th January 2021 (snow plus rain). The soil moisture fluctuations are responding to the rainfall events adequately. Analysis of the hydrometeorological data reveals that the measurements are adequately done at this site. The summer season is characterized by irrigation events and the soil moisture and ET are adequately responding to these events.

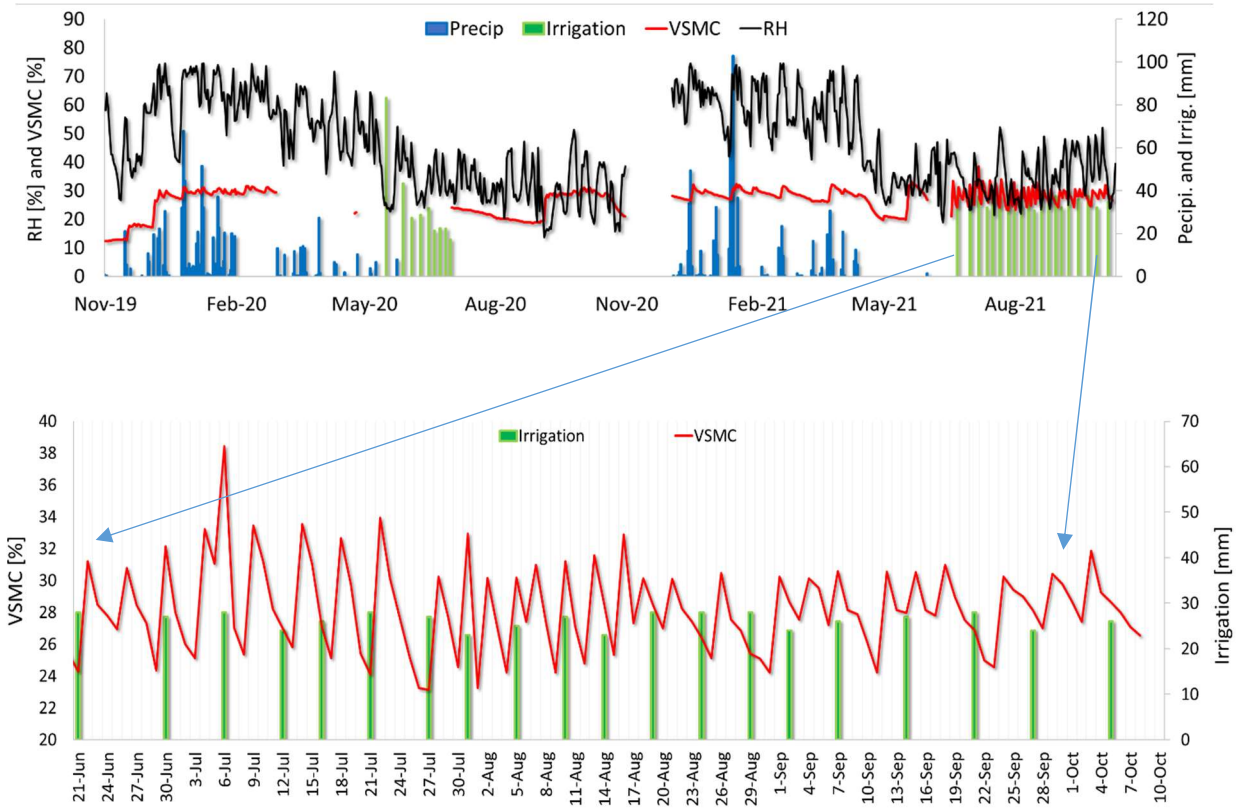

Figure 23 Hydrometeorological variables at the Tal Amaara Site.

5.4.6. Pressure-Windspeed Components

The atmospheric pressure at this site during this season did not show a unique trend. It was highly fluctuating on a day-to-day basis. However, the windspeed signals also showed some inverse relationship to the pressure differences (fig. 24). The region being in the Bekka valley, it's possible to have horizontal drainage of valley winds from the neighboring mountains that creates complexity of wind patterns other than the regional surface pressure differences. Nevertheless, we see slight indicators of pressure-wind relationships from the data collected. The location of Tal Amara is at a relatively higher altitude, which explains why the air pressure is less than that reported by other locations.

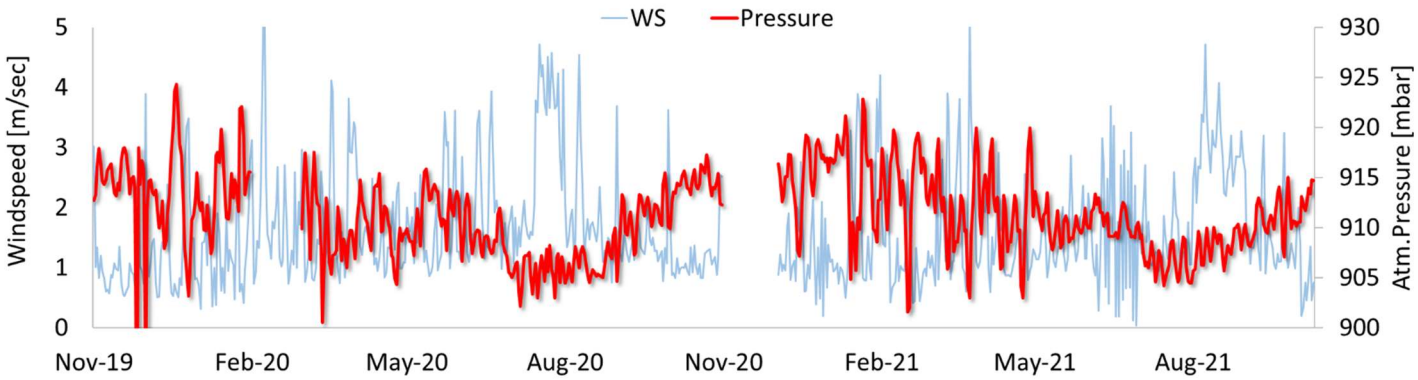

Figure 24 Pressure-Wind dynamics at the Tal Amara, Lebanon.

5.5. Brief data results discussion

1. ETo is realistically captured by in-house approach (Agromet data) and the CORDOVA-ET station.
2. The measured ET trends look reasonable. Although ET_SMD and ET_COR were comparable, ET_COR exhibited some spurious "overshoots" on certain days.
3. The lack of energy balance components is noted, and it is recommended to retrieve it from the CORDOVA-ET system as it will help to discuss the nature of the land surface and mass-energy relationships.
4. This site has the unique feature of being at higher altitude well above mean sea level, so it has to be augmented, if possible, with other methods (Lysimeter).
5. This relatively humid site has snowfall also. The impact on snow on soil water balance needs to be explored further.
6. The data gaps have been almost negligible in Season 3 and 4 which is quite interesting. The CORDOVA-ET data gaps are however significant, and it seems that some sensors need replacement.

6. MOROCCO, Berrechid Site.

6.1. Location Details

In Morocco, the university of Hassan II and its Institute of Agronomic and Veterinary Sciences (IAV Hassan II) is responsible for agrometeorological station maintenance and managing the measurements. The site is managed by IAV on a private farm of 20 ha. The farm is owned by Mr. Bentika (fig. 25) who was committed to participate in the project and ensure the safety of the station and to facilitate access for the project team members. He also agreed to follow the standard practice of the region and specific to the winter season. The site is secured with easy access and ready to adapt the crops according to the project's needs.

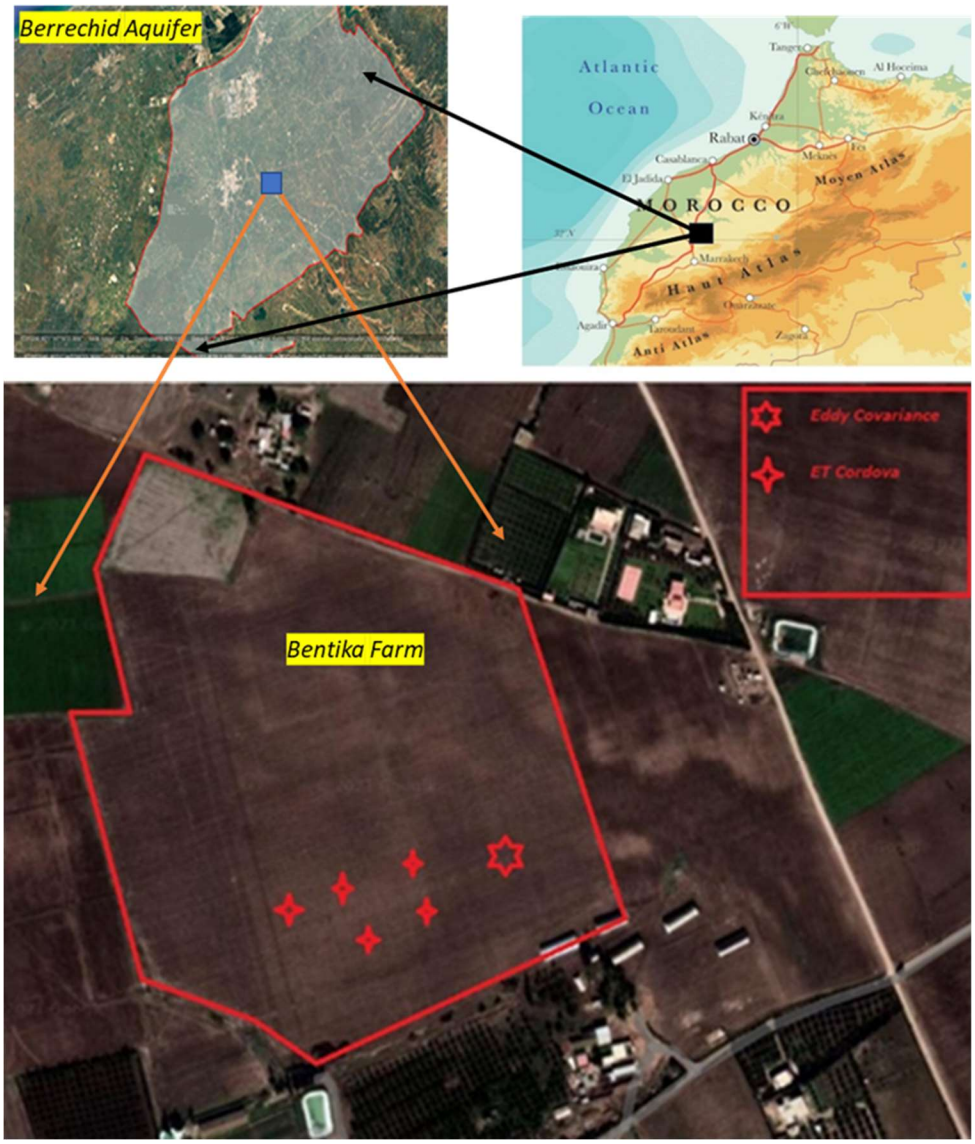

Figure 25 Location of the Berrechid Site (a private farm) in Morocco, administered by the Institute of Agronomic and Veterinary Sciences (IAV Hassan II), Morocco.

6.1.2. People involved

Table 31 People associated with the Berrechid site in Morocco.

Name/surname	Function/organisation	Role
Ali Hammani	IAV Hassan II	Country Manager
Ehssan El Meknassi	Lecturer researcher/ IAV Hassan II	implementation, data collect and analysis
Abdeljalil Nadif	Engineer / independent	Field assistant
Abla Kettani	Lecturer researcher/IAV Hassan II	CORDOVA-ET assembly
Merdas Mohamed	Project Manager/CRTS	Data manager of eddy covariance
Mohamed Zakour	Technician/IAV	field data collect assistant
Omar Makroum	Technician/IAV	Soil analysis
Bentika Wasiaa	Farmer	Farming

6.1.3. Soil characteristics

In November 2020, soil samples were taken at 2 locations at 3 depths in the experimental plot. Gravimetric analysis showed that the texture of the soil is homogeneous and sandy loam (Table 32).

Table 32 Physical properties of the soil at Berrechid site in Morocco.

Sample Number	Coarse Sand	Fine Sand	Silt	Fine Loam	Clay
B II 20 cm	4.1	45.1	25.8	20.6	4.5
B I 40	7.6	40.1	37.2	9.7	5.4
B II 60	10.1	24.9	22.5	24.7	17.8
C III 20	7.4	40.5	24.6	6.7	20.9
C I 40	11.1	35.1	23.0	10.9	19.9
C I 60	10.2	35.7	24.6	9.0	20.5

Table 33 Chemical properties of the soil at Berrechid site in Morocco (EC=electrical conductivity).

Samples	pH	K_2O	$CaCO_3$	Organic mater	P_2O_5	EC	NH_4^+	NO_3^-
0-40C	7.8	164	8.59	2.01	22.65	2.53	8.82	25.9
0-40B	7.6	128	7.88	1.21	18.65	1.71	5.88	22.4

6.1.4. Water characteristics

Irrigation water comes from the Berrechid aquifer, collected by borewells and stored in an irrigation basin. Salinity and pH measurements are taken at a basin level (Table 34).

Table 34 Physico-chemical properties of irrigation water at Berrechid site in Morocco (EC=electrical conductivity; SAR=sodium adsorption ratio).

Source of water	Ca^{++} (ppm)	Mg^{++} (ppm)	Na^{+} (ppm)	SAR	pH	EC (dS/m)
Borehole (ground water)	-	-	-	-	7.82	1.56

6.2. Crop cultivation and agronomic practices

The farmer cultivates various crops, in particular cereals irrigated by drip irrigation, fodder corn, potatoes and carrots. The experimental plot was cultivated with maize during the summer season. Durum wheat is the predominant cereal crop in the region. However various other crops are also grown. For this project the following crops were grown and monitored in the different seasons: Quinoa in season 1 (Feb 23,2020-July 3, 2020); Beetroot in season 2 (Aug. 27, 2020-Nov. 11, 2020); and Durum wheat in season-3 (Jan 11, 2021 – May 31, 2021)

Table 35 Agronomical practices adopted for the quinoa crop (winter 2020) at Berrechid site in Morocco.

Operation	Date	Notes
Land preparation	19 Feb. 2020	7. Land preparation using disc plough.
Planting	23 Feb. 2020 1 March 2020 1 April 2020 11 April 2020 19 April 2020	8. Grain corn was cultivated. 9. 90% seedling emergence 10. maximum canopy cover. 11. Beginning of canopy senescence. 12. Beginning of flowering.
Irrigation events	Dates of Irrigation 22 Feb. 2020 28 Feb. 2020 5 March 2020 10 March 2020 19 March 2020 12 April 2020 16 April 2020 29 April 2020 2 May 2020 6 May 2020 22 May 2020	Applied Water (mm) 8.3 4.2 4.2 5 5 5 8.8 12 13.5 16.7 24.7
Fertilizer application		No fertilizers applied
Weed control		manual weeding

Table 36 Agronomical practices adopted for the beetroot crop (Summer 2020) at Berrechid site in Morocco.

Operation	Date	Notes
Land Preparation	July 5	Deep ploughing with disc plough
Installation of the 1.4 m wide boards	July 20	
Installation of the Drip network	July 25	
Fertilizer application	July 30	NPK 10-20-20
Sowing	8 August	6.7 kg/ha
Pesticides		Takumi
Harvest	10 October	1.5 ha

Table 37 Agronomic practices adopted for durum wheat (winter 2021) at Berrechid site in Morocco.

Operation	Date	Notes
Land Preparation	20 November, 2020	Deep ploughing with disc plough
Installation of the Drip network		Not used as it was a rainfed crop
Fertilizer application	25 November, 2020	NPK 10-20-20 @ 1.5 q/ha N 33 kg/ha Urea 80 kg.ha
Sowing (Kanakis variety)	13 December, 2020	Seed rate is 170 kg/ha
Pesticides	1 January, 2021 15 March, 2021 20 April, 2021	Herbicide: Palace+Mistank Anti-fungus: Bixor
Harvest	27 May, 2021	yield: 38 quintal /ha

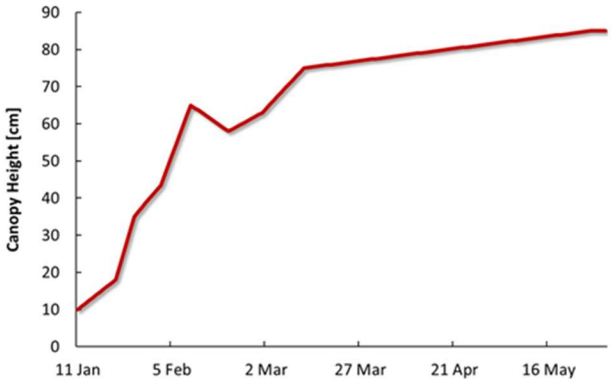

Figure 26 Temporal variability of canopy height of the durum wheat crop (winter 2021) .

6.3. ET Sensing Equipment and Allied Instrumentation

6.3.1. Eddy Covariance Technique

An eddy covariance station owned by the Royal Center of Remote Sensing (CRTS) was installed. The CRTS made the station available to IAV to conduct the experiment. ICARDA financed the repair of the station in order to fix or replace some components. The eddy covariance system has the following components: Open path gas analyzer with a 3D sonic anemometer, specifically designed for studies of turbulent flows. It measures absolute carbon dioxide, water vapor density, air temperature, atmospheric pressure, three-dimensional wind speed and sonic air temperature simultaneously. It has an aerodynamic shape for minimal distortion to the wind and to the sensor heating. It has an optimal housing of the analyzer and wind measurements. It has low power consumption and can be powered by a solar panel. The measurements were temperature-compensated without active thermal control. Integrated mounting of the sonic analyzer and anemometer ensured that the measurements of the gas analyzer and the sonic anemometer were time synchronized. Field installation, configuration and calibration were done and the maximum sampling frequency of this system was 50 Hz. It was already factory calibrated to ensure smooth functioning for all ranges of CO_2, H_2O, pressure and temperature in all combinations encountered in the field. The meteorological system consists of air temperature and relative humidity sensors, soil heat flux, soil temperature sensor providing the average temperature at 6 to 8 cm deep from the ground for energy balance measurement systems and net radiation sensor on the canopy cover. The biomet system also consists of volumetric soil moisture measurements using TDR. The data acquisition is based on a micro-logger that also has a small energy balance calculation program. The solar panels did not work after the station was installed. The repair took a long time due to the COVID19-related country closure for nearly 20 days. The TDR was installed on 7 July 2020. The field was changed from the season 2 site to another plot, the eddy covariance system was also moved and reinstalled by the same company.

Figure 27 Location of various facilities at the Berrechid Site, Morocco. It is a different farm than season 2 but within the Berrechid aquifer system

6.3.2. CORDOVA-ET Station

The sites were equipped with one CORDOVA-ET station with four nodes and calibrated against the established measurement protocol. The CORDOVA-ET station was installed in February 2020 and has been moved twice. The first time in August 2020 and the last time in December 2020. The four nodes started

functioning in February 2020 together with the CORDOVA weather station. However, the nodes and the CORDOVA weather station paused and stopped sending data until it was reset again. These interruptions have happened many times throughout the last year. The CORDOVA weather station (Frogitt) seems to have a problem sending data from October 2020 onwards even if it works. Table 38 lists main points relating to the functioning of the CORDOVA ET Station.

Table 38 Status of CORDOVA-ET Station deployed at Berrechid site in Morocco.

Item	Installation date	Remarks
Frogitt Cordova Weather Station	August 2020	Many times, it stopped functioning between August 2020 and December 2020. The weather station is functioning but not sending data to Grafana from 2020-10-02
Node 1	August 2020	Not functioning only air temperature and RH sensors working
Node 2	August 2020	Not functioning. It was working for and temperature and RH, but, stopped 2021-01-29
Node 3	August 2020	Not functioning. Canopy temperature recording stopped on 29 Jan 2021
Node 4	August 2020	Not working well.

6.4. Data results, analysis and reporting

In general, the data reported from the Berrechid site during the measurement phase (season1, 2 and3) tells that only 43% of the season days had measurements in the L3 data (days when gaps were small, or measurements were on-going) with respect to CORDOVA-ET station. On the other hand, with respect to the eddy covariance approach and the energy balance approach, 99-100% of the winter season had measurements in the L3 data. The following detailed analysis is performed for the Berrechid site with respect to the different meteorological variables. For the ease of analysis, the ET and the associated variables were grouped into the clusters for analysis and discussion. While quantitative statistical comparisons were performed for ET variables, qualitative interpretations are given for other data clusters. Unlike in seasons 1 and 2, this site started reporting ET_EB in season 3 onwards using the measurements of energy balance components made by the Biomet system of the eddy covariance tower. Nevertheless, ET_EC will be invariably reported as the main estimate of this site obtained using the eddy covariance technique (high frequency windspeed and humidity measurements).

6.4.1. Potential Evapotranspiration (ETo)

The comparison between ETo estimated by the CORDOVA-ET Station (ETo_COR) as well as the one obtained using meteorological sensors mounted on the eddy covariance tower (ETo_SELF) are shown in figure 28. The CORDOVA-ET station was active in season 1, but discontinued operations during early season 2 and ceased functioning. As a new set of CORDOVA-ET station equipment was installed by late March 2021, the CORDOVA-ET measurements were rather limited in the season 3. Although the two estimates were comparable (ETo_SELF and ETo_COR), they were different with some systematic bias, particularly in season 3, rather than a random bias. This reflects the fact that there is some inconsistency in the measurements of some meteorological variable that are used to compute ETo using the simplified Penman-Monteith equation (FAO-56 method). Because ETo is a biophysical indicator that is computed only based on a combination of meteorological variables, a bad agreement between various estimates of ETo, reflects the fact that the same meteorological variables are being measured differently by different sensors based at this site and the data thus lack consistency. Thus, a meteorological sensor inter-comparison is recommended for this site. Details of the sensors determining the meteorological variables that were used to compute ETo_SELF are provided in the Annexure-I.

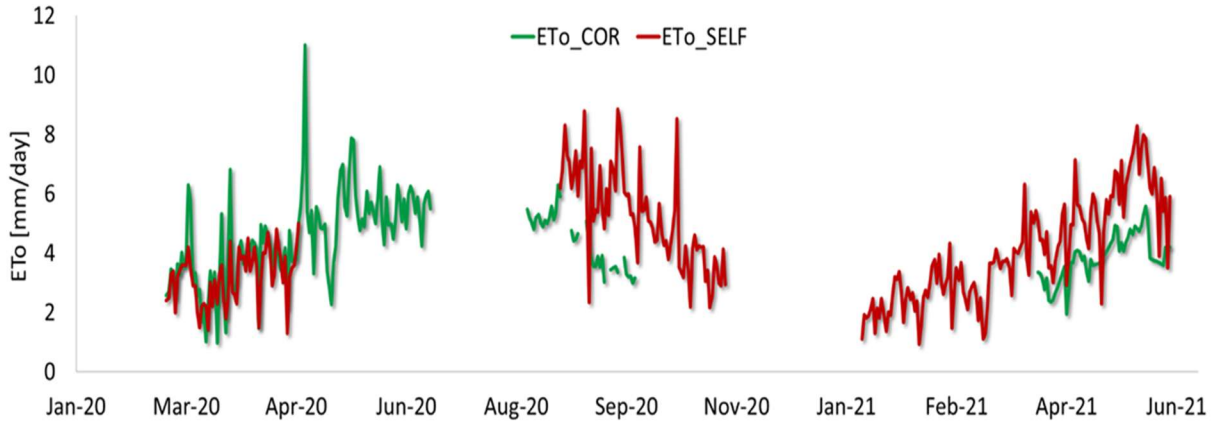

Figure 28 ETo measured at the Berrechid Site, Morocco, by CORDOVA-ET Station and inhouse approach.

6.4.2. Actual Evapotranspiration (ETa)

The comparison of the ETa at the Berrechid site, for season 1 and season 2 were done only for two ET methods. However, for the season 3 comparisons were done based on four estimates: [1] the CORDOVA-ET Station-based (ETa_COR), [2] eddy covariance approach (ETa_EC), [3] soil moisture depletion-based (ETa_SMD) and [4] Energy Balance based (ETa_EB). The general pattern shows that the estimates greatly differed although the temporal patterns were comparable. While ETa_SMD was highly underestimated in season 3 and overestimated in season 1, ET_EB and ET_COR were positively biased relative to ETa_EC. The magnitudes and trends of the two energy balance approaches (ET_EB and ET_COR) reflects the fact that there is a systematic error in the energy balance method. This is proved by the fact that ET estimated by these methods are unrealistically larger than ETo on these days. (fig. 29). One of the reasons for the differences in various estimates might be attributed to the differences in the footprints of the sensors of the two approaches. While the eddy covariance footprint is slightly dynamic (due to the prevailing wind patterns), the footprint of the CORDOVA-ET Station energy balance components is essentially circular depending on the height of sensors, assuming the fact that in the energy balance approach only 1D energy

fluxes are assumed. In season 2 and in season 3 the large magnitudes of ET_COR relative to ETo_COR (see Fig 28) makes us believe that there is some important fault in the manner in which some variables are sensed by the CORDOVA-ET Station and by the energy balance method, that is reflected in the ETa estimates. ETa should be smaller than ETo during these days when the vegetation is sparse (towards the end of growing season). One possible explanation is the underestimation of the sensible heat flux (H). This underestimated H component when deducted from Rn gives a larger LE, thus the overestimation of LE (or ETa). The underestimation of H can be manifold (either it could be due to the incorrect temperature differences or due to the incorrect estimation of ra).

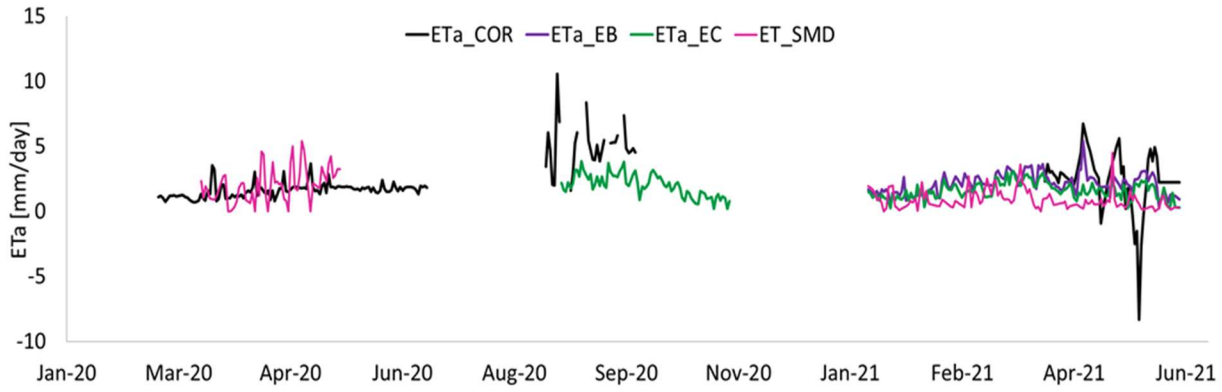

Figure 29 ETa estimated at the Berrechid Site, Morocco, by the CORDOVA-ET Station (ETa_COR) and the inhouse approach, Eddy Covariance (ETa_EC).

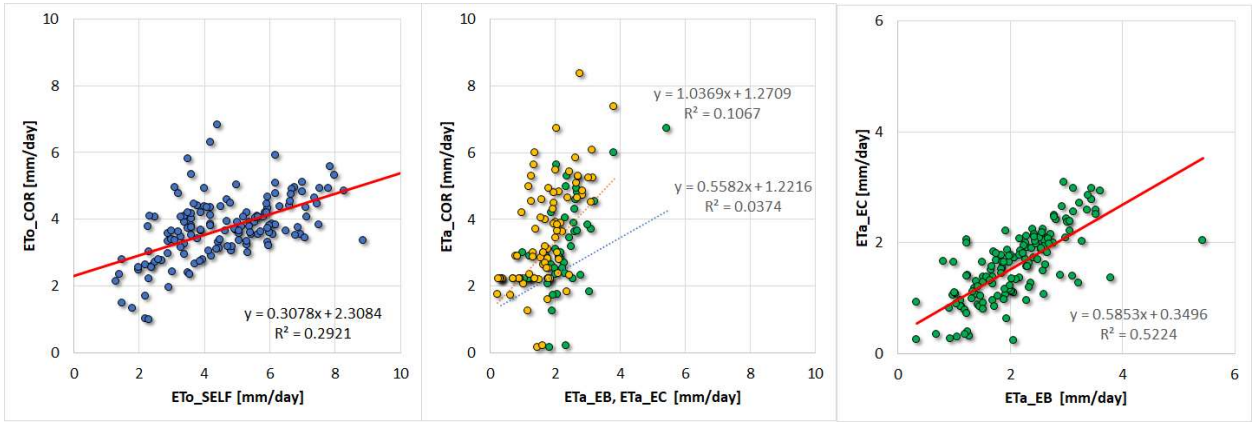

Figure 29b Statistical comparisons between the different estimates of ETo and ETa, respectively. A linear regression ($y=\beta_1 x+\beta_0$) was evaluated. R^2 explains the percentage of the variance in the dependent variable that the independent variables explain collectively.

6.4.3. Energy Balance Components

Analysis of the various surface energy balance components sensed at the site reflects the fact that the net radiation (Rn) was predominantly fluxed as latent heat flux (LE) rather than sensible heat flux (H) in the active vegetative phase of the crop. However, towards the end of the crop season, in summer, the Rn was mostly fluxed as H (fig. 30). There is a major problem in the magnitude of Rn for season-1 which combined with the unavailability of other energy balance terms makes it unrealistic. There seems to be an increasing trend in the season on Rn as the crop enter the summer season. There were days when the latent heat flux was ~70-90 W/m^2. The sensible heat at the Berrechid remained relatively smaller (50-75 W/m^2) on a daily basis reflecting the fact that the plot had adequate moisture. However, towards crop maturity, sensible hear flux increased to as much as 120 W/m^2. This is justified in the irrigation events as showed in the following panel where we see that frequent events were common at this site. The G also showed small but significant amount of energy flux (0-10 W/m^2). This is true on the days that overlapped with the irrigation events. This reflects the facts that assumption of G=0 in the surface energy balance as adopted by the CORDOVA-ET Station is not always reasonable to adequately capture the ETa signals.

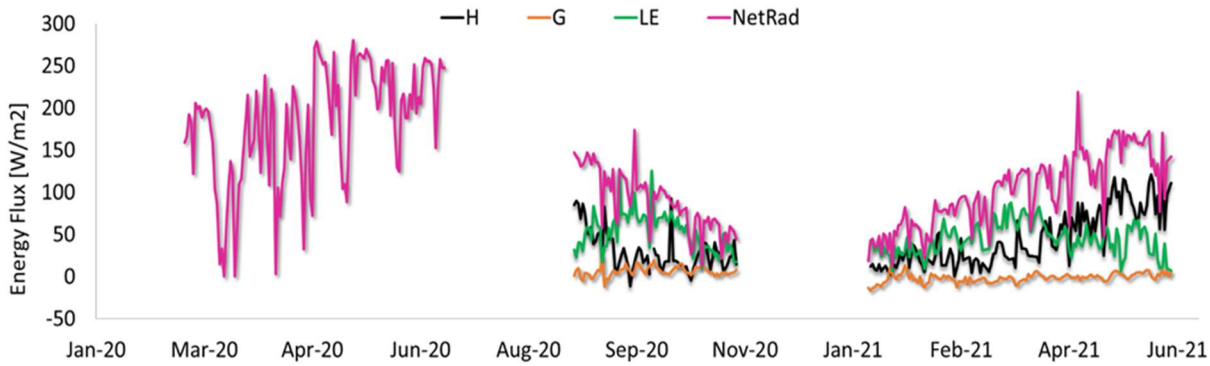

Figure 30 Components of the surface energy fluxes (H sensible heat flux, LE latent heat flux, G- soil heat flux along with Rn, the net radiation flux) at the Berrechid Site, Morocco.

6.4.4. Temperature Components

It can be observed from the data (fig. 31) that all the temperature components tended to increase in value towards the summer. The soil temperature remained larger than the air temperature across most parts ofn the crop season except for a few days towards the end of May 2021. In seasons 1 and 3 the temperature components were similar implying the dense nature of the canopy. In season 3, canopy temperature sensing commenced only towards the end of March and showed some unrealistic values as large as 33 degrees when the corresponding air and soil temperature were in the 20-degree range, a 15-degree bias. This has implications on ET retrieval by the CORDOVA-ET system, and it is recommended that the performances of these temperature be carefully checked. The reason for this could be due the incorrect alignment of the temperature senor (may be facing the soil instead of vegetation) or the faulty performance of the sensor itself. There are useful recommendations for deployment of infrared thermometers given in the papers by Gardner et al. (1992a,b). Citations for these are given in an earlier

comment. It would be worthwhile to explore how the IR sensors are deployed (view and azimuthal angles, number of sensors, etc.) in the CORDOVA-ET stations.

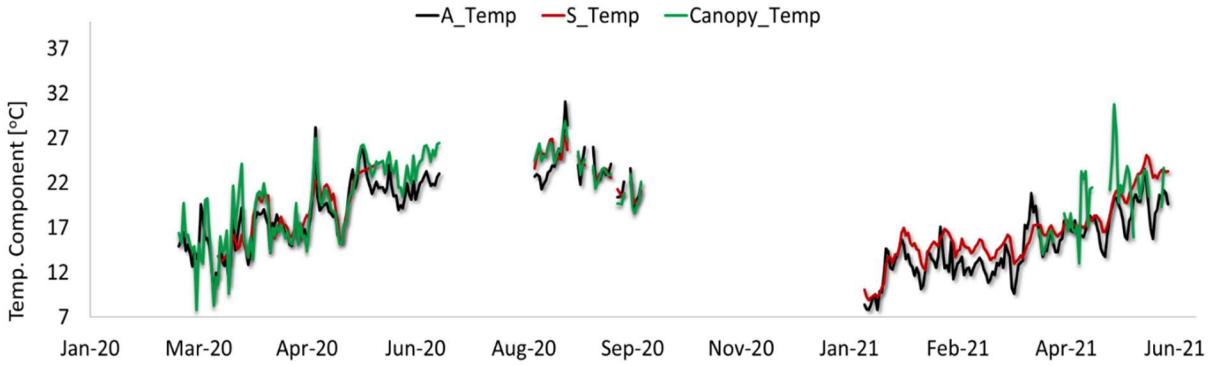

Figure 31 Temperature components at the Berrechid Site, Morocco.

6.4.5. Hydrometeorological Components

The hydrometeorological variables of various types were plotted together in a time series manner and analyzed (fig. 32). The patterns of these hydrometeorological variables were linked to one another. For example, on the 17th of May 2020 (season 1) and 5th of March 2021 (season 3), there were heavy precipitation events of ~40mm and there were corresponding increases in the atmospheric RH and the VSMC. It can be observed that the RH at this site fluctuated on a day-to-day basis and declining dramatically as the season approached summer. The summer is almost dry with no rainfall, and copious amounts of irrigation are needed to sustain the crop. The pattern of VSMC is good with the influx of water as rain or irrigation and realistically captures the influence of precipitation-ET trends and their influence on soil moisture. Overall speaking, the Biomet sensors seems to be working satisfactorily.

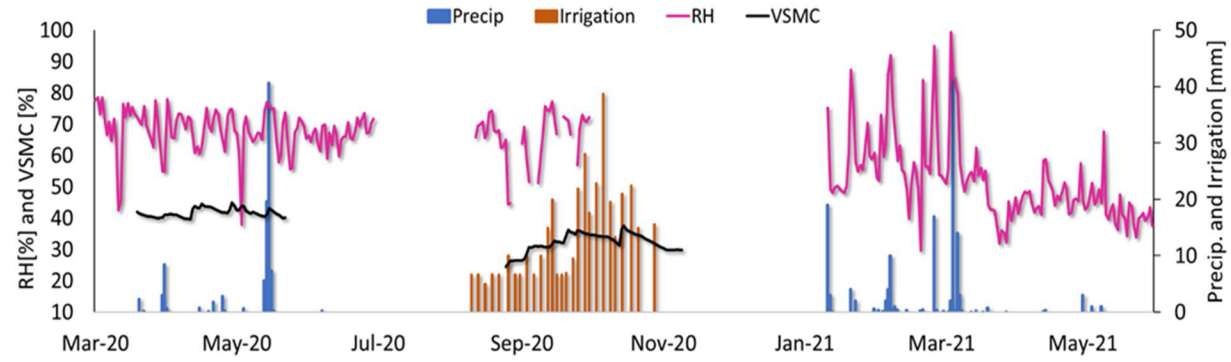

Figure 32 Hydrometeorological variables at the Berrechid Site, Morocco.

6.4.6. Pressure-Windspeed Components

The season-1 windspeed exhibited unlikely large magnitudes that require careful scrutiny. The atmospheric pressure pattern seemed to decrease slightly as the Summer season approached in late March and early April. Regional wind patterns as a function of surface pressure heterogeneities are however a large-scale phenomenon. We see that there were certain days even during the winter the windspeed was strong and the corresponding atmospheric pressure declined (e.g., 5th Feb 2021). Nevertheless, we see (fig. 33) slight indicators of pressure-wind relationships from the data collected. The location of Berrechid near to the coast is often influenced by weather systems and this may have an influence on the surface pressure patterns and hence the wind.

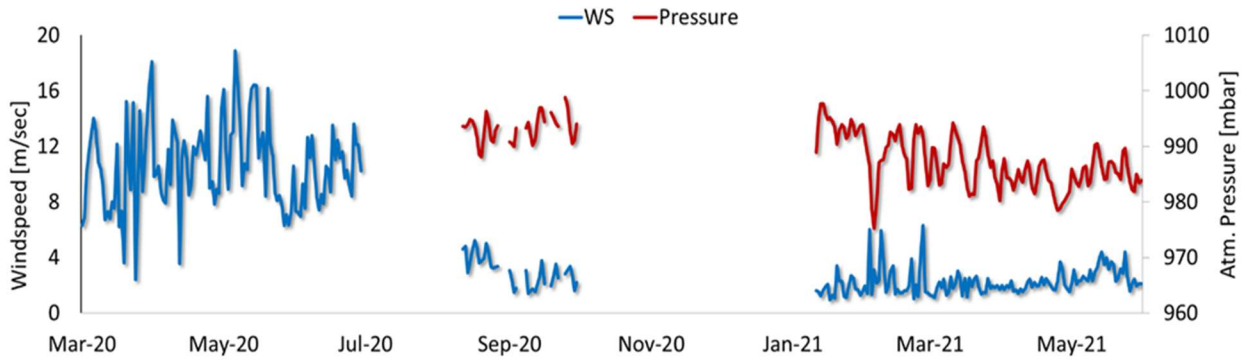

Figure 33 Pressure-Wind dynamics at the Berrechid Site, Morocco.

6.5. Brief data results discussion

1. ETo observations were comparable between ETo_COR and ETo_SELF but there remains a need to evaluate why magnitudes were different.

2. ETa,The ETa_COR showed spurious readings > ETo.

3. Energy Balance approaches (ETa_COR and ETa_EB) provided ETa values larger than those from ETa_EC probably due to the assumption of 1D energy flux in the EC system calculations and incomplete closure of the EB.

4. Towards the end of the crop season, canopy temperature greater than soil and air temperature was noted. What implications this has on ETa retrievals by ETa_COR needs to be deliberated.

5. ETa_EC may be considered as the standard calibration and validation data for of RS-based estimates.

6. The CORDOVA-ET station needs to be replaced with a new one with better functioning sensors urgently.

7. TUNISIA, the El Koudia Site

7.1. Location details

The field ET data were collected at El Koudia experimental station (36°32'47.83''N; 9°00'50.00''E, fig. 34) of the National Institute of Field Crops (INGC) located in the Governorate of Jendouba (Bou Salem Region) in northwest of Tunisia. The farm was equipped with an agrometeorological station. Several experiments on crop diseases and on evaluating new varieties are conducted. Within the framework of this project, an eddy covariance station was installed by the National Institute for Research in Rural Engineering, Water and Forests (INRGREF). The INRGREF team has several other eddy covariance sites across Tunisia and has a sound technical expertise in this methodology of ET determination. Conducting ET estimation at El Koudia station is a new task. As a result, this makes it necessary to gather additional information in order to obtain an agro-ecological characterization of the site with required information to interpret results. The field consists of sedimentary rocks from Mio-Pliocene and Quaternary. The average annual temperature is 18 °C, with the maximum temperature reaching 35°C (July - August) and minimum temperature of about 5-6 °C (December- -February). The average annual rainfalls are 542 mm/year. More than 70 to 75 % of the rainfall corresponds to the period between October and March. The lowest average precipitation is recorded in July with only 4 mm, while the highest values are recorded in December with about 83 mm. The site has a deep clay soil. The eddy covariance station and the CORDOVA-ET system were installed in a 2.4 ha plot (130 m x 185 m) located in the middle of the farm and planted with durum wheat during the winter season. The EC instruments and CORDOVA base station were placed in the middle of the plot with a distance of at least 62 m from the edge. The agrometeorological station was located in the northwest of the farm on a bare soil plot with a distance of approximately 7 m from the road.

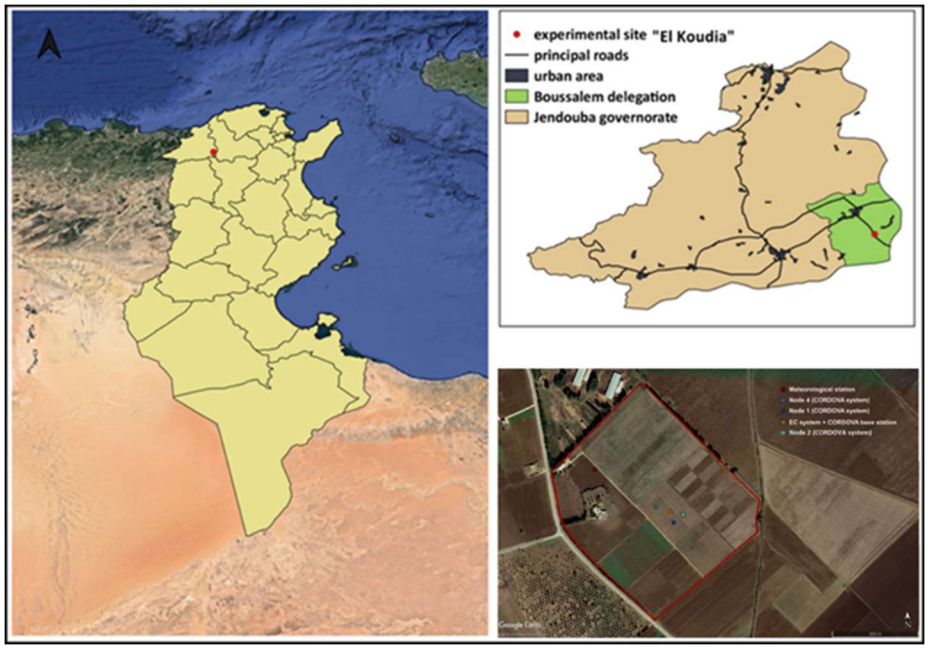

Figure 34 Location of the El Khoudia site (in the experimental farm station of INGC) in Tunisia where the eddy covariance and other facilities (CORDOVA-ET Station) are managed by the INGREF team.

7.1.1. People involved

Table 39 People associated with the El Khoudia site in Tunisia.

Team member	Position/ organization	Contribution
Rim Zitouna	Associate Professor/ INRGREF	INRGREF coordinator, data analysis and exploitation
Itidel Alaya	Engineer INRGREF	Instrumentation (CORDOVA-ET), field sampling and data handling
Zayneb Hammami	ICARDA Technician	Soil Moisture
Rim Louati	Technician/ INRGREF	Eddy Covariance system maintenance

7.1.2. Soil characteristics

The El Koudia soil belongs to a little-known soil class according to the Commission de Pedologie et de Cartographie des sols (CPCS, 1967) (Tunisian agriculture map). In order to have additional information on soil characteristics, fieldworks were undertaken in August. These measurements were planned before but were delayed due to COVID 19. Tables 40 and 41 show the results of soil analysis carried out at the INRGREF laboratory in November 2020.The site has a deep, non-saline (EC = 0.2 dS/m; pH=8), calcareous soil (total carbonate is 22.5% and active carbonate is 7.2%) with clay loam texture. The site soil has low organic matter (1.1%) and a high cation exchange capacity (16.0 meq/100g) according to the soil analysis conducted by INGC using the laser induced breakdown spectroscopy (LOGIAG).

Table 40 Physical properties of soil at the El Khoudia site in Tunisia (BD=bulk density; FC=field capacity; PWP=permanent wilting point).

Soil depth (cm)	BD (kg/m^3)	Field Capacity (%)	Permanent welting point (%)
10	157	23.60	13.00
20	173	22.50	10.80
30	176	21.80	10.80
40	179	21.80	10.70
50	165	23.40	11.70
60	160	23.70	11.30
70	164	22.90	13.00
80	155	24.70	12.60

90	168	21.80	10.50
100	172	22.90	11.20

Table 41 Chemical properties of soil at the El Khoudia site in Tunisia (EC=electrical conductivity).

Soil depth (cm)	Organic matter (%)	N (g/kg)	P (mg/kg)	K (g/kg)	pH	EC (dS/m)
20-40	1.1	1.5	18.1	1.2	8.1	0.2

7.1.3. Water characteristics

The field is located in the Bouhertma catchment area. Irrigation water is supplied with water from the Bouhertma dam at a rate of 5 L/s. According to the irrigation water analysis, performed at the INRGREF laboratory, the water is non saline with an electrical conductivity of 0.657 $dS.m^{-1}$ but with a high pH level of 10.5. No detailed studies have been conducted on the physico chemical properties of irrigation water at this site and will be undertaken in the future.

7.3. Crop cultivation and agronomic practices

The experimental site is located at Boussalem region known for the dominance of field crop cultivation. The main cultivated crops in this experimental farm during the winter season are durum wheat, faba bean, sugar beet and rapeseed using conventional or direct sowing methods. During summer, the fields are generally not cultivated due to irrigation water shortage. No irrigation was applied due to water problems in the summer but in winter it is predominantly rainfed. Glyphosate herbicide is usually applied during the sowing. Crops grown were a wheat crop in season 1 (Dec 3, 2019-June 23, 2020); maize crop in season 2 (July 19,2020-Nov 3, 2020); faba bean crop in season 3 (Dec. 19, 2020 – May 26, 2021) and sorghum crop in season 4 (Aug. 9, 2021 – Nov. 2, 2021. The full set of field agronomic practices during the four seasons (2020-2021) are described in the Table 42-45 below.

Table 42 Agronomic practices for the winter 2020 wheat crop at the El Khoudia site in Tunisia.

Operation	Date	Notes
Lands preparation	-	No Land Preparation applied
Planting (Wheat)	Dec. 03,2019	Direct sowing using a no-till drill 170 Kg/ha Durum wheat variety: Carioca
Weeds control	Feb. 26, 2020	Recommended herbicides application
Irrigation event	-	7. No irrigation applied (Rainfed cultivation)
Harvesting	June 23, 2020	

Table 43 Agronomic practices for the summer 2020 maize crop at the El Khoudia site in Tunisia.

Operation	Date	Notes
Land preparation	-	No Land Preparation applied
Planting (maize)	Jul. 19,2020	Direct Sowing using a no-till drill
Irrigation event sprinkler irrigation	August 24,2020 August 31,2020 September 4,2020 September 21,2020 September 25,2020 September 29,2020 September 30,2020 October 5,2020 October 8,2020	24 mm 24 mm 24 mm 24 mm 24 mm 24 mm 24 mm 24 mm 24 mm
Harvesting	Nov 3, 2020	

Table 44 Agronomic practices for the winter 2021 Fababean crop at the El Khoudia site in Tunisia.

Operation	Date	Notes
Land preparation	-	No Land Preparation applied
Sowing	December 18, 2020	Seed rate 130kg/ha Variety Najeh
Irrigation events	NA	Completely Rainfed
Harvesting	June 11, 2021	

Table 45 Agronomic practices adopted for the summer 2021 maize crop at the El Khoudia site in Tunisia.

Operation	Date	Notes
Land preparation		Direct sowing of sorghum
Sowing /Planting	August, 09 2021	45 kg/ha
Fertilizers		No fertilizer
Irrigation Events	August 90 mm September 120 mm	Sprinkler irrigation

7.3. ET Sensing Equipment and Allied Instrumentation

In late November 2019, an eddy covariance system was installed at the middle of the experimental plot. A CORDOVA-ET system (composed of a base station and two nodes) was mounted on the same field as well. The farm is equipped with an agrometeorological station that provides the data for ETo calculation. The relative placement of each station is shown in figure 34.

7.3.1. Eddy Covariance System

Although there were no active ETa monitoring activities in this site before, INRGREF recently acquired an eddy covariance system, and it was set up as per the standard protocols. A three-dimensional sonic anemometer, CSAT3 (Campbell Scientific, Inc., Logan USA) and a Krypton hygrometer, KH20, (Campbell

Scientific, Inc., Logan USA) were installed in December 2019 (36°32'47.9"N 9°00'50.1"E). The data were acquired and recorded at 20Hz frequency. The four components of solar radiation (incoming and outgoing short- and long-wave solar radiation) are sensed using a net radiometer (model NR01, Hukseflux, Inc., Netherland). Finally, soil heat flux was recorded using three heat flux plates (model HFP01, Hukseflux, Inc., Netherlands) at 1s then averaged and stored over 15 min. There is no historical data to characterize the turbulence of the site. The site used the standardized EC data processing and quality control protocol adopting the ECPACK software (Van Dijk et al., 2004). The coordinate rotation correction method was used to ensure that all the EC sites follow the same approach of processing EC data. Using the the four-energy component data, the balance 'closure' was analyzed at hourly and daily scales in the EC-data processing chain in the ECPACK procedure. In addition, quality control using integral turbulence test and stationarity test was employed. In order to obtain daily data for sensible and latent heat, and a gap filling using the EddyProc method was applied. Two datasets of daily ETa were calculated from the EC station; [1] ETa-EC for the eddy covariance station (observed latent heat), ETa-EB from the energy balance (ET deduced as the residual of the sensed Energy Balance components: Rn, H, and G).

7.3.2. CORDOVA-ET Station

On 23 January 2020, the CORDOVA-ET base station, the Froggit weather station and two nodes were installed at the site. The nodes were installed on a faba bean plot near to the wheat field. The system was composed of a commercial weather station (froggit, Germany) and multiple nodes connected to a base station and controlled using wireless communication. ETo was calculated from the commercial weather station data using the FAO 56 Penman-Monteith equation, while ETa is determined using the energy balance approach with the nodes' data. The base station and the weather station were mounted on the same mast (36°32'47.5"N 9°00'50.3"E) close to the Eddy Covariance system. The nodes "tn_001" (36°32'46.6"N 9°00'50.6"E) and «tn_004» (36°32'48.4"N 9°00'48.1"E) were placed to the sides of the base station with at least 40 m distance from the plot edge. Each node of the system integrated four sensors connected to a data logger that includes the Microcontroller Board, Pycom LoPy4. The sensors used were: [1] Air temperature and humidity sensor (model SHT35D, Sensirion, Switzerland); [2] Pyranometer: multi-spectral sensor (model AS7262, AMS AG, Austria); [3] Canopy temperature sensor, a non-contact infrared thermometer (modelMLX90614, Melexis NV, Belgium); and [4] Soil temperature sensor (model DS18B20, Maxim Integrated). The microcontroller sent the instantaneous data from the sensors to the "Things Indoor Gateway" in the base station using the LoRaWAN radio technologies. Then, the Indoor Gateway used a 4G modem Wi-Fi to connect to the IoT network (over the cellular telephone network).

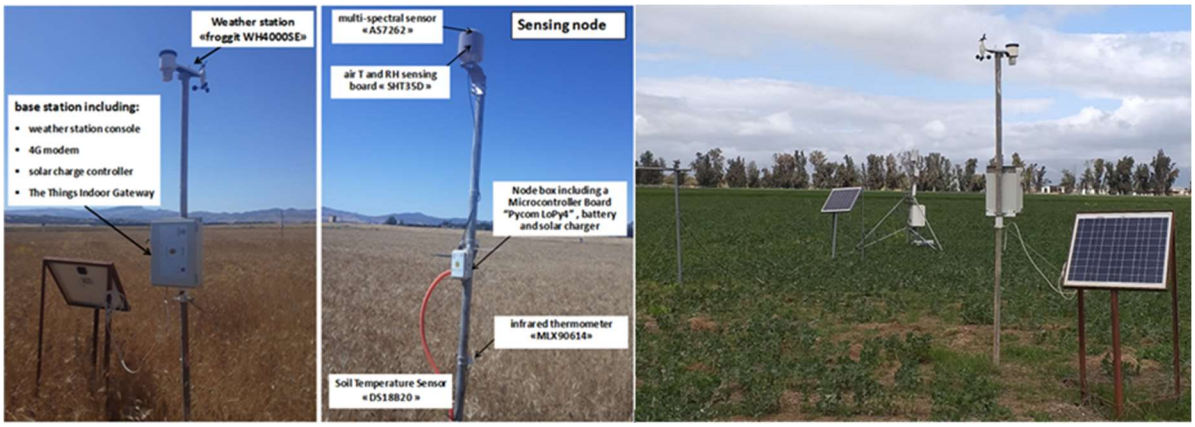

Figure 36 The location and the assembly details of the CORDOVA-ET Station at the El Khoudia site, Tunisia.

The Wi-Fi weather station «froggit WH4000SE» provides precipitation, air temperature and humidity, wind speed and direction, and solar radiation data. Both the Indoor Gateway and the weather station console use the 4G modem of the base station for internet connection and real time data upload. The data transmitted are stored in an open-source time series database "InfluxDB". The nodes and the weather station were operating normally during the first few hours on 23 January 2020. But due to a problem of connectivity between the nodes and the gateway, the base station was no longer sending data from the nodes. The Indoor gateway could not detect the nodes again until resetting them. The connectivity interruption was corrected with a new program for the microcontrollers. This program has led to a dysfunction of the pyranometers. The air T and RH sensors also are not working for all the nodes. During the first two week of installation, the system functioning was interrupted each day in the early morning due to low power. To avoid this problem, on February 4, 2020, the solar panel was changed with a larger one (50W). However, the site confronted the same problem from the summer season where the system shut down several times even after changing the base station battery with a new one. From late November 2020, the site has no access to the Froggit station data at the Grafana website.

Table 46 Current status of the CORDOVA-ET Station deployed at the El Khoudia site in Tunisia.

item	Installation date	Remarks /Condition
Weather station	January 2020	Data was not transmitting from the CORDOVA-ET server from mid November 2020. The problem was corrected after changing the station configuration on WS View on February 16, 2021. An update of the console firmware was carried out on April 20, 2021 to fix the gaps on GRAFANA interface
Node 1	January 2020	
Node 2	January 2020	Soil temperature sensor fixed and re-installed on January 6, 2021 Replacement of the solar charger node was done on April 1, 2021
Node 3	January 2020	Not operational during the current season
Node 4	January 2020	Canopy temperature sensor was fixed and re-installed on January 6, 2021.

7.4. Data results, analysis and reporting

7.4.1. Potential Evapotranspiration (ETo)

There was reasonably good agreement between the ETo estimated by the CORDOVA-ET Station (ETo_COR) and the on-site estimate of ETo calculated using the modified Penman Monteith equation (FAO56 approximation), or using meteorological variables measured at the Agromet station (ETo_SELF) (Fig. 36). In general, the seasonal dynamics of ETo from Winter to Spring to Summer to Autumn varied as expected during the four seasons in 2020 and 2021, implying the nature of atmospheric demand for evaporative flux from the land surface. This was primarily because of the seasonal changes in net radiation and the vapor pressure deficit of the atmosphere. The comparison between the two ETo estimates indicated that there was no real divergence between the two estimates in any part of the crop season. This reflected the good congruency in the manner in which the instruments at this site (Agromet station vs the CORDOVA-ET Station) estimated the values of various meteorological variables although the ETo_COR was available only for a brief period. Statistical analysis showed that ETo_SELF was 11 % larger relative to ETo_COR and the regression between the two estimates suggested that 99% of the variability could be explained between the two estimates, which is quite encouraging.

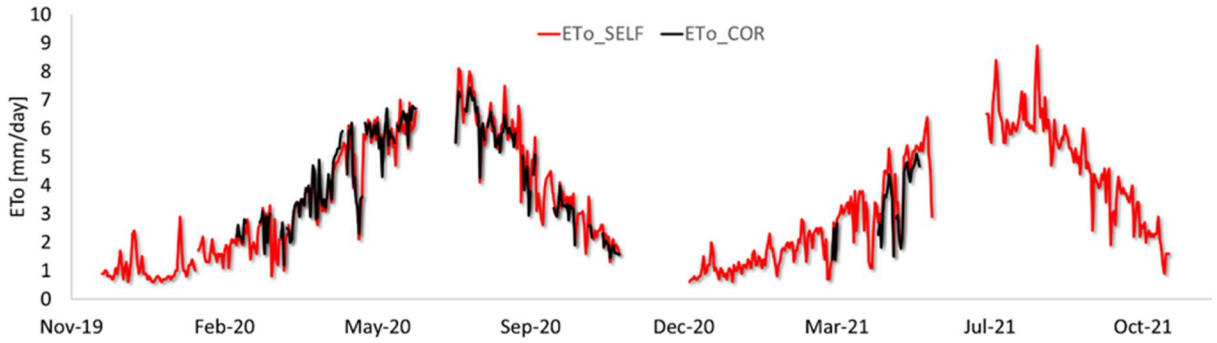

Figure 36 ETo determined at the El Khoudia Site, Tunisia, by CORDOVA-ET Station (ETo_COR) and on-site approach (ETo_SELF)

It has to be acknowledged that ETo is a biophysical indicator that is computed based on a combination of meteorological variables using the modified Penman Monteith equation (FAO56 approach or ASCE approach) and it is not surprising to have a good agreement between various estimates of ETo, which necessarily implies how well various meteorological variables are observed by sensors based on different systems. This analysis implies that the meteorological retrievals using various approaches were reasonably good at this site and that sensors/ instruments need not be cross calibrated at this stage.

7.4.2. Actual Evapotranspiration (ETa)

The comparison of the ETa retrievals at El Khoudia, based on three approaches imply relatively less congruency (Fig. 37) between the CORDOVA-ET Station (ETa_COR) and the two inhouse approaches [1] using eddy covariance approach (ETa_EC) and [2] using energy balance approach (ETa_EB). The temporal patterns of ETa_EB and ETa_EC agree but the magnitudes do not agree very well. In season 2 (summer), sudden decreases in ETa_COR were common, which is something we observed across all the sites, leading us to believe that there was some serious fault in the manner in which some variables were sensed by the CORDOVA-ET Station that was reflected in the ETa estimates. In the initial phase of the crop (between DOY 200-260), ETa_COR values were negative. This is theoretically impossible, and we can never get negative ET at a daily time step. In season 3, ET_COR agreed well with ET_EB, implying that the energy balance approaches agreed among themselves. However, looking at the magnitudes of the measured ETa, ETa_EC seemed to be more realistic in season 3, however in season 4, ETa_EC showed very small values although the crop was tall sorghum. There is a possibility that the tall crop have interfered with the eddy covariance system. This boils down to the question as to what was the vertical distance between the top of the crop canopy and the sonic anemometer/air temperature/humidity sensing system. The increasing difference between ET_EB and ET_EC as the sorghum grew indicates that this might have been part of the problem.

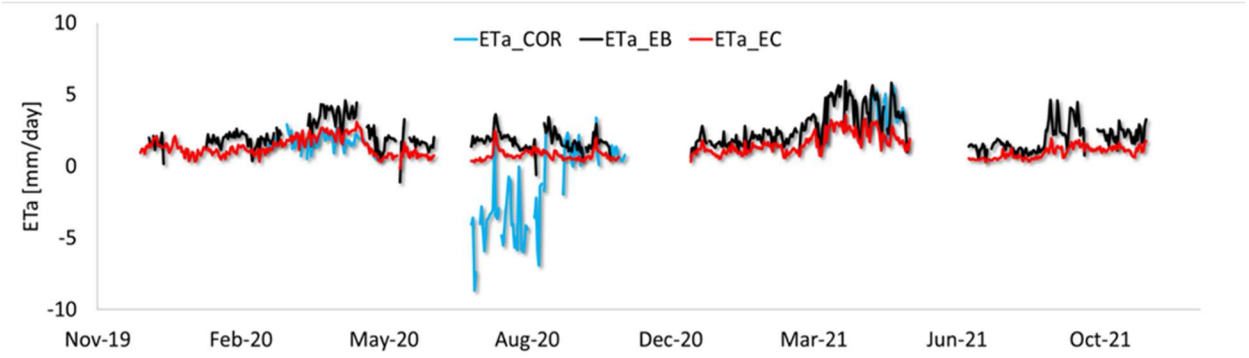

Figure 37 ETa determined at the El Khoudia Site, Tunisia, by CORDOVA-ET Station (ETa_COR) and inhouse approach [1] Eddy Covariance (ETa_EC) and [2] Energy Balance (ETa_EB)

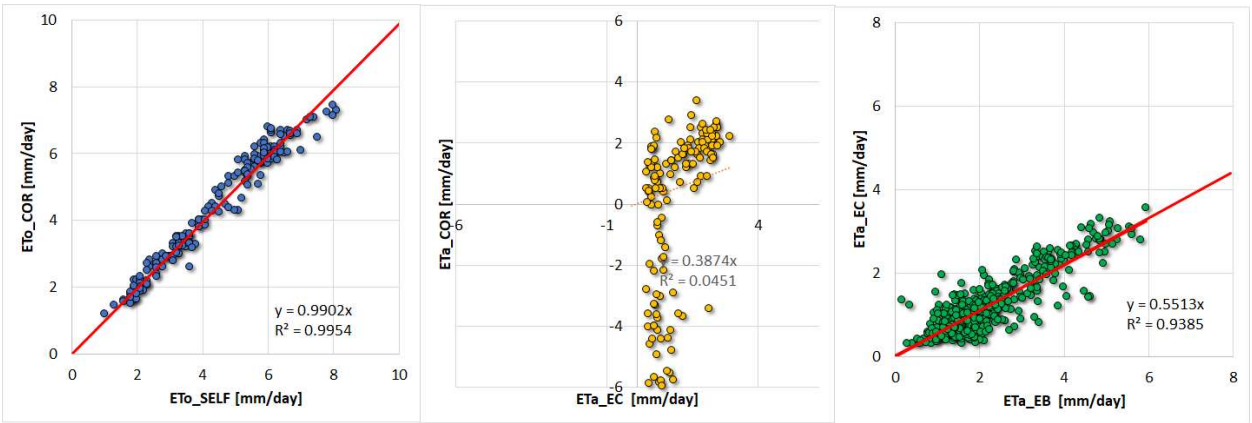

Figure 37b Statistical comparisons between the different estimates of ETo and ETa, respectively. A linear regression ($y=\beta_1 x+\beta_0$) was evaluated. R^2 explains the percentage of the variance in the dependent variable that the independent variables explain collectively.

This may apply to season 3 as well although faba bean does not get nearly as tall as sorghum. In season 3, the peaks and troughs were captured by both the approaches coinciding with the seasonal patterns. However, discrepancies in ETa_EB and ETa_EC is also significant and cannot be ignored in all the seasons. The differences may be slightly attributed to the differences in the footprints of the sensors of the two approaches. While the eddy covariance footprint is slightly larger and dynamic (due to the prevailing wind patterns), the footprint of energy balance components is essentially circular depending on the height of sensors, assuming the fact that in the energy balance approach only 1D energy fluxes are assumed. Nevertheless, the footprints should have been well within the cropped area. The assumption of energy balance component footprint to be circular may be also invalid because the sensible heat flux footprint follows the eddy covariance system footprint, and the sensible heat flux is a major component of the energy balance. Nevertheless, A careful diagnosis of the energy balance approach (ETa_COR and ETa_EB) is recommended for this site. Looking at the fact that ETa_EB was nearly always larger than ETa_EC, one would be justified in thinking that ETa_EC underestimated ETa. The energy balance closure should be carefully examined.

7.4.3. Energy Balance Components

Analysis of the various surface energy balance components sensed at the site reflects (fig. 38) the fact that the net radiation (Rn) was predominantly converted into latent heat flux (LE) rather than sensible heat flux (H) in El Khoudia during the active vegetation stages in all the seasons. Along the season, there was an increasing trend for Rn and H in the winter seasons (season 1 and season 3) and decline in the summer seasons (seasons 2 and 4), however, the LE showed seasonality congruent with the crop growth even if the crop was completely rainfed and no irrigation water was applied to the crop. It can also be seen that the LE showed increasing trends for a few days after the rainfall events (e.g. Mid-March 2020 and 2021, mid-April etc.). The G also showed a small but significant amount of energy. This was particularly true on the days that overlapped with the irrigation events. This reflects the fact that the assumption of G=0 in the surface energy balance as adopted by the CORDOVA-ET Station was not always reasonable to adequately capture the ET signals.

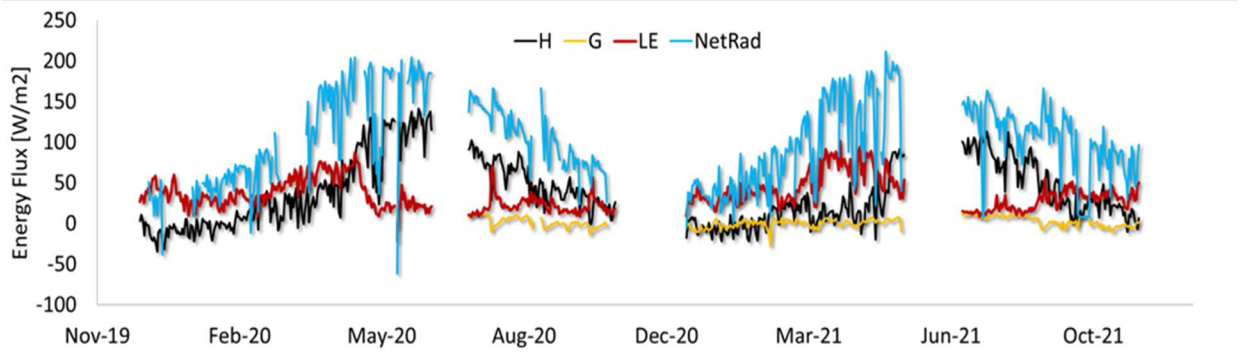

Figure 38 Components of the Surface Energy at the El Khoudia Site, Tunisia.

7.4.4. Temperature Components

It can be observed from the data that all the reported temperature components tended to increase from winter to spring to summer during the course of crop growth. At this site, in general, the soil temperature was slightly larger than canopy temperature on most of the days, but the differences were subtle. The reason for this could include the uniform spread of vegetation on the land surface or the decreased sensitivities of the microsensors. Nevertheless, the differences between the soil and canopy temperature were not conspicuous for this site, which warrants a careful examination of the canopy temperature sensor used by the CORDOVA-ET Station for calculating various process in the surface energy balance. It can be observed that the dramatic dip in the temperature on 17th February 2020 was realistically captured by all the temperature components and its influence on other micrometeorological variables was evident (see Figs. 36, 38, and 40).

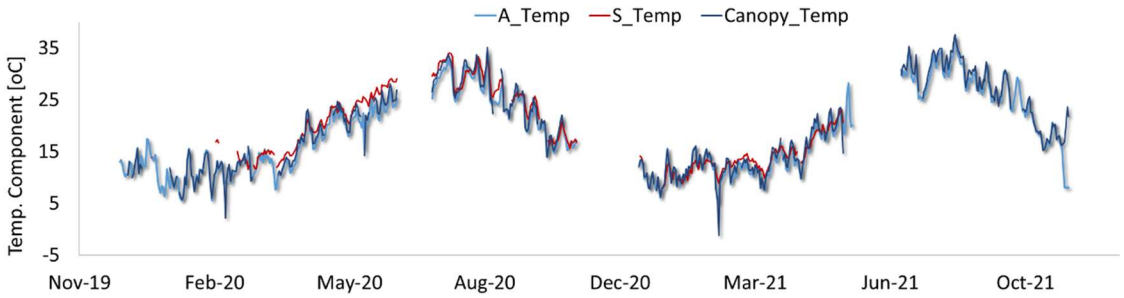

Figure 39 Temperature components at the El Khoudia Site, Tunisia.

7.4.5. Hydrometeorological Components

The hydrometeorological variables observed at the El Khoudia site during the four seasons 2020 to 2021 were plotted together and analyzed. It can be observed (fig. 40) that the RH at this site fluctuated on a day-to-day basis, showing an decreasing trend as the season changed from Winter to Spring to Summer, and towards the mid-summer the RH dramatically reduced. There were days during the winter when the RH was smaller which is plausible. The humidity of the atmosphere has a role in the evaporative process vis the drying power of the atmosphere. This has an implication on the ET probably via the lowered atmospheric demand for water resulting in ET reductions. The plot also shows the well distributed rainfall events implying that during the winter season, rainfed crops could be adequately cultivated. The soil moisture was lacking on a continuous manner at this site. It is strongly encouraged to monito VSMC in the subsequent seasons. Discussions with the country coordinator clarified that this site has been attempting to do soil moisture analysis using gravimetric approaches (which is tedious) and a TDR system at this site could provide continuous VSMC. This site is under severe water stress in the summer and the crop performance is often affected by inadequate irrigation possibilities. Thus, routine VSMC monitoring is vital.

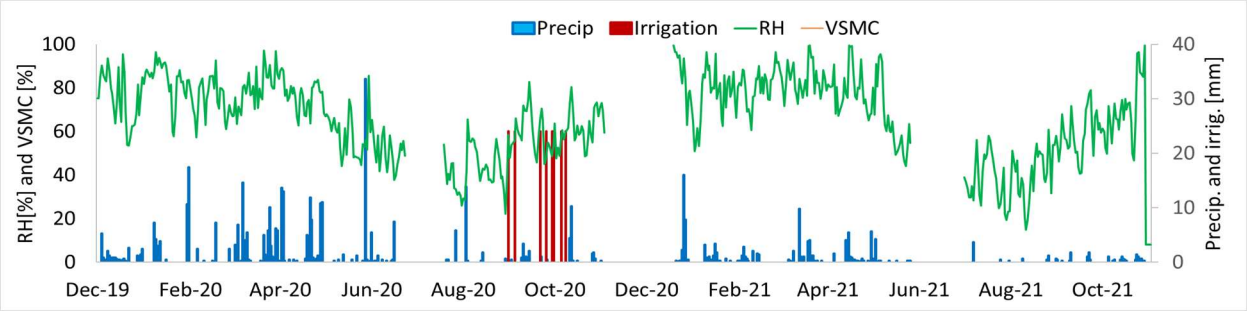

Figure 40 Hydrometeorological variables at the El Khoudia Site, Tunisia.

7.4.6. Pressure-Windspeed Components

The atmospheric pressure pattern seemed to decline slightly as the summer season approached in late April and early May and vice versa as the winter seasons approached. The windspeed observed did not follow a temporal pattern and was observed to be rather random (fig. 41). Regional wind patterns as a function of surface pressure heterogeneities is however a large-scale phenomenon. Nevertheless, we see slight indicators of pressure-wind relationships from the data collected. Wind affects ET via it influence on the biosphere-atmosphere coupling manifested via the aerodynamic resistance. The pressure affects the psychrometric constant calculation. Both of which are critical elements in the Penman Monteith equation. Accurate wind speed and pressure are vital micrometeorological variable

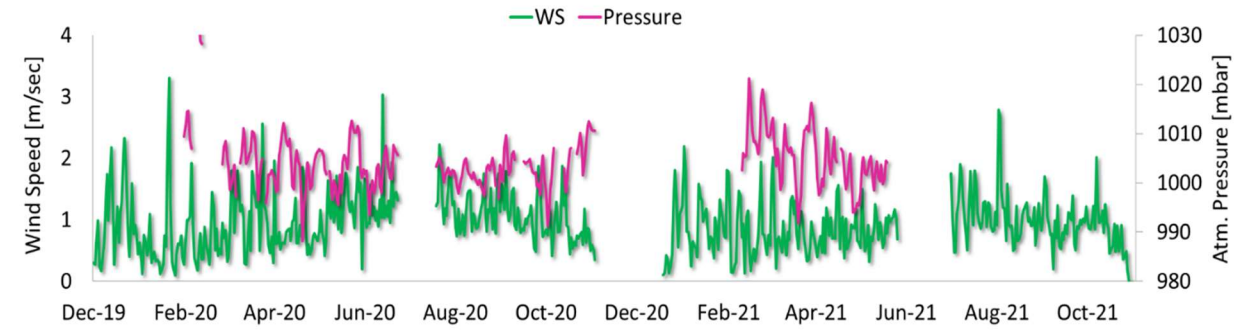

Figure 41 Pressure-Wind dynamics at the El Khoudia Site, Tunisia.

7.5. Brief data results discussion

1. ETo was realistically captured by the in-house approach (Agromet data) and with ETo_COR, but data of ETo_COR were sparse, which limits any conclusion.

2. For ETa, The ETa_EB showed realistic trends, but with larger magnitudes than ETa_EC . The performance of ETa_COR was uncertain due to the poor performance in season 2 and the lack of data points in seasons 1 and 3.

3. The sudden temperature drop on 17 Feb 2021 and 15 July 2021 and its impact is reflected in all the variables, which is a good sign.

4. ETa_SMD method may be established due to the availability of a new TDR system. Also, the biomet system of EC has VSMC that should be used to compute ETa_SMD.

5. The role of VSMC is quite important and its temporal analysis along with precipitation and irrigation (if applied) should be done in the next season.

8. Data Analysis and Lessons Learned

After completing the first phase of data acquisition during the four seasons and the subsequent data analysis, we learnt the following lessons that help us improve our understanding of the complexity of data acquisition, processing and reporting.

We started towards the end of 2019 with a lot of excitement by strengthening the instrumental capacities at all the sites. As season 1 ended, unfortunately the COVID-19 pandemic set in and this had a deep impact on our overall operations, which still continues (e.g., swift shipping of CORDOVA-ET systems). These include creating continued challenges in implementing observations from season 2 onwards in terms of lockdown, unavailability of technical staff to work on the ground, delays in procurement, shipment and replacement of faulty parts, delays in data acquisition and data processing and reporting. Even with these extraordinary challenges, we were able to get a solid set of datasets for season 3 that has been subjected to rigorous peer review and scrutiny by the Quality Assessment and Quality Control (QAQC) team at ICARDA. The quality of data acquisition and reporting has improved from season 1 to season 4. What we reported in the previous sections was an unbiased evaluation of the various ET (and the related) observations.

What was observed in seasons 1 through 3 was that retrieval of ETo is much easier and more reliable than determination of ET, across the sites and across all the methodologies. We observed that the CORDOVA-ET Station performance improved dramatically from season 2 to season 3, but again deteriorated in season 4. The improvements were noted especially at those sites where new instrumentation was deployed (e.g., Jordan) or where the site PI collaborated with UCO bilaterally to retrieve the data correctly (e.g., Lebanon). This boils down to the fact that constant replacement of CORDOVA-ET parts is essential, and the instrument has some durability issues with respect to the sensors. This is reflected in the nature of the measured data and the anomalies we saw while comparing with other estimates. We saw anomalous data patterns retrieved by CORDOVA-ET Stations and the energy balance approach in general (e.g., Morocco and Tunisia where ET was of unrealistically larger magnitudes) or rapid spikes when the vegetation was lower (e.g., Jordan, Lebanon). It can be concluded that, CORDOVA-ET was an acceptable method for ETo retrievals, however, it is still in a rapidly improving stage for ET. In the current form it needs a lot more effort in terms of: [1] proper functioning of various parts that can measure the necessary variables to compute ET; [2] need for proper data transmission mechanisms via the interface; and [3] need for auxiliary data, which, in the current situation demands extra effort from the user (e.g., canopy height). In the ideal situation, it should operate in a standalone manner and provide reliable estimates of ET without relying on the additional facilities for either gap filling or calibrating the system. The team is looking forward to building an active collaboration with UCO. It has to be acknowledged that ETo is a biophysical indicator that is computed based on a combination of several meteorological variables using the modified Penman Monteith equation (FAO56, Allen *et al.*, 1998, approach or ASCE approach). As it is merely a combination of several measured meteorological variables it is imperative to have a good agreement between various estimates of ETo, which necessarily implies how well various meteorological variables are observed by sensors based on different systems. If there is a discrepancy in ETo at any site, it implies that there is a need to cross validate the meteorological retrievals using various approaches and the instruments may need to be cross-calibrated.

It can be observed from the comparisons done in the four seasons that the results appear to have improved from one season to the other despite COVID19 related complexities. The striking characteristic of season 3 and season 4 was the decreased amount of data gap, which reflects the ability of the partners to do the gap filling of L1 in a robust manner. The availability of gap free data makes it possible to do seasonal calibration and testing of RS-derived ET estimates. We recommend the following ground-based estimates be used for RS calibration and testing activities. Egypt (*ETa_EB*), Jordan (*ETa_Lysi*), Lebanon (*ETa_SMD*), Tunisia (*ETa_EC*), Morocco (*ETa_EC*).

	Egypt	Jordan	Morocco	Tunisia	Lebanon
ETo_COR	25	89	61	36	88
ETo_SELF	97	85	76	99	88
ETa_COR	13	77	58	30	43
ETa_Lysi		73			
ETa_EB	88		38	83	
ETa_EC			59	98	
ETa_SMD	28	10	56		57
H	70	60	59	98	4
G	64	60	59	61	
LE	64	60	59	98	
Precip	75	89	98	100	96
A_Temp	84	83	82	100	100
S_Temp	76	71	70	59	95
Canopy_Temp	25	71	56	84	83
SW_In	66	60	18	86	45
SW_Out	55			86	4
LW_In	55			86	
LW_Out	55			86	
NetRad	70	60	93	86	
RH	75	83	82	100	100
VSMC	58	65	78	1	81
WS	98	83	82	99	100
LAI				2	2
NDVI				3	
Cnpy_Ht	4	9	41	6	8
Irrigation	1	58	26	1	4
Runoff					
Capillary					
Pressure	18	83	49	53	96

Figure 42 Data completeness matrix for the Season-3 across all the sites displayed as the percentage of the crop duration specific to each location. Grey shade represents those variables that are not measured at the site. The red tones indicate data that was not reported either due (1) inability to retrieve the variable from the CORDOVA-ET system (e.g., Lebanon) or (2) not reported at the discretion of the site PI as it was not mandatory. Note that Morocco had only measurements for 3 seasons and the % is calculated based on this.

The seasonal data submissions were subjected to a rigorous QA/QC based on the network protocols. Still, we were able to accumulate a good amount of data for inter-comparison and analysis at the L3 level. Nevertheless, we have acquired and archived the data at half hourly time step in the native (L1) and gap filled (L2) formats for future sub-daily analysis. We defined that a day qualifies for an L3 reporting only if that day has <10% of data gaps that facilitated robust temporal scaling to daily time step. The following figures shows the number of days reported at each site (or crop) for both ETo and ETa (related variables follow the same pattern). It can be generalized that on an average there were only 1-5% data gaps across the network (although there is variability across the site), which reflects the fact that things are in a good shape towards the end of season 4.

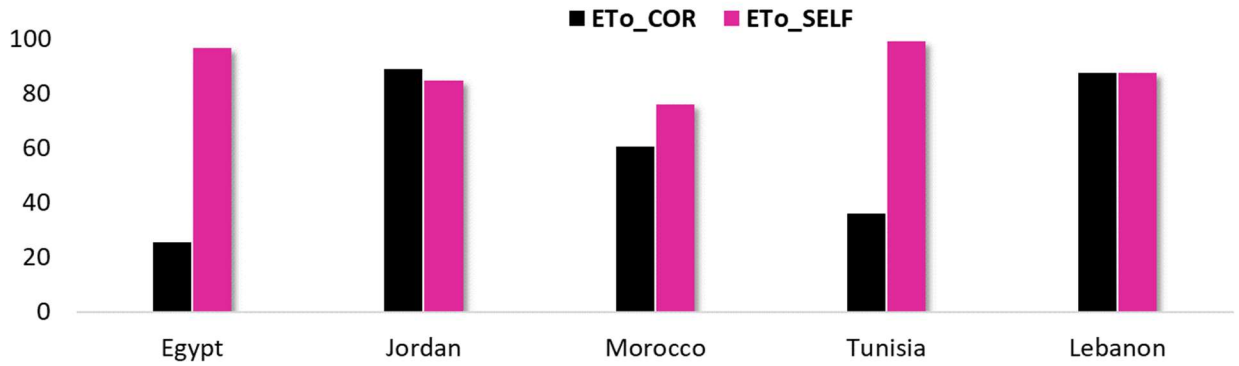

Figure 43 Comparison of the level of availability of high quality ETo measurements at the different sites as a percentage of the crop duration by the two different methods for Seasons 1-4.

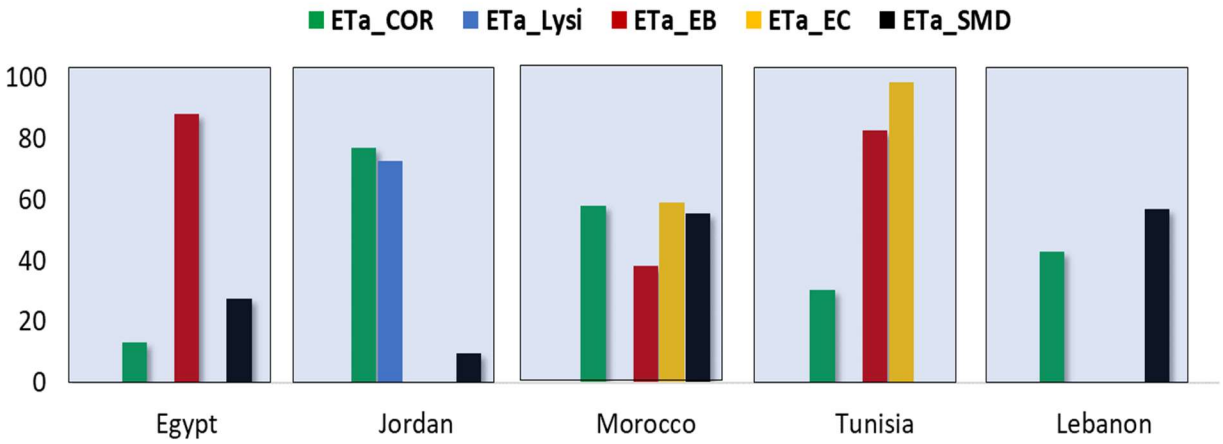

Figure 44 Comparison of the level of availability of high quality ETa measurements at the different sites as a percentage of the crop duration by different methods (ETa_COR, ETa_Lysi, ETa_EB, ETa_EC, ETa_SMD). We see that Morocco has the highest diversity of ETa estimates whereas Egypt has only a single method for Seasons 1-4.

9. Comparing actual evapotranspiration retrieved through various remote sensing-based models with field measured data

Actual evapotranspiration was measured for every country using the best estimation technique for that particular area. For each location, observed ETa data was retrieved for three seasons from December 2019 to May 2021. **Error! Reference source not found.** shows the month-wise exact span of the seasons. Season 3 and 4 had continuous and more data points (figs. 45 and 46) than seasons 1 and 2 for ground measured actual ET values.

Table 47: Month-wise classification of multiple crop seasons for all five study locations

Country	Season-1	Season-2	Season-3	Season-4
Egypt	Winter Wheat *(Dec 1,2019 – May 13, 2020)*	Summer Maize *(July 20, 2020 – Oct 21, 2020)*	Winter Wheat *(Nov. 25, 2020 – April 30,2021)*	Summer Rice *(June 16, 2021 – Oct. 20, 2021)*
Jordan	Winter Wheat *(Dec 25, 2019 – May 5, 2020)*	Summer Maize *(July 15, 2020 – Oct. 20, 2020)*	Fodder Vetch *(Jan. 13, 2021 – April 30, 2021)*	Maize *(June 14, 2021 – Sep. 9, 2021)*
Lebanon	Wheat *(Dec 7, 2019 – July 2, 2020)*	Potato- Fallow *(March 1, 2020 – July 31, 2020)*	Faba bean *(Dec. 3, 2020 – May 6, 2021)*	Maize *(June 17, 2021 – Oct. 8, 2021)*
Morocco	Maize *(Feb 23,2020 – July 3, 2020*	Beetroot *(Aug. 27, 2020 – Nov. 11, 2020)*	Durum Wheat *(Jan 11, 2021 – May 31, 2021)*	NA
Tunisia	Wheat *(Dec 3, 2019 – June 23, 2020)*	Maize *(July 19,2020 – Nov 3, 2020)*	Faba bean *(Dec. 19, 2020 – May 26, 2021)*	Sorghum *(Aug. 9, 2021 – Nov. 2, 2021)*

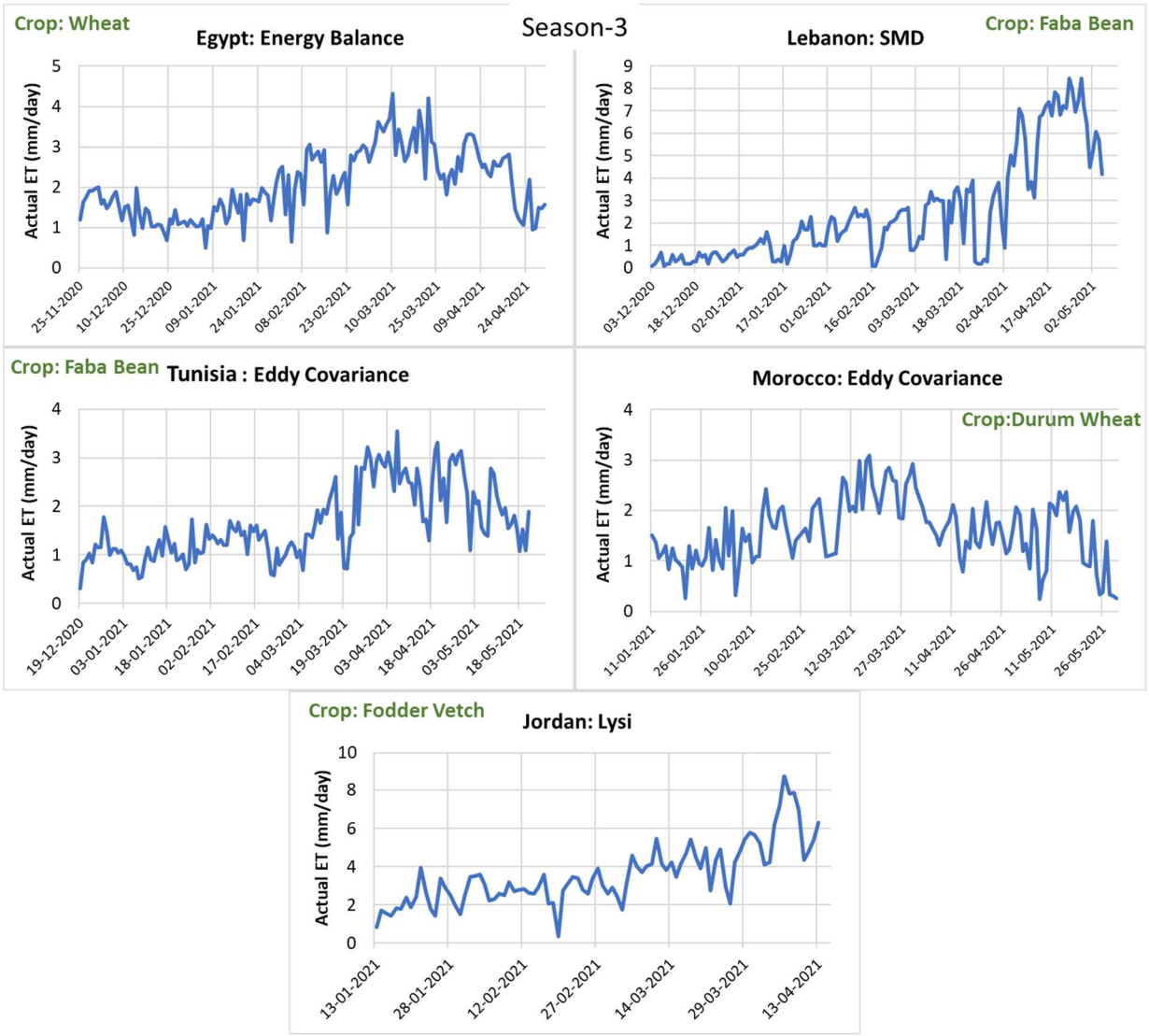

Figure 45: Ground measured actual ET plots for season 3.

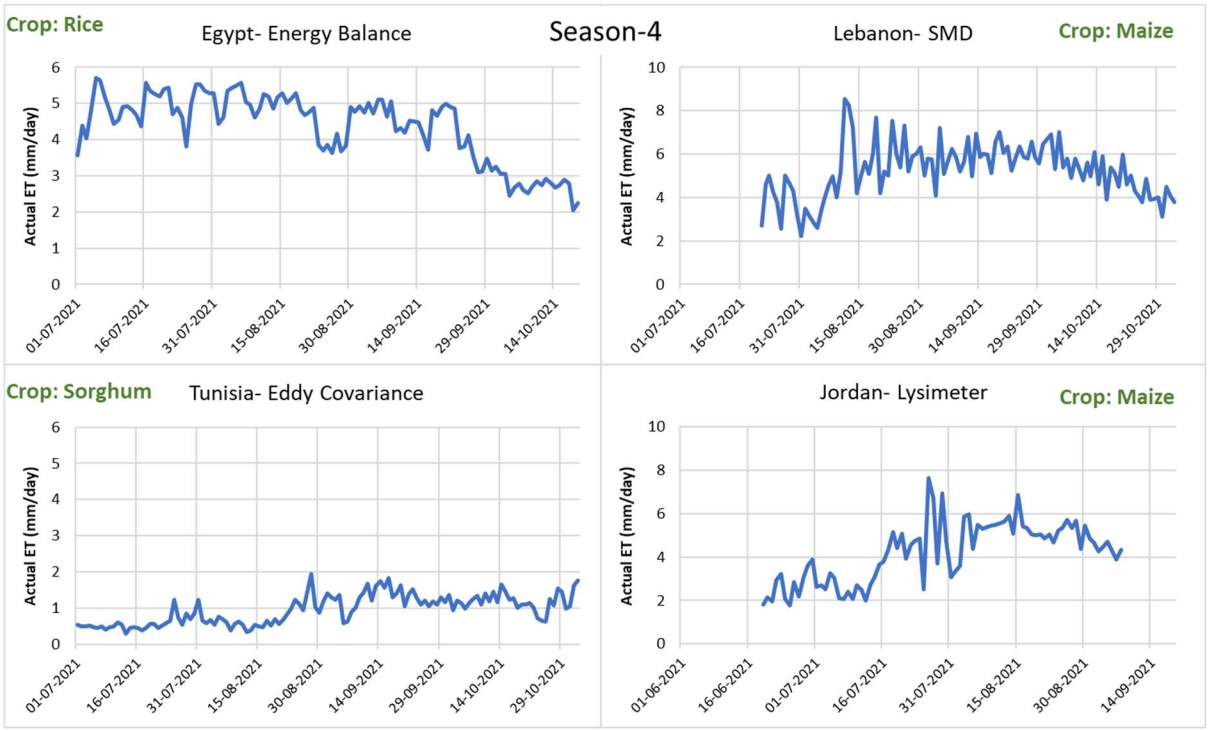

Figure 46: Ground measured actual ET plots for season 4.

9.1 Description of ET models and ETa data extraction

9.1.1 Water Productivity Open-access Portal (WaPOR)

The FAO developed WaPOR portal provides actual evapotranspiration data for continental to national levels (*WaPOR, FAO*). Sub-national level ETa data is for very few experimental locations at 30 meters spatial resolution. Continental ETa product is of 250 meters spatial resolution, and national level is of 100 meters. At present, the portal offers actual evapotranspiration and interception for decadal, annual, and monthly frequencies for Africa and Near East regions. For our comparative analytics, we used national-level products, which are available at a monthly frequency. This was the best dataset for study countries on WaPOR (available for download) as sub-national level products do not cover our study area sites.

As per the WaPOR portal's description, from January 2020 onwards, all the base input layers (NDVI, albedo and fAPAR) for 100 m products were derived from the Copernicus Sentinel-2 satellite data. Before this until December 2019, Proba-V satellite data was used for the same.

The WaPOR's ETa is based on the ET-Look model described by Bastiaanssen et al. (2012). Here, the ETa and interception is the sum of the soil evaporation (E), canopy transpiration (T), and evaporation from rainfall intercepted by leaves (I). The monthly total is obtained by taking the ETa and interception in mm/day, multiplying by the number of days in a decade, and summing the decades of each month. The broad approach for ET-Look (WaPOR) ETa computation is given in fig. 47.

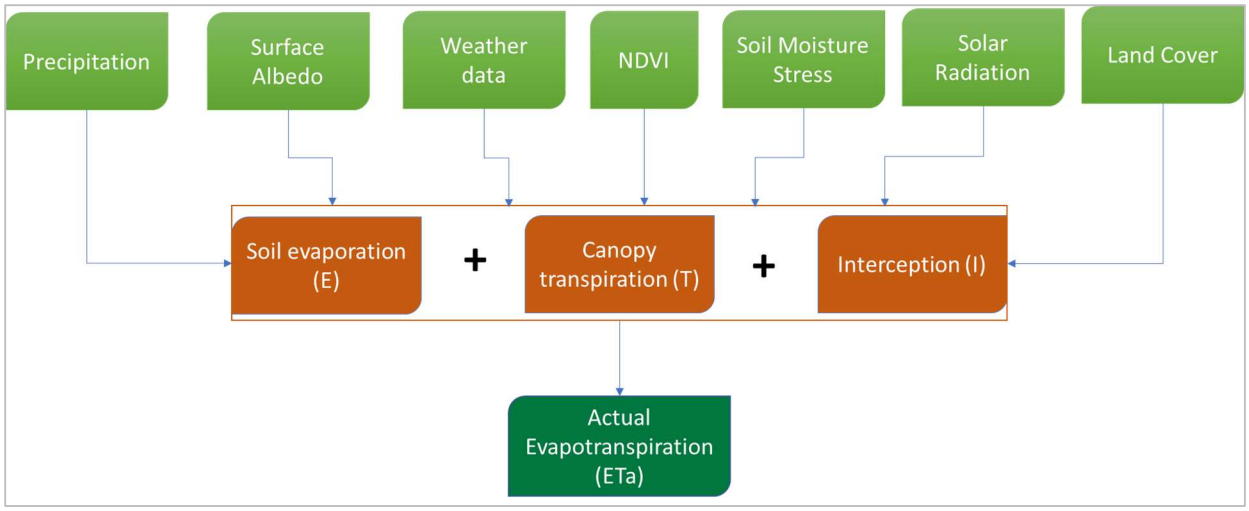

Figure 47: Brief indicative methodology for ET estimation using ET-Look model, ETa data available on Water Productivity Open-access Portal (WaPOR)

9.1.2 Mapping EvapoTranspiration at high-Resolution with Internalized Calibration (METRIC)

METRIC model was developed based on SEBAL (Surface Energy Balance Algorithm for Land) algorithm. SEBAL was proposed by Bastiaanssen et al. in 1998. The development of METRIC was started in 2000. Broad methodological steps are given in fig. 48. SEBAL was developed to model ET with minimum ground-based measurements. METRIC uses the alfalfa reference for calibration because of the near-maximum ET represented by alfalfa. The primary difference between SEBAL and METRIC is that the Reference ET is used to calibrate H and dT (near Surface Temp. Difference) in METRIC but not in SEBAL (Allen & Kilic et al.).

In this study, we downloaded the METRIC-based ETa using EEFLUX Google Earth Engine (GEE)-driven application. This platform uses Landsat 7 and Landsat 8 satellite data (30-meter spatial resolution) and its thermal bands (120-meter spatial resolution for Landsat 7 and 100-meter for Landsat 8). Due to the use of both 7 and 8 series, imagery is available at eight days intervals. The Landsat-7 data has stripped gaps. The EEFLUX GEE application allows users to download the ETa imagery for the area of interest. Then, using a GIS overlay, the pixel value of the point of interest can be extracted. The resolution of the ETa product is 30 meters.

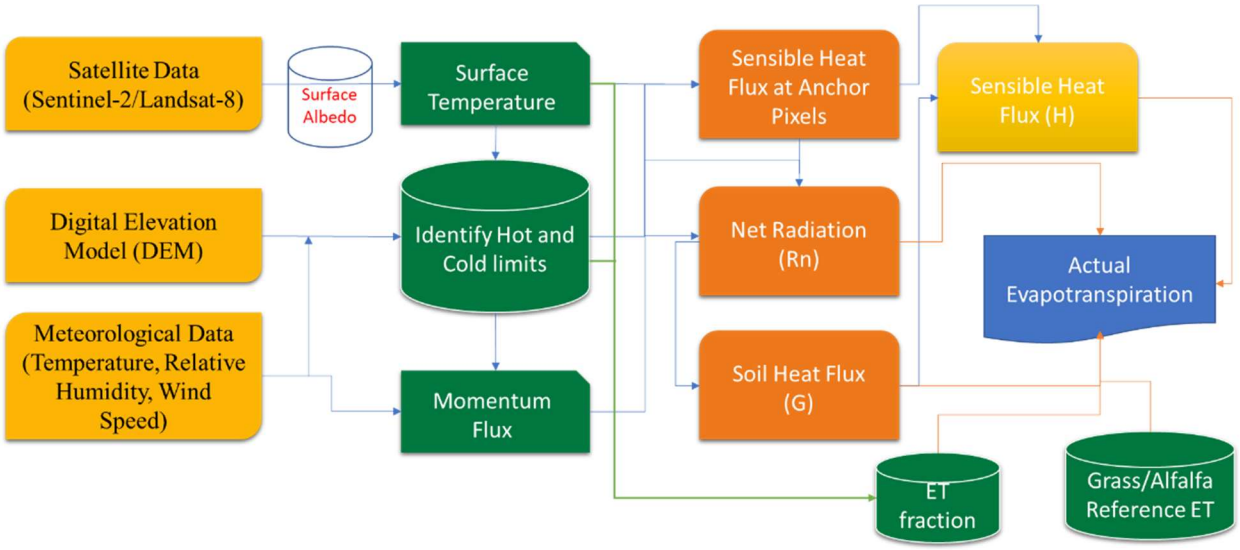

Figure 48: Broad steps for SEBAL and METRIC models

9.1.3 Surface Energy Balance Algorithm for Land (SEBAL)

A brief description of the SEBAL model can be expressed as given below-

$$LE = R_n - G - H \qquad \text{EQUATION 1}$$

where LE is the latent energy consumed by ET, Rn is net radiation (sum of all incoming and outgoing short-wave and long-wave radiation at the surface), G is sensible heat flux conducted into the ground, and H is sensible heat flux convected to the air. Energy absorbed into the canopy and photosynthesis is generally less than a few % and is ignored in the Equation given above (Allen et al., 2011).

The model was scripted in GEE (Figure49, 50) by utilizing Sentinel-2 satellite data of 10-meter spatial resolution and MODIS Land Surface Temperature (LST) of 100-meter resolution. The ETa produced by this model has a 10-meter spatial resolution. Note that the spatial and temporal resolutions of the three methods used were different, specifically 10 m, 30 m and 100 m spatial resolution at 5 days, 8 days and monthly frequency for SEBAL, METRIC and WaPOR respectively.

MODIS LST has a daily frequency and sentinel 2 series satellite data has a 5-day temporal resolution. Most of the time, we got only 2-4 (out of at least 6) sentinel-2 imageries due to cloud cover. This frequent availability of satellite data generates more probability of getting cloud free scenes compared to less frequent data. Land Surface Temperature (LST) at higher spatial resolution was obtained by downscaling MODIS LST through the disaggregation method. The approach suggested by Sánchez et al,2020 was tried to be implemented for the LST disaggregation. Although disaggregated to a lower resolution, there might be a variation in LST because of coarse pixel size. IT may impact ET values if there are a lot of variations in the LULC temperature due to different land use features. But We are mostly concerned with agricultural areas. That is a homogenous area, therefore, we didn't observe a higher degree of variation in LST values. With the help of MODIS LST and Landsat 7-8 combined LST, we intend to develop a 5-day interval interpolated LST product that we would utilize in our SEBAL Model to improve its efficiency. We are trying

to generate a 10-meter spatial resolution LST with 5 days frequency by interpolating the Landsat-7 and 8 LST. This may improve the efficiency of our SEBAL model.

This high spatial and temporal resolution based and SEBAL model derived RS-ET can be used for crop water consumption mapping at smallholder farmers' level.

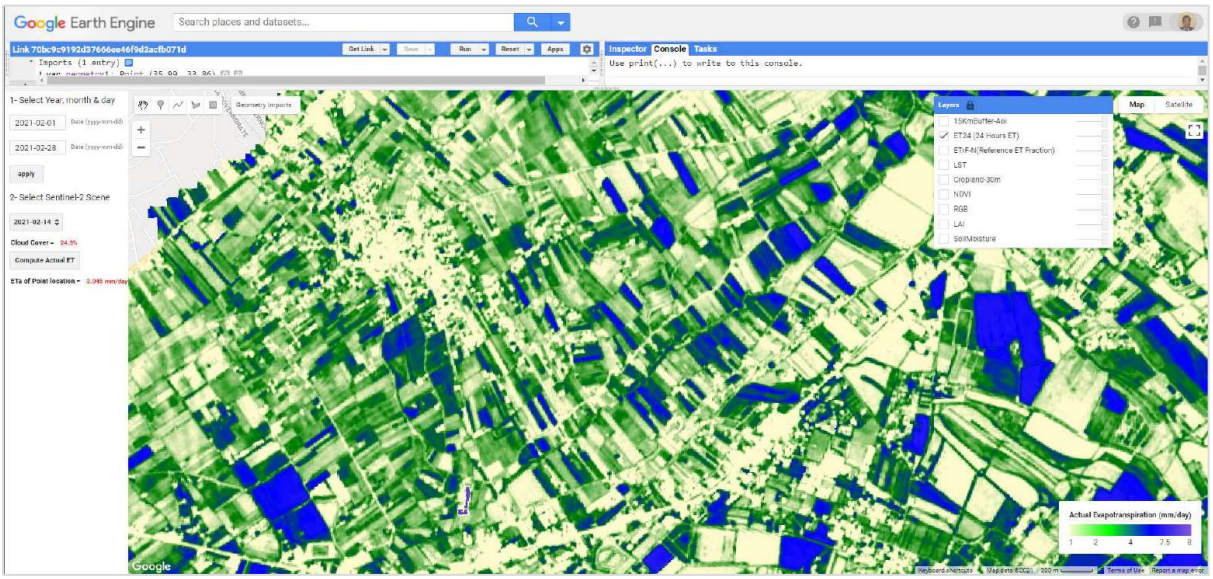

Figure 49: Screenshot of SEBEL GEE model

9.2 Remote Sensing based ETa Data extraction and arrangement

The ETa from the SEBAL model was extracted using the location point's pixel value extraction method. We also tried to extract SEBAL ETa using a 3x3 pixel window and a 9x9 pixel window. But a very little variation at decimal places was observed for the Egypt location. Therefore, the point extraction method was utilized throughout the analysis. Similarly, the location point's pixel value extraction was applied to obtain the METRIC ETa values. WaPOR enables a user to insert a latitude and longitude value of the point of interest, and then a time series can be generated by providing date ranges. Overall, all the RS-based ETa were extracted using the location point's pixel value extraction method. To break ETa data into daily ETa values, monthly (WaPOR ETa), 8-16 days interval (METRIC ETa) and 5-8 days interval (WaPOR) ETa values were divided by the number of days in a particular month. Though this method may not be exhaustive, it certainly provides an approximation of the daily values. We would try to interpolate data using a weather parameter or any other relevant parameter during the further study.

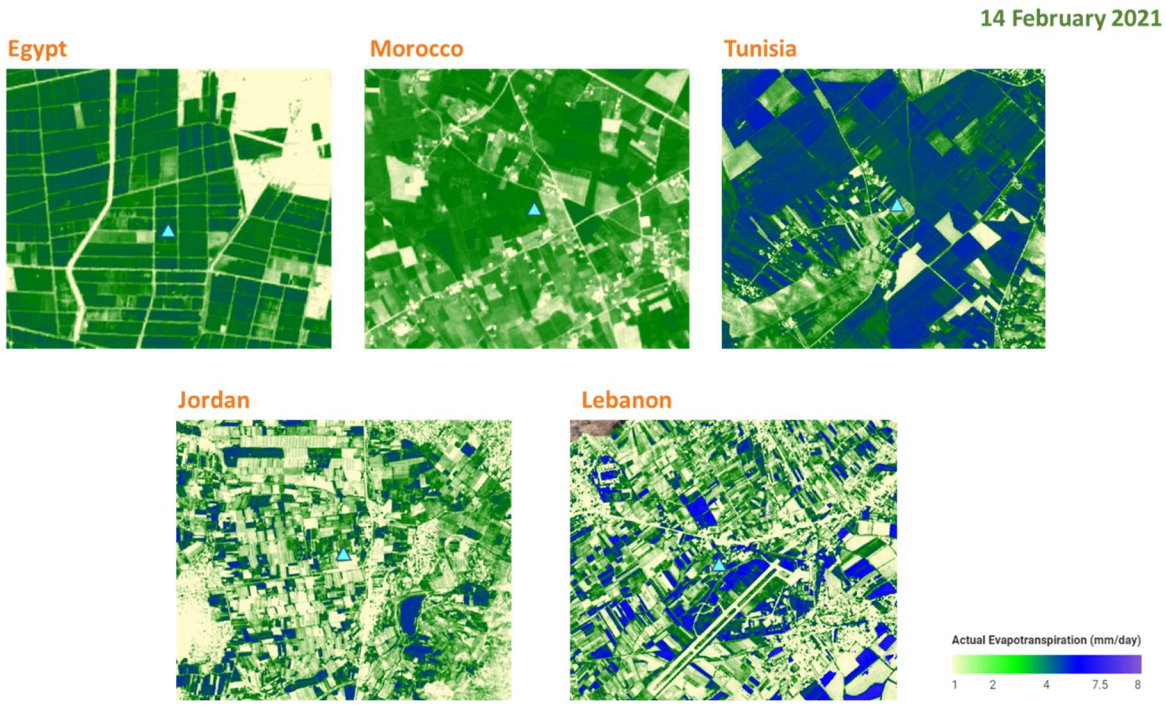

Figure 50: SEBAL GEE based actual evapotranspiration of study locations during peak vegetative stage of different crops during 2021. The triangle (cyan colored) depicts the field ETa observation site

9.3 Model performance indicators

The regression modelling generates coefficient of determination (r^2), which is not an exhaustive method to evaluate the model's efficiency. To evaluate the model's performance, we computed normalized Root Mean Squared Error (nRMSE), uncertainty/standard error, Ratio of Performance to Deviation (RPD) and index of agreement (d). The index of agreement (d) proposed by Willmott (1981) is considered as a standardized measure of the degree of model prediction error which varies between 0 and 1 (AgriMetSoft (2019)). The value of d near 1 shows the model's perfect agreement between observed and estimated values. Smaller values of RMSE & uncertainty and larger values of RPD and d reflect a model's high efficiency. Mathematically, these parameters can be explained as given below-

$$RMSE = \sqrt{\frac{\sum_{i=1}^{N}(Observed_i - Predicted_i)}{N}} \qquad \text{EQUATION 2}$$

$$Uncertainity = \frac{Std\ Dev}{\sqrt{N}} \qquad \text{EQUATION 3}$$

$$Uncertainity\ \% = \frac{\frac{Std\ Dev}{\sqrt{N}}}{max} \times 100 \qquad \text{EQUATION 4}$$

$$RPD = \frac{Std\ Dev}{RMSE} \qquad \text{EQUATION 5}$$

$$\textbf{\textit{Index of Agreement}}\ (d) = 1 - \frac{\sum_{i=1}^{N}(O_i - P_i)^2}{\sum_{i=1}^{N}(|P_i - \bar{O}| + O_i - \bar{O})^2} \qquad \text{EQUATION 6}$$

where O = Observed values, P = predicted/estimated value, N = count of data points.

9.4 Comparison of remote sensing-based ETa models with field measured data

To determine the efficacy and suitability of remote sensing (RS) based models, a detailed comparative analysis was carried out between each RS based model mentioned in this report and the observed ETa from field sites.

As mentioned in the model description section, the ET obtained from WaPOR was of monthly frequency. The ground-based ET (GB-ET henceforth) was of daily frequency for season-3 and roughly fortnightly for seasons 1 and 2. Here, to compare GB-ET with WaPOR ET, we used two approaches. In the first approach, we converted daily data to monthly data by summing all month days and comparing it to WaPOR ET. In another approach, to see the response and variability, we converted the monthly WaPOR ET data into daily data by dividing it by the number of days in a particular month and then comparing those daily ET values with GB-ET.

9.4.1 Remote Sensing-based ETa model-wise intercomparison for mutual satellite overpasses

The scatter plot depicting all locations in a plot for each model separately for each season and corresponding models' performance metrics were generated to identify the best modelling technique for ET estimation using remote sensing. Season wise plots, models' performance metrics and description has been given below. Here, this is to note that ground-based and RS-based ET values were selected for the dates of satellite pass only. As mentioned earlier, the RS-ET obtained from FAO's WaPOR is of monthly frequency. SEBAL based RS-ET was based on sentinel-2 satellite data. The frequency of the satellite image was 5 days and ET could be obtained at 5-day frequency except for the cloudy days. WaPOR monthly RS-ET data was scaled to the daily RS-ET using the daily reference ET of the respective locations. For daily WaPOR based ET generation, the monthly value of WaPOR based RS-ET was divided by the reference ET for that month. This output value was used for scaling the monthly ET to daily ET by multiplying it to the daily reference ET. The reference ET was calculated by site-specific weather parameters. For comparative plotting, the WaPOR derived daily ET values were obtained synchronized with the SEBAL ET dates because SEBAL ET dates are more compared to METRIC ET dates. This was done just to compare daily approximation of WaPOR, SEBAL and METRIC derived daily RS-ET (for the dates of satellite overpass only) with corresponding GB-ET. RS-ET values were compared with the ground-based ET values determined on the same day of satellite passing. METRIC based ET was also synchronized with SEBAL based ET dates, but a smaller number of values were obtained as METRIC is based on 8 days Landsat series satellite data and cloud cover during rainy season map widen the gap between two images. For Jordan, the least number of ET values can be obtained because here cloud-free satellite data were available for a smaller number of days compared to other study locations.

9.4.1.1 Observations for Season-1

For Season-1, scatterplots (fig 50) and models' performance metrics (This observation infers that soil moisture depletion (SMD) based ET estimation showed lowest correlation with the RS-Derived ET values as most of the RS based ET values were below the reference line. Both WaPOR and METRIC overpredicted the ET values whereas most SEBAL based ET values were observed to be near the reference line. Each RS-based model underpredicted the ET values for Morocco and Tunisia locations. ET values for Jordan generated poor R2 values using WaPOR and METRIC (0.03 and 0.15 respectively) compared to SEBAL (0.56).

*Table*48) were generated for all five study locations employing three RS-based ET estimation models. For Egypt's location, the largest R^2 (0.71) and lowest nRMSE (19%) were observed by using the SEBAL model. In fact, the SEBAL model generated the lowest nRMSE and better index of agreement (d) for each location. The overall nRMSE was the lowest for SEBAL compared to METRIC and WaPOR generated outputs. The overall RPD values were the best for SEBAL based ET followed by WaPOR and METRIC. The d values were largest for SEBAL followed by METRIC and WaPOR. The largest d value (near 1) denotes better agreement between ground-based and estimated data. The ET regression modelling for Lebanon showed the largest underprediction using all RS-based models.

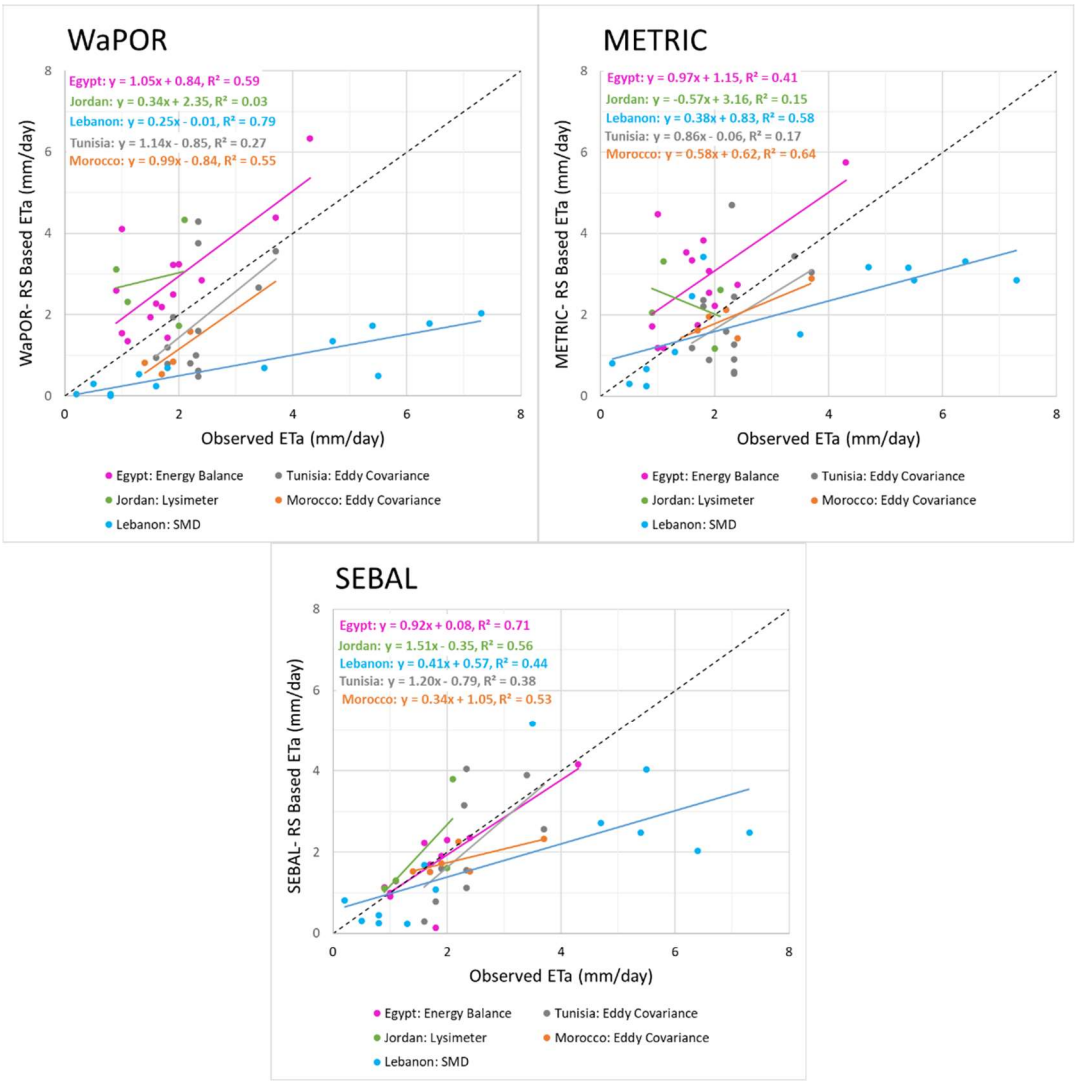

Figure 50: Model-wise intercomparison of RS-ET with observed ET for study locations for season 1. The dotted line represents the identity/reference line

This observation infers that soil moisture depletion (SMD) based ET estimation showed lowest correlation with the RS-Derived ET values as most of the RS based ET values were below the reference line. Both WaPOR and METRIC overpredicted the ET values whereas most SEBAL based ET values were observed to be near the reference line. Each RS-based model underpredicted the ET values for Morocco and Tunisia locations. ET values for Jordan generated poor R^2 values using WaPOR and METRIC (0.03 and 0.15 respectively) compared to SEBAL (0.56).

Table 48: Models' Performance metrics for Remote Sensing based ET Model's intercomparison analysis for season 1. Cells colored in green depicts the best model for the season based on nRMSE, d and RPD.

Season-1

Location	**nRMSE (%)**	**Uncertainty (%)**	**RPD**	**Index of Agreement**

		WaPOR		
EGYPT	44	8.5	1.1	0.71
Tunisia	51	9.9	1.1	0.51
Lebanon	88	2.7	0.3	0.41
Jordan	58	14.1	0.7	0.46
Morocco	40	6.1	0.9	0.30
Overall	56	8.2	1.1	0.37
		METRIC		
EGYPT	60	8.6	0.8	0.56
Tunisia	50	9.3	1.1	0.46
Lebanon	63	13.7	0.6	0.69
Jordan	110	8.8	0.5	0.27
Morocco	32	2.4	1.2	0.78
Overall	71	8.6	1.0	0.57
		SEBAL		
EGYPT	19	6.7	0.8	0.91
Tunisia	41	12.3	0.9	0.65
Lebanon	71	5.9	0.9	0.66
Jordan	27	5.8	1.6	0.69
Morocco	19	5.6	1.4	0.62
Overall	35	7.3	1.5	0.70

9.4.1.2 Observations for Season-2

For Season-2, both SEBAL and METRIC performed well in terms of small nRMSE and higher values of the d and RPD (*Table* 9). The largest d (0.88 for Jordan) was generated by the WaPOR model followed by SEBAL (0.87 for Egypt) and METRIC (0.84 for Jordan). Largest d was accompanied by smallest nRMSE and highest RPD values show better performance of the model for these locations. For the Lebanon location, SMD-based GB-ET was negatively correlated with RS-ET and generated negative d (Figure). Lower RS-ET efficiency was observed for the Morocco location too. SEBAL based RS-ET was the best correlation among all locations and all models for season-2. For Jordan, WaPOR followed by METRIC and SEBAL performed well as d is above 0.8 except for SEBAL (0.48). The correlation between GB-ET and RS-ET was the least for this season for the Morocco location. For Morocco location, ET values were observed of lower range (between 0 to 4) and the correlation between GB-ET and RS-ET was unexpectedly poor.

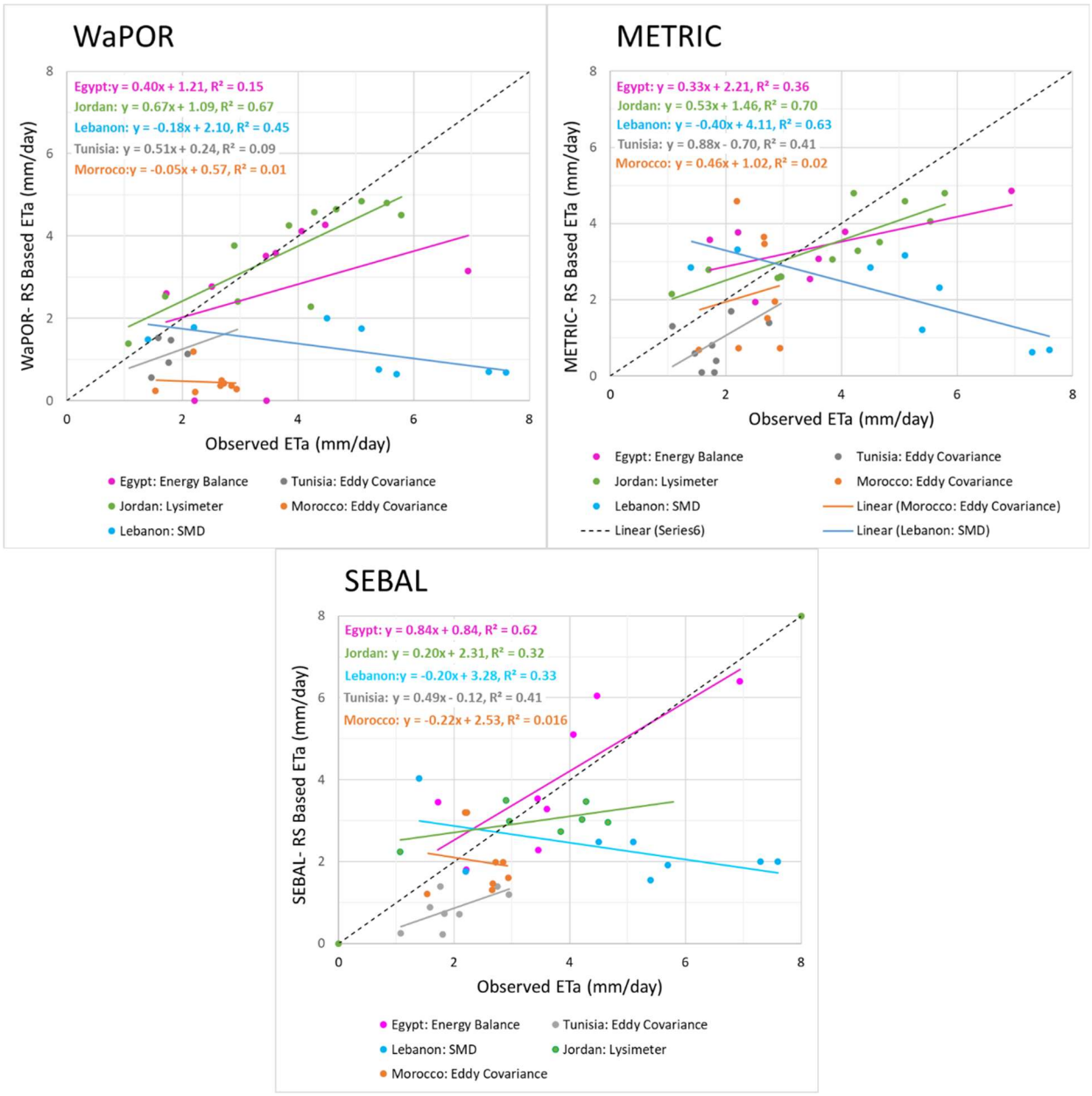

Figure 51: Model-wise intercomparison of RS-ET with observed ET for study locations for season 2. The dotted line represents the identity/reference line

ET observations were less in number for season-1 and season-2 compared to season-3 and season-4. For Lebanon and Jordan locations, lower ET values can be attributed to heterogeneous land cover features.

Table 49: Models' Performance metrics for Remote Sensing based ET Model's intercomparison analysis for season 2. Cells colored in green depicts the best model for the season based on nRMSE, d and RPD-

Season-2

Location	nRMSE (%)	Uncertainty%	RPD	Index of Agreement
		WaPOR		
EGYPT	71	7.7	0.9	0.49
Tunisia	84	6.0	0.2	0.16
Lebanon	90	2.7	0.1	-0.18
Jordan	22	6.5	1.8	0.88
Morocco	85	3.8	0.2	-0.01
Overall	70	3.2	0.8	0.38
		METRIC		
EGYPT	38	5.2	0.7	0.67
Tunisia	57	9.4	0.7	0.48
Lebanon	83	5.2	0.3	-0.71
Jordan	24	5.0	1.7	0.84
Morocco	60	18.5	0.3	0.14
Overall	52	3.2	1.0	0.40
		SEBAL		
EGYPT	26	8.6	1.6	0.87
Tunisia	63	5.6	0.4	0.30
Lebanon	75	3.6	0.2	-0.35
Jordan	28	2.8	1.4	0.48
Morocco	42	9.6	0.5	0.21
Overall	47	3.2	1.1	0.49

9.4.1.3 Observations for Season-3

For Season-3, the GB-ET data was better compared to previous seasons. In this season, SEBAL outperformed the other two RS-ET models (*Figure*). The SEBAL was followed by METRIC and WaPOR. Overall, a larger coefficient of determination values was observed. RS-ET generated by SEBAL was the nearest to the reference line. This itself tells that SEBAL outperformed other two models. SEBAL showed the larger d for Lebanon followed by Egypt. The SEBAL and METRIC estimated RS-ET satisfactorily for all locations but the highest accuracy was observed for Jordan followed by Egypt as smaller nRMSE & uncertainty values and higher RPD values were observed (

Table). Unexpectedly SEBAL performed poorly in the prediction of RS-ET for Tunisia where both d and RPD were smaller (0.32 and 0.6) and comparatively higher nRMSE (50%). For Lebanon, both WaPOR and METRIC underpredicted the RS-ET. Underprediction of RS-ET for Lebanon was larger for WaPOR compared to METRIC followed by SEBAL. This underprediction can be attributed to the coarse spatial resolution of the WaPOR model. WaPOR predicted RS-ET value for Tunisia with higher accuracy compared to METRIC and SEBAL. For Jordan, the largest r^2 and RPD values were observed throughout the seasons. Though d was comparatively less, the nRMSE was exceptionally low (10% only). That can also be seen in the SEBAL plot of *Figure* where most of the ET points are located near the identity line.

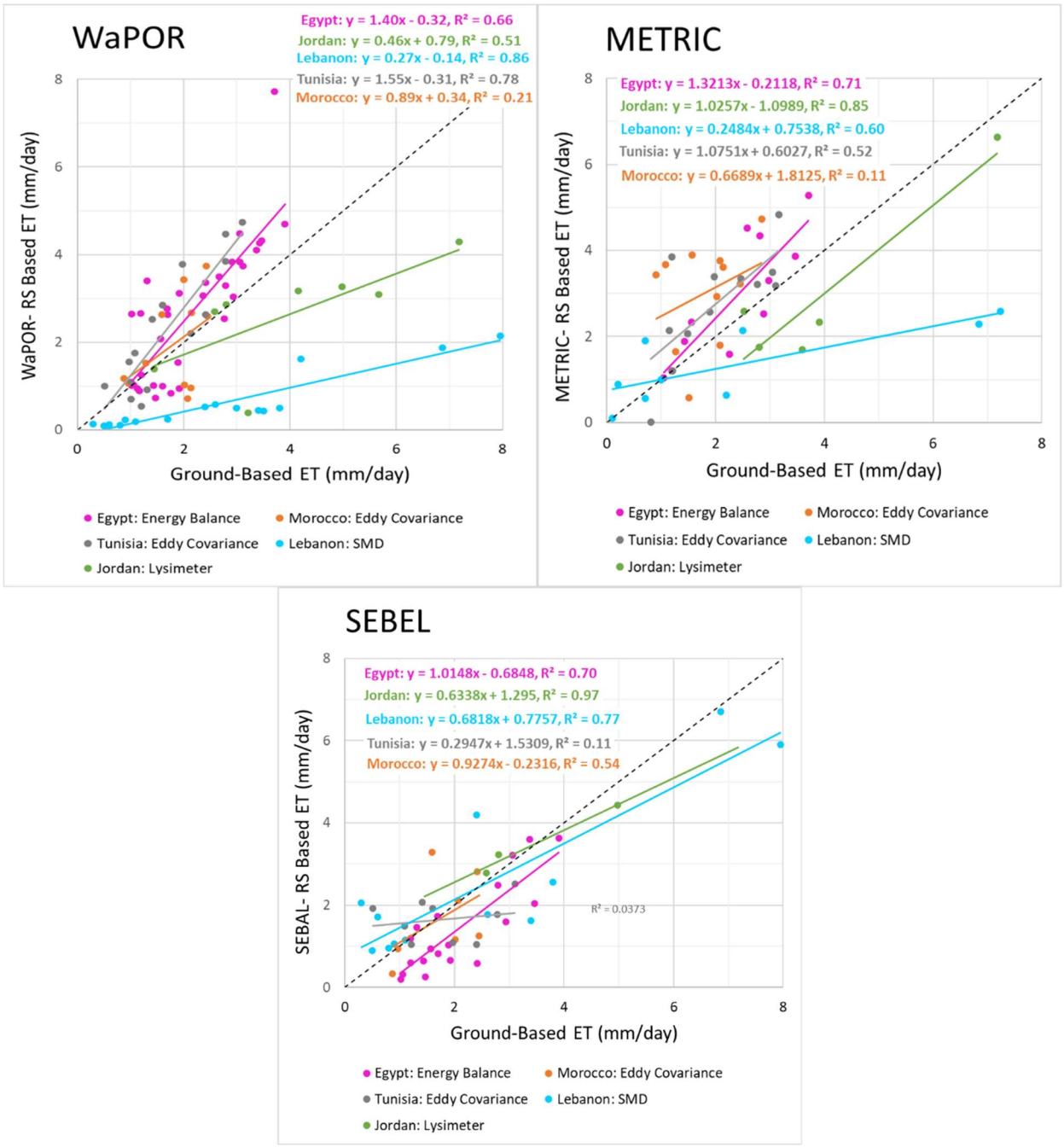

Figure 52: Model-wise intercomparison of RS-ET with observed ET for study locations for season 3. The dotted line represents the identity/reference line

Table 50: Models' Performance metrics for Remote Sensing based ET Model's intercomparison analysis for season 3. Cells colored in green depicts the best model for the season based on nRMSE, d and RPD

Season-3

Location	nRMSE (%)	Uncertainty (%)	RPD	Index of Agreement
		WaPOR		
EGYPT	40	3.5	1.8	0.78
Tunisia	58	7.5	1.4	0.79
Lebanon	97	8.1	0.3	0.42
Jordan	46	10.0	1.0	0.63
Morocco	51	4.4	0.6	0.53
Overall	60	6.7	1.0	0.61
		METRIC		
EGYPT	41	8.3	1.5	0.82
Morocco	91	7.7	0.7	0.25
Tunisia	56	7.7	1.1	0.69
Lebanon	108	11.5	0.3	0.56
Jordan	31	13.9	1.7	0.88
Overall	66	3.1	0.9	0.65
		SEBAL		
EGYPT	40	7.0	1.3	0.81
Morocco	44	12.3	1.4	0.59
Tunisia	50	7.3	0.6	0.32
Lebanon	44	8.5	1.6	0.94
Jordan	10	11.1	2.0	0.59
Overall	41	3.1	1.5	0.89

9.4.1.4 Observations for Season-4

For Season 4, we received data from four locations except Morocco. The data from Morocco location was not obtained because farmer did not plant any crop and they decide to move the station. Our SEBAL model is based on ERA-5 Land hourly climate data. This data is available till September 29, 2021 (last checked on 12th December 2021). Therefore, we didn't extract October month's RS-ET values for all locations by all models. During this season larger ET values were observed for the Egypt location whereas smaller ET values were seen for Tunisia location (*Figure*). Satellite data for the Tunisia location was infrequent compared to other locations. WaPOR performed well for the Egypt location followed by SEBAL and METRIC. nRMSE was quite small for RS-ET estimated by all models. WaPOR model performed poorly for all other locations as both RPD and d were quite low and nRMSE was high (Table). For Lebanon and Jordan, this poor performance can be attributed to the coarse spatial resolution of the WaPOR based RS-ET. METRIC worked comparatively well for Jordan and Egypt locations with some underprediction of RS-ET values. The poor correlation was observed for Lebanon by METRIC as all the points were underpredicted and were observed far from the identity line. The SEBAL based RS-ET was comparatively better. High underprediction of RS-ET values was observed for Lebanon location whereas some

overprediction of RS-ET values for Egypt and Jordan was observed. For Tunisia the performance of SEBAL was good and most of the points were observed near identity line and this is corroborated by a higher value of d (0.87) throughout this season.

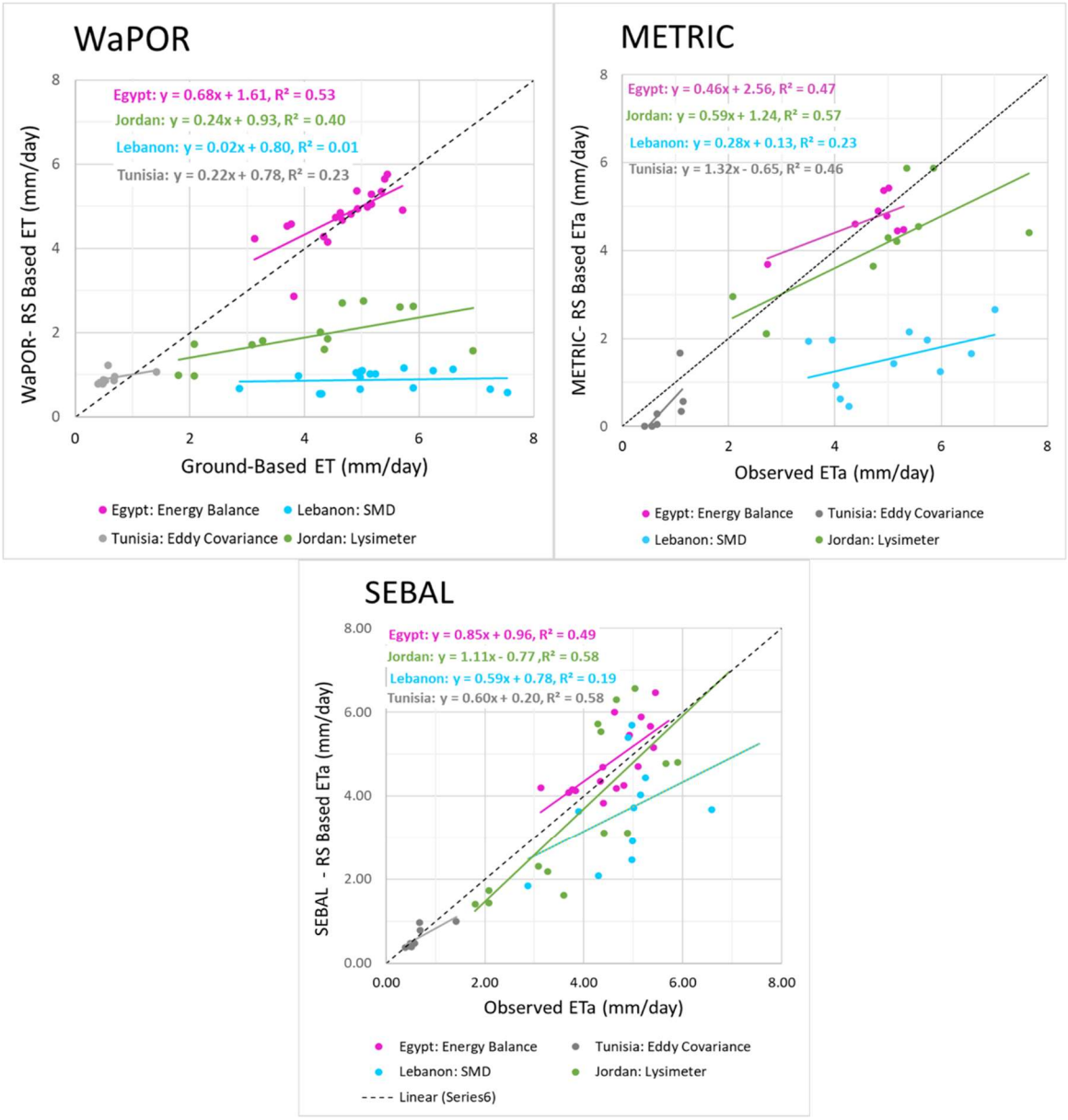

Figure 53: Model-wise intercomparison of RS-ET with observed ET for study locations for season 4. The dotted line represents the identity/reference line

Table 51: Models' Performance metrics for Remote Sensing based ET Model's intercomparison analysis for season 4. Cells colored in green depicts the best model for the season based on nRMSE, d and RPD

Season-4

Location	nRMSE (%)	Uncertainty%	RPD	Index of Agreement
		WaPOR		
EGYPT	11	2.58	1.30	0.73
Tunisia	60	4.40	0.40	0.36
Lebanon	86	4.79	0.05	0.00
Jordan	61	6.09	0.24	0.26
Overall	54	4.14	0.90	0.31
		METRIC		
EGYPT	12	7.78	0.98	0.78
Tunisia	70	9.45	1.04	0.56
Lebanon	72	7.55	0.19	0.10
Jordan	27	7.17	1.36	0.80
Overall	45	5.36	1.25	0.66
		SEBAL		
EGYPT	16	3.20	1.14	0.78
Tunisia	20	8.43	2.02	0.87
Lebanon	30	6.63	0.52	0.41
Jordan	28	7.83	1.13	0.82
Overall	23	4.12	1.53	0.91

9.5 Overall Observations

Based on all observations from scatterplots and models' performance metrics, SEBAL based RS-ET estimation was found to be the best method for this study. SEBAL based RS-ET values were more accurate compared to the other two models. This fact can also be statistically proved as lower nRMSE and higher d values were observed for SEBAL based RS-ET. SEBAL failed to predict accurately for Tunisia during season 3. The SMD method-based GB-ET was found to be least correlated with RS-ET during all seasons. For all seasons, SEBAL followed METRIC and WaPOR was the trend of performance of RS-based ET models. WaPOR based RS-ET accuracy was higher for Egypt location except for season 2. METRIC worked well for all seasons except for seasons 2 and 3 for Morocco. METRIC-based RS-ET was underpredicted for Jordan and Lebanon. The poor correlation reported in Lebanon for all seasons is related to the overprediction of smaller ET values and the underprediction of larger ET values. This can also be attributed to the 30 m resolution of METRIC ET, which might have contributed to the underprediction of ETa values for Lebanon and Jordan, where non-agricultural land-uses are located near the agricultural land of the ground-based ET estimation locations.

Most aligned regression lines to the identity line, low RMSE & uncertainty and comparatively higher RPD values indicate that SEBAL can be considered the best prediction model for RS-based ETa estimation followed by METRIC and WaPOR. Here, this is worth mentioning that SEBEL has produced ETa at fine (10 m) spatial resolution compared to METRIC (30 m) and WaPOR (100m). This finer resolution ETa could be beneficial for smallholder farming to pave the way for clever water use. This study also reflects that fine resolution ETa can be considerably useful in areas where homogeneity is absent, or non-agriculture

features are present. Fine resolution RS-based ET could solve the problem of mixed pixel, hence could provide more accurate RS-ET values for small farms.

9.6 Limitations of the remote sensing analyses

The ground-based ET observations were determined using different methods (i.e., EB, EC, SMD, and Lysi) for diverse locations (one method for each location). Therefore, there are likely underlying variations in the values of the ET obtained. Contrary to this, each RS-based ET model has a universally applicable method for all locations. Therefore, some errors may creep in after comparing ground-based ET (obtained from different methods) for the different areas with RS-based ET data.

METRIC model is based on Landsat series data and has 8 days frequency whereas the SEBAL model is based on Sentinel-2 data with the 5-day frequency. During comparative analysis, there might be some difference due to different input satellite imagery. This is one of the limitations. We have scaled WaPOR based monthly ET values to daily ET values based on daily reference ET. This could introduce some error.

9.7 Data analysis and lesson learnt

This research work investigated the use of remote sensing-based evapotranspiration modelling at a broader scale for assessing ET in smallholder farming. Smallholder farming-based RS-ET estimation would be more feasible and accurate after its robust optimization and time-to-time validation in different geographies. The results reflect that the most reliable remote sensing-based method for ET modelling in this study was SEBAL (smallest RMSE and uncertainty values and larger RPD values), followed by METRIC and WaPOR. Most of the ETa predictions by SEBAL, moderately underpredicted ground ET measurements. On the contrary, METRIC had moderate over predictions of measured ET. Probably due to coarse spatial resolution, the WaPOR model exhibited the largest RMSE, higher uncertainty and smallest RPD values.

There is a need to establish at least one common ground-based ET estimation technique across the locations for better comparison with RS model output. Another aspect can be the use of the same RS data for each remote sensing-based model. Inverse calibrated ET methods have great strength, especially for reasons where less data is available, like in the NENA region for site-specific advisories. The SEBAL model presented here could be upgraded by developing five-day interval land surface temperature data using interpolation of 8-16 days interval Landsat LST. This may bring improvements in the model. Besides this, to interpolate monthly or weekly RS based ET values to daily ET values, a separate analysis could be conducted by utilizing a suitable Mateo input. More modelling techniques like Operational Simplified Surface Energy Balance (SSEBop) could also be included for comparison with ground-based estimates.

10. Challenges faced

- Unexpected COVID19 related lockdown in several countries disrupted data collection and equipment maintenance
- Some CORDOVA ET Station spare parts could not be ordered or delivered to do supply chain disruptions

- The reliability of functioning of CORDOVA ET Stations was not very good – need to improve robustness and make it a standalone station not dependent on other instruments for gap filling
- In Lebanon, there were frequent power cut and also telecom network did not support the data loggers
- Such data collection should continue and should be sustained at institutional level
- Rodents often chewed on the cables, need conduits to prevent this
- There's no one common baseline field data for comparison with RS

11. Lessons learnt

- COVID19 taught us that to a large extent face-to-face interaction can be replaced with virtual and the two webinar series - field measurement methods for evapotranspiration, and the remote sensing methods for evapotranspiration complimented each other and helped share knowledge and build capacity under virtual mode of operation
- SMD method is tedious and erroneous, and does not give good field ET measurement results in places we tried
- Performance and completeness of data kept improving from season 1 to season 4. Implementing partners are now better equipped to troubleshoot, resolve issues and operate with limited backstopping. Further support is needed to enable this process.
- CORDOVA ET Station has a new version that has resolved problems identified in the project. This version maybe provided to partners for further validation of its performance
- Need to simplify data collection and reporting templates

12. Opportunities

- This project fills ET data, information and knowledge gap. There's no other standardized measurement of ET in the region. Long-term field measurement important to FAO to help deliver their regional mandate
- Crop Kc values can be revisited using the generated data
- Special issue of a regional journal can be recommended to report all project results in one place
- Sensors have been repaired or replaced in recent months; this will make performance more reliable. Refurbishment of lysimeter in Lebanon will give an opportunity to bridge major gap
- More involvement of field measurement implementing partners in remote sensing validation
- Training of students
- Consider conducting ET measurement method footprint analysis
- In-depth analysis of good quality portion of measured ET data
- Comparison between the three agro-ecologies

- Consider using infrared thermometers for canopy temp estimation
- Consider introducing one common ET measurement technique across all sites
- Soil-water balance-based ET estimation for comparison
- When ready, CORDOVA ET Station can be a standard ET measurement equipment for use across the region
- Efforts need to continue to solve remaining issues
- Strengthen training component
- Start thinking of how to sustain beyond project lifecycle
- Parameterization per crop per agroecology
- Compare global (used by RS models) versus field measured weather datasets
- Need to bridge gap between science and policy aspects of information coming out of project results

13. Conclusion and Recommendations

In conclusion, the data set obtained (seasons 1-4) can be considered a success given the unique challenge posed on all the operations directly and indirectly because of the pandemic and the high levels of gap free high-quality data that was accumulated across the 5 sites. We used this opportunity to understand the limitations and strengths in the collected data and the consortia now has a thorough idea on data reporting, analysis and quality standards. Some suggestions include:

[1] It is vital for the UCO to correct the issues in the CORDOVA-ET systems in terms of parts replacements and functioning across the network to make it a successful and cost-effective product so that it can be scaled across the region to understand water scarcity issues. There are signs of its improvement (e.g., Jordan) from season 2, but the overall performance is still far from adequate. ICARDA and the consortia offer full support and cooperation to take this forward.

[2] It may be interesting to study crop phenology at these sites as phenology can help us better understand and simulate evapotranspiration

[3] As we proceed in this mission, more sites across the region can be considered under this network.

[4] It is apt time to make use of this data for RS-based ET retrievals and testing of crop simulation models. Seasons 1, 2, 3, and 4 combined provide 2000+ days (minimum estimate) of ET data. This is when we bin all the high-quality data across the 5 sites, 4 seasons and ~100+ days of gap free data at each site.

[5] Finally, it is recommended that, based on the learnings from this phase of the project, the field measurements be continued for developing additional datasets free of gaps and errors. Comparison with remote sensing products be done with the additional datasets.

[6] Efforts be made for information and knowledge sharing beyond the project implementing partners by making data accessible, by organizing dissemination events such as webinars, conferences or symposiums.

14. References

AgriMetSoft (2019). Online Calculators. Available on: https://agrimetsoft.com/calculators/Index%20of%20Agreement

Aguilos, M., Stahl, C., Burban, B., Hérault, B., Courtois, E., Coste, S., Wagner, F., Ziegler, C., Takagi, K., & Bonal, D. (2018). Interannual and seasonal variations in ecosystem transpiration and water use efficiency in a tropical rainforest. Forests, 10(1), 14. https://doi.org/10.3390/f10010014

Allen R, Kilic A (2021) METRIC -- Mapping EvapoTranspiration at high Resolution with Internalized Calibration in FAO water scarcity initiative Webinar Series 'Remote Sensing Determination of Evapotranspiration, Algorithms, strengths and weaknesses, uncertainty and best fit-for-purpose' Allen R, Morton C, Kamble B, Kilic A, Huntington J, Thau D, et al. (2015) EEFlux: A Landsat-based evapotranspiration mapping tool on the Google Earth Engine. 2015 ASABE / IA Irrigation symposium: emerging technologies for sustainable irrigation—a tribute to the career of terry howell, Sr Conference Proceedings. St. Joseph, MI: ASABE; pp. 1–11.

Allen, R. G., Tasumi, M., & Trezza, R. (2007). Satellite-based energy balance for mapping evapotranspiration with internalized calibration (metric)—model. Journal of Irrigation and Drainage Engineering, 133(4), 380–394. https://doi.org/10.1061/(asce)0733-9437(2007)133:4(380)

Allen, R. G., Pereira, L. S., Raes, D., and Smith, M. (1998). Crop evapotranspiration: guidelines for computing crop water requirements. Roma: Food and Agriculture Organization of the United Nations Available at: https://appgeodb.nancy.inra.fr/biljou/pdf/Allen_FAO1998.pdf.

Angus, D. E., & Watts, P. J. (1984). Evapotranspiration — how good is the Bowen Ratio Method? Agricultural Water Management, 8(1-3), 133–150. https://doi.org/10.1016/0378-3774(84)90050-7

Baldocchi, D., Falge, E., Gu, L., Olson, R., Hollinger, D., Running, S., Anthoni, P., Bernhofer, C., Davis, K., Evans, R., Fuentes, J., Goldstein, A., Katul, G., Law, B., Lee, X., Malhi, Y., Meyers, T., Munger, W., Oechel, W., … Wofsy, S. (2001). FLUXNET: A new tool to study the temporal and spatial variability of ecosystem–scale carbon dioxide, water vapor, and energy flux densities. Bulletin of the American Meteorological Society, 82(11), 2415–2434.

Bastiaanssen, W. G. M., Menenti, M., Feddes, R. A., & Holtslag, A. A. M. (1998). A remote sensing surface energy balance algorithm for land (sebal). 1. formulation. Journal of Hydrology, 212-213, 198–212. https://doi.org/10.1016/s0022-1694(98)00253-4

Bastiaanssen, W. G., Cheema, M. J., Immerzeel, W. W., Miltenburg, I. J., & Pelgrum, H. (2012). Surface Energy Balance and actual evapotranspiration of the transboundary Indus Basin estimated from satellite measurements and the ETLOOK model. Water Resources Research, 48(11). https://doi.org/10.1029/2011wr010482

Berni, J. A. J., Zarco-Tejada, P. J., Sepulcre-Cantó, G., Fereres, E., and Villalobos, F. (2009). Mapping canopy conductance and CWSI in olive orchards using high resolution thermal remote sensing imagery. Remote Sens. Environ. 113, 2380–2388. doi: 10.1016/j.rse.2009.06.018.

Cuenca, R. H., Stangel, D. E., & Kelly, S. F. (1997). Soil Water Balance in a boreal forest. Journal of Geophysical Research: Atmospheres, 102(D24), 29355–29365. https://doi.org/10.1029/97jd02312

Eastham, J., Rose, C. W., Cameron, D. M., Rance, S. J., & Talsma, T. (1988). The effect of tree spacing on evaporation from an agroforestry experiment. Agricultural and Forest Meteorology, 42(4), 355–368. https://doi.org/10.1016/0168-1923(88)90043-3

Edwards, W. R. (1986). Precision weighing lysimetry for trees, using a simplified tared-balance design. Tree Physiology, 1(2), 127–144. https://doi.org/10.1093/treephys/1.2.127

Hemakumara, H. M., Chandrapala, L., & Moene, A. F. (2003). Evapotranspiration fluxes over mixed vegetation areas measured from large aperture scintillometer. Agricultural Water Management, 58(2), 109–122. https://doi.org/10.1016/s0378-3774(02)00131-2

Jensen, M.E.; Burman, R.D.; Allen, R.G. (1990) Evapotranspiration and Irrigation Water Requirements; ASCE Manuals and Reports on Engineering Practice No. 70; ASCE: Reston, VA, USA.

Kyaw Tha Paw U, Qiu, J., Su, H.-B., Watanabe, T., & Brunet, Y. (1995). Surface Renewal Analysis: A new method to obtain scalar fluxes. Agricultural and Forest Meteorology, 74(1-2), 119–137. https://doi.org/10.1016/0168-1923(94)02182-j

Maes, W. H., and Steppe, K. (2012). Estimating evapotranspiration and drought stress with ground-based thermal remote sensing in agriculture: a review. J. Exp. Bot. 63, 4671–4712. doi:10.1093/jxb/ers165.

Montazar, A., Krueger, R., Corwin, D., Pourreza, A., Little, C., Rios, S., & Snyder, R. L. (2020). Determination of actual evapotranspiration and crop coefficients of California date palms using the residual of energy balance approach. Water, 12(8), 2253. https://doi.org/10.3390/w12082253

Pelgrum, H.; Miltenburg, I.J.; Cheema, M.J.M.; Klaasse, A.; Bastiaanssen, W.G.M. (2012) ET Look: A novel continental evapotranspiration algorithm. IAHS-AISH Publ., 352, 120–123.

Sánchez, J. M., Galve, J. M., González-Piqueras, J., López-Urrea, R., Niclòs, R., & Calera, A. (2020). Monitoring 10-m LST from the Combination MODIS/Sentinel-2, Validation in a High Contrast Semi-Arid Agroecosystem. Remote Sensing, 12(9), 1453. doi:10.3390/rs12091453

Senay, G. B., Bohms, S., Singh, R. K., Gowda, P. H., Velpuri, N. M., Alemu, H., & Verdin, J. P. (2013). Operational evapotranspiration mapping using remote sensing and weather datasets: A new parameterization for the SSEB approach. JAWRA Journal of the American Water Resources Association, 49(3), 577–591. https://doi.org/10.1111/jawr.12057

Van Dijk, A., Moene, A.F., and De Bruin, H.A.R., 2004: The principles of surfaceflux physics: theory, practice and description of the ECPACK library, Internal Report2004/1, Meteorology and Air Quality Group, Wageningen University, Wageningen,the Netherlands, 99 pp

Wagle, P., Bhattarai, N., Gowda, P. H., & Kakani, V. G. (2017). Performance of five surface energy balance models for estimating daily evapotranspiration in high biomass sorghum. ISPRS Journal of

Photogrammetry and Remote Sensing, 128, 192–203. https://doi.org/10.1016/j.isprsjprs.2017.03.022

WaPOR, FAO. FAO Water Productivity. (n.d.). Retrieved November 19, 2021, from https://wapor.apps.fao.org/home/WAPOR_2/1.

Wegehenkel, M.; Gerke, H.H. (2015) Water table effects on measured and simulated fluxes in weighing lysimeters for differently- textured soils. J. Hydrol. Hydromech., 63, 82–92, doi:10.1515/johh-2015-0004.

Willmott, C. J. (1981). On the validation of Models. Physical Geography, 2(2), 184–194. https://doi.org/10.1080/02723646.1981.10642213

Yang, Y., Scott, R. L., & Shang, S. (2013). Modeling evapotranspiration and its partitioning over a semiarid shrub ecosystem from satellite imagery: A multiple validation. Journal of Applied Remote Sensing, 7(1), 073495. https://doi.org/10.1117/1.jrs.7.073495

15. Annexure-1

15.1. Meteorological Instruments used in Egypt

Name	Make	Remarks /Condition/action
ET Instrumentation (EB Tower with EC used to measure H)		
Sonic Anemometer	81000 Young USA	- In good physical condition - Working well - Cleaning and height readjustment of sonic anemometer
Net Radiometer	NR01	In good physical condition - Working well - Out of calibration - Cleaning and height readjustment of Net Radiometer - Inversion test has been conducted to check instrument operation and results matched the expected output
Soil Temperature Sensors	HFP01 Soil Heat Flux Plates and TCAV	-The cables of the two sets connected to the weather station were cut - The sensors were tested and found to be in a good condition - The excess and broken cable parts were cut, and the sensors were reconnected directly to the datalogger instead of replacing them - The cables were routed in a new solid plastic cable conduit for better protection -The sensors were reinstalled and tested.
Temperature & RH sensor	HMP45C	-Not working -In a very bad physical condition -Traces of water has been found on the sensor's main board which caused rusting of some components - The sensor reached its end of life and has been damaged beyond repair and should be replaced

Soil Volumetric Water Content Sensor	CS650	-Malfunction -Wrong measurements -The sensor output bad measurements that doesn't match the range of measurement, replacing the sensors with another model with shorter rods is recommended
Datalogger	CR3000	- In good physical condition - Working well - OS out of date -The operating system of the datalogger has been updated to the latest version Std 32.05
3G Modem	M100	In good physical condition - Working well
Solar Panel	------	- in good physical condition - Working well - Needs repositioning -repositioned to south direction and cleaned
Solar Charger and Battery	------	-The cables connecting the battery and solar charger was found to be cut in several points by mice, the mice chewed through the cable and caused damage to several spots. -The cables were repaired and routed in a new solid plastic cable conduit to avoid further damage by mice, however, it is highly recommended to use mice repellents and make sure that the cable is properly buried in the soil after planting and harvesting
CORDOVA-ET Station		
Main station and nodes	------	-Stopped working and Egyptian team waiting spare parts coming from CORDOBA University.

15.2. Meteorological Instruments used in Jordan

Name	Make	Remarks /Condition
Weather station		
data logger	Campbell CR10x data logger	Working well
Wind Monitor	Series 05103	Working well
Precipitation mm	TE525WS Precipitation mm Tipping-bucket rain gauge with 0.254 mm per tip (TE525MM-L, 24.5 cm	Working well
Pyranometer	LI200R Pyranometer	Working well
Digital Air Temperature and Relative Humidity Sensor	CS215-L Digital Air Temperature and Relative Humidity Sensor	Working well
ET Instrumentation (Method-1)) – Lysimeter		
data logger	Campbell data logger CR6	Working well
-Wind speed m s^{-1}	- Sonic anemometer (Wind Sonic-L)	Working well
Solar radiation W m-2	Solar radiation W m-2	Working well
Silicon pyranometer	Silicon pyranometer (LI200X-L Li-Cor)	Working well
Air temperature and relative humidity °C and % Temperature and RH probe	(HMP45C-L-GM) with gill radiation shield (41003-5)	Working well
Barometric pressure Pa	(CS100 Setra 278)	Working well
Net radiation W m-2	Net radiometer (NR-Lite-L, Kipp and Zonen)	Working well
Precipitation mm	Tipping-bucket rain gauge with 0.1 mm per tip (TE525MM-L, 24.5 cm	Working well
CORDOVA-ET Station		
Weather station and 4 Nodes	Working well except node 3 that need reprogramming, air and humidity sensors of node 1,2 and 3 that need update, soil sensor of node 1. Working well	

15.3. Meteorological Instruments used in Lebanon

Name	Make	Remarks /Condition
Automated Weather station		
Pyranometer	173388/Pessl Inst.	Functions well, needs calibration every two years
Air Temperature	A660611/Pessl Inst. (PT1000 1/3 Class B)	Function well; cleaning monthly in summer, twice in winter
Relative Humidity	A660611/Pessl Inst. (ROTRONIC Hygromer®)	Functions well
Barometer	Pessl Inst.	
Rain Gauge/ Double tipping bucket rain gauge	IM523/Pessl Inst.	Functions well, Cleaning is necessary monthly
Wind Direction	IM511CDI/ Pessl Inst.	Functions well
Wind Speed	IM512CD/ Pessl Inst.	Functions well
CORDOVA-ET Station		
Froggit Cordoba-ET Weather Station	Forggit German made	The base Cordoba weather station is well.
Four nodes of Cordoba weather station	Cordoba setup of Pycom technologies	LoRa communication is used to communicate between nodes and data logger; the datalogger is connected to modem that sends data through GPRS format.

15.4. Meteorological Instruments used in Tunisia

Name	Make	Remarks /Condition
Weather station		
Air Temperature	PESSL INSTRUMENTS HYGROCLIP; PT1000 1/3 Class B	Well-functioning
Relative Humidity	PESSL INSTRUMENTS HYGROCLIP; ROTRONIC Hygromer® IN-1	Well-functioning
Rain	PESSL INSTRUMENTS RAIN GAUGE; Double tipping bucket rain gauge collector Surface=200 cm2	Not functioning
Solar radiation	PESSL INSTRUMENTS PYRANOMETER; LI-200SZ	Well-functioning
Wind speed	PESSL INSTRUMENTS WIND SPEED; 12 cm diameter cup wheel assembly, 40 mm diameter hemispherical cups	Well-functioning
Leaf wetness	PESSL INSTRUMENTS LEAF WETNESS	
ET Instrumentation (EDDY COVARIANCE		
Data logger	CR3000 (Campbell Sc)	Working well
Sonic anemometer	CSAT3 (Campbell Sc)	Working well
Krypton Hygrometer	KH20 (Campbell Sc)	Working well
Soil heat flux	HFP01 (Hukseflux)	Working well
Thermo-hygrometer	HMP45 (Vaisala)	Working well
Net radiometer	NR01 (Hukseflux)	Working well
Leaf wetness	237 (Campbell Sc.)	Working well
CORDOVA-ET Station -if applicable		
		General status summarizing Table 13

15.5. Meteorological Instruments used in Morocco

Sensor Type	Model/Brand
Solar Radiation	**CS300-L** Pyranometer
Air Temperature	**CS215-L** Digital Air Temperature and Relative Humidity Sensor
Relative Humidity	
Barometer	**CS100** Barometric Pressure Sensor
Rain Gauge	Double tipping bucket rain gauge IM523/Pessl Inst.
Wind Direction	**03002-L** Wind Sentry Set
Wind Speed	

16. Annexure-2

Based on consultation meetings with FAO team and focal points in each participating country, Cordoba method was adopted to be the standardized measurement protocol. This is based on the sound theoretical basis. The attractiveness here is the development and use of cost-effective instrumentation that can measure various components of the energy balance equation. The cost-effective sensors were developed subjected to extensive research, testing and calibration. In this project, it is planned that we install 5 stations in each of the participating country and connect them in a local and regional network. The CORDOVA-ET station yields ET_a measurements based on the surface energy balance principles. Its complete functionality, along with hardware specifications, is well described in the UCO CORDOVA-ET report (Berni et al., 2018). This station consists of multiple sensors which communicate via wireless connections. There are multiple micro-meteorological stations which are called 'nodes' that integrate the sensors required for measuring the components of the energy balance. These nodes are powered with solar photovoltaic cells and related batteries. Along with nodes, there is a base station which receives the data from the nodes and forwards them to a main server through Internet. A server-based software stores and manages the data from the nodes and helps their visualization to the users. The CORDOVA-ET station (makes use of the surface energy balance approach to derive ET_a, through the Energy Balance method, where *Rn* and *G* are measured, and *H* is calculated as

$$H = \rho Cp \frac{(Tc - T\ )}{ra}$$

where: ρ is the air density

C_p is the air specific heat capacity

Tc and Ta are the canopy and air temperature, respectively

r_a is the aerodynamic resistance.

The main issue is that net radiometers are expensive and not commonly available in most weather stations. Following what proposed in the FAO-56 publication, approaches for estimating *Rn* from measurements of solar radiation (*Rs*) can be adopted, as *Rs* is most commonly measured in agrometeorological weather stations. The other critical parameter is r_a which depends mainly on the wind speed and on canopy attributes (height and roughness). There are multiple formulations for estimating r_a. However, being a critical variable in the calculation of *H*, and therefore for estimating *LE*, the assumptions behind its calculation can have very important impacts on the results of the surface energy balance. For a detailed sensitivity analysis of the estimation of *LE* from canopy temperature measurements, see (Leinonen et al., 2006; and Maes and Steppe, 2012). The methodology used to calculate r_a in the CORDOVA-ET station is based Berni et al. (2009) the model of Viney (1991) has been used given the simplicity of that parameterization and good results.

Figure 54. Illustration of a typical CORDOVA-ET station

Description of the Cordoba System

N.B. The information in this Section is provided by Dr. Jose Antonio Jiménez-Berni, Instituto de Agricultura Sostenible (IAS), Consejo Superior de Investigaciones Científicas (CSIC), Córdoba, Spain.

The CORDOVA-ET system consists of different components that are interconnected using wireless technologies, which allows real-time data recording and monitoring of the field observations (Figure A1). The components of the system are:

- Multiple micro-meteorological stations or nodes that integrate the sensors required for measuring the components of the energy balance. It resembles a weather station because of the appearance of the radiation shield used to avoid the heating of the air temperature and humidity sensors (Figure 55). The nodes are powered with solar photovoltaic cells and operate with batteries.
- A base station or gateway that receives the measurements from the nodes and forwards the data to the Internet. This gateway can be installed indoors and connected to the internet using WiFi or Ethernet or it can be integrated into a weatherproof enclosure with solar power. One base station can receive data from the nodes in a theoretical range of about 10km, depending on the topography, location of the antenna, etc.
- Server-based software for managing and storing the data from the nodes and providing visualization to users. This normally runs on cloud services, but it could be deployed on embedded computers (e.g., Raspberry Pi) or local servers.

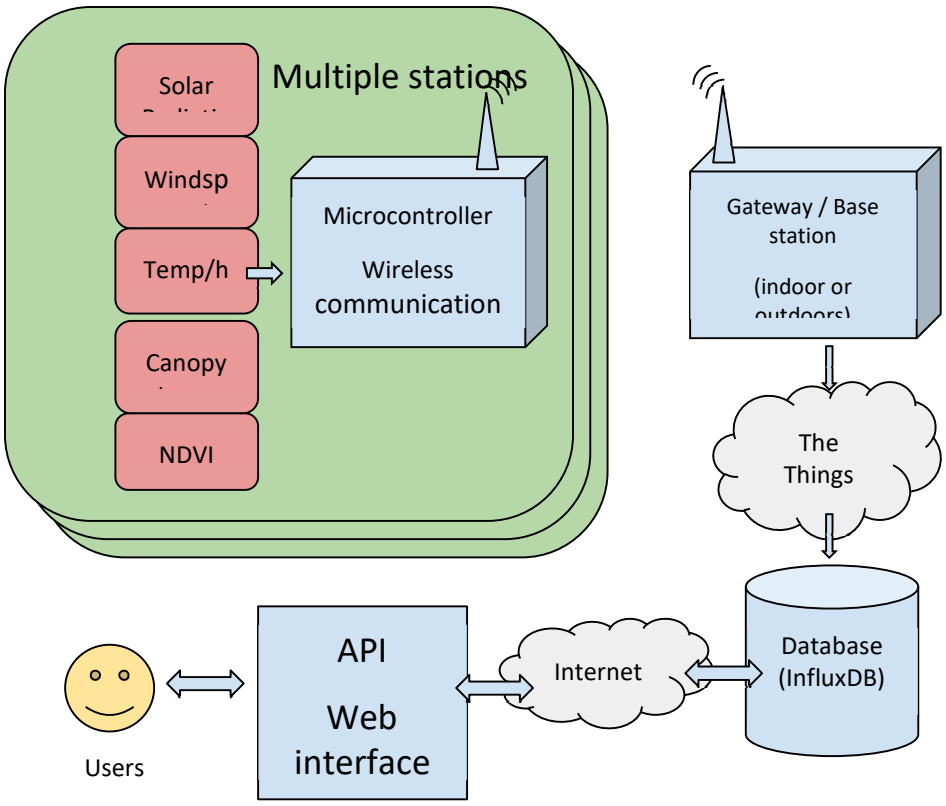

Figure 55. Overview of the CORDOVA-ET system. Multiple stations with the sensors and wireless communication (LoRaWAN) are deployed in the field. A gateway/base station receives the information from the stations and forwards the information to the Internet. The data is stored in a database and it is exposed to the users through a web interface and a programming API accessible with R and Python.

***Figure 56.** 3D printed radiation shields and sensor boxes containing the air temperature, humidity and barometer, hot wire anemometer and solar radiation sensor (on the right).*

Validation of Cost-Effective Sensors

Air temperature, humidity and atmospheric pressure

The sensor used for measuring simultaneously air temperature, humidity and barometric pressure provides a digital output (protocol I2C) of factory-calibrated air temperature, humidity and pressure. According to the specifications from the manufacturer, it is capable of measuring humidity with ±3% accuracy, barometric pressure with ±1 hPa absolute accuracy, and temperature with ±1.0°C accuracy.

The comparison with the air temperature (Figure 57) and humidity (Figure 58) measured with the weather station shows a r^2=0.987, RMSE=1.0ºC, MAE=-0.75ºC and a slope 1.0 for air temperature, and r^2=0.989, RMSE=2.1% RH, MAE=-0.32 % RH and a slope of 0.985 for relative humidity. Atmospheric pressure has not been validated as the barometer is not part of the standard payload of agrometeorological weather stations.

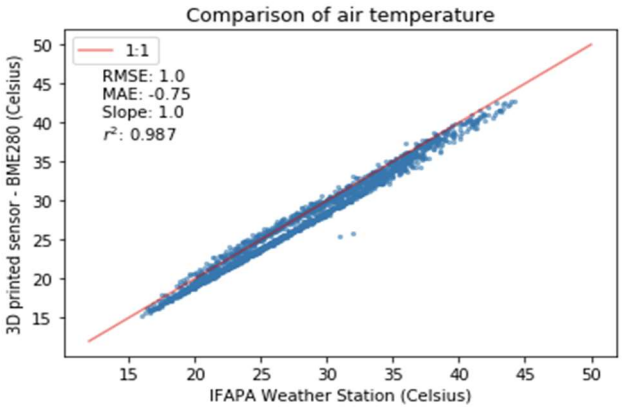

Figure 57: *Validation of air temperature sensor, comparing the CORDOVA sensor in the 3D printed radiation shield and the standard sensor in the IFAPA weather station.*

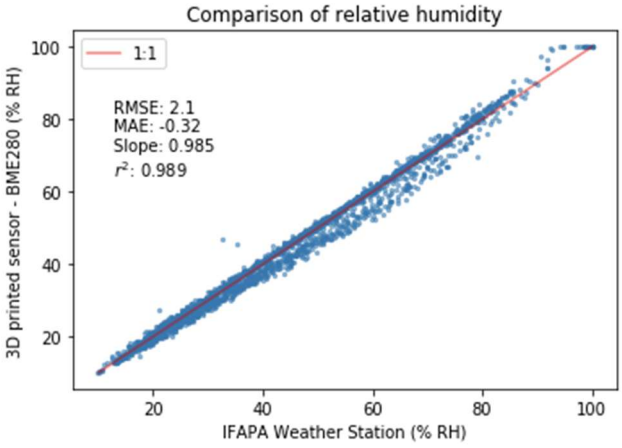

Figure 58. *Validation of air humidity sensor, comparing the CORDOVA sensor in the 3D printed radiation shield and the standard sensor in the IFAPA weather station.*

The results are very satisfactory and within the specifications of the sensors. It is important to highlight that shielding the sensor from solar radiation is critical to achieve these accuracies. Incorrect shielding of the sensor would result in the heating of the sensor and therefore an overestimation of air temperature. The 3D printed radiation shield proved to be very effective, and no positive bias has been observed. On the contrary, there is a negative bias of -0.75ºC in the observations of air temperature.

Solar Radiation

Incoming solar radiation is measured with pyranometers that measured the total solar radiation on the shortwave range of the spectrum (350-2500 nm). Even though pyranometers are critical in agrometeorological observations, they are not usually included in standard low to medium cost weather stations, becoming an option with a high cost which ranges from a few hundred to thousands of euros depending on their capabilities. There are two types of pyranometers: thermopile (expensive) and silicon-based (cheaper). Thermopile pyranometers measure the solar radiation for the full solar spectrum, while the silico-based are only sensitive to a spectral range of 400-1.000 nm.

In the CORDOVA system case, a multispectral light sensor has been used to implement a low-cost pyranometer. An initial prototype was built (Jimenez-Berni & Estevez-Gualda, in preparation) and demonstrated to provide results comparable to standard pyranometers. The advantage of a multispectral sensor compared with a broad, single band silicon pyranometer is that the band combination in a multivariate analysis can provide more accurate results and enable better estimations of PAR vs. total solar radiation or even improved results in the estimation of longwave radiation (as discussed below).

The spectral sensor is integrated in a 3D-printed enclosure that provides the housing for the detector (Figure 59) as well as for the optic broadband diffuser that acts as cosine corrector to integrate the total light from the sky. The detector provides a digital signal (I2C) with the intensity of the six spectral bands as well as the internal temperature that is used for the calibration. The calibration of the CORDOVA sensor was performed against a four-component net radiometer (model NR-01, Hukseflux, The Netherlands) installed on the same mast (Figure 59). Data was recorded at 10 min intervals for the net radiometer and at 1 min interval in the multispectral sensor, so data was resampled to 10 min using the average value for the 10 minutes to match the data from the net radiometer.

A multivariate model, using ordinary least squares, was built to predict solar radiation from the net radiometer using the six spectral channels and the sensor temperature. The model showed very strong significance for all the bands except for band 6 (650 nm) that shower a weaker significance (p=0.029).

Figure 59: *(a) Top view of the spectral sensor in the enclosure with the optic diffuser. In this test model, two sensors can be installed for simultaneous observation or for including visible and near infrared versions of the spectral sensor. (b) pyranometer and net radiometer (NR-01, Hukseflux, The Netherlands) used for the calibration.*

The predicted values for the model were plotted against the solar radiation measured by the net radiometer for 4 days with variable cloud conditions (figure 60), showing that the spectral sensor followed perfectly the pattern of clouds. When plotting the predicted values against the net radiometer (figure 61), there is very strong agreement between them (r2=0.997) with a slope of 1, RMSE=16.35 W/m2 and MAE=-0.05.

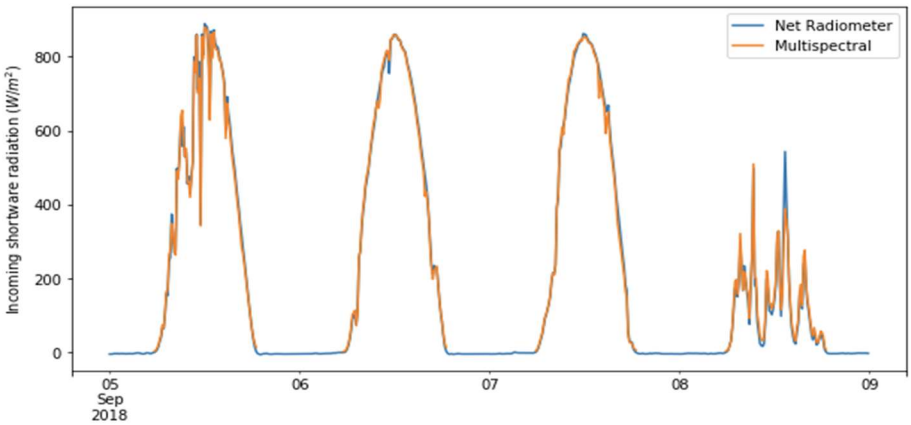

Figure 60: *Evolution of solar radiation measured with the net radiometer and modelled from the multispectral sensor.*

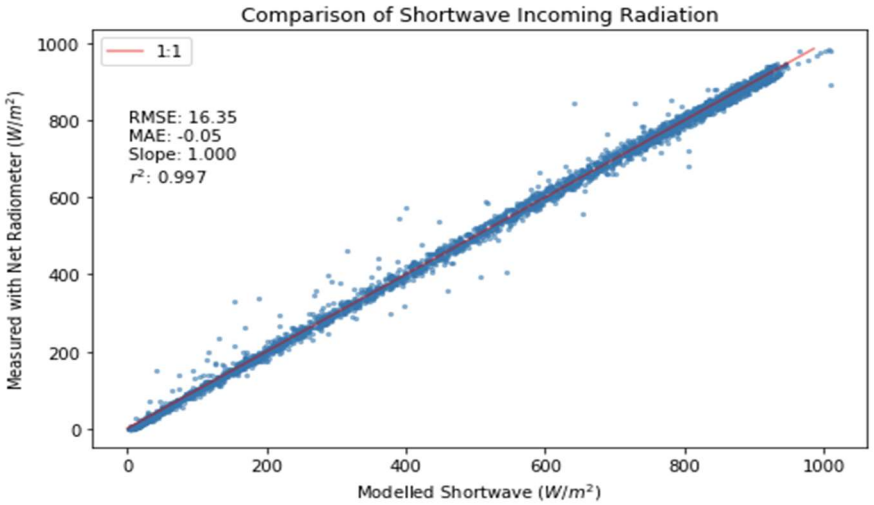

Figure 61: *Comparison of solar radiation for the multispectral sensor and the pyranometer from the net radiometer. The calibrated values from the multispectral sensor are obtained using multivariate regression that combines all the spectral bands and sensor temperature.*

Wind Speed

Wind speed can be measured in weather stations using different instrumentation such as cup anemometers, propellers, sonic, and hot-wire anemometers. While cup and propeller anemometers are the most common, they have moving parts which makes them prone to maintenance and if the quality of the bearing is not very good, low wind speeds can be underestimated. Sonic anemometers provide the best accuracy and do not have any moving parts, but their cost is also much higher. Hotwire anemometers do not have any moving parts and they use a heating and a temperature sensing element so that wind cools down the heater. This temperature difference can be measured and converted into wind speed.

Hotwire anemometers have traditionally been expensive because of the cost of heater and sensing technologies and the accuracy required for processing the analog signal provided by them. However, recent developments in low-cost instrumentation have made some affordable solutions. The CORDOVA Wind-Sensor integrates an ambient temperature sensor and a voltage output that is proportional to the wind speed (non-linearly though). Previous studies with this same sensor (Prohasky and Watkins, 2014) suggest that it can measure average wind speed with an accuracy of ±0.5m/s.

For the evaluation of the sensor, a 3D-printed case with a ring element for protecting the sensor was built. The sensor required an input voltage of >9V. Since the system is powered with Li-Po batteries with a nominal voltage of 3.7V, a DC-DC converter was required to step-up the voltage from 3.7V to 9-12V.

Figure 62: *Test prototype for the CORDOVA wind speed sensor. A ring protective ring was added to protect the sensor from birds and any accidental damage. The box contains the electronics for powering and sensing.*

The following equation was used to relate the wind speed and the output voltage:

$$V_{out} = a + bT + cv^d$$

Where a, b, c and d are the calibration coefficients, T is the ambient temperature and $v$is the wind speed.

The comparison with the wind speed measured at the weather station showed a large scatter (figure 63) that was attributed to the influence of the wind direction, probably caused by the large protective ring. The newer prototype avoids this by creating a design that mimics the 3D anemometers and provides protection but without big obstructions that could cause issues with the wind direction. The issue of direction dependency was also reported in (Prohasky and Watkins, 2014), so further analysis is required to investigate how the new design will behave under different conditions and characterize the dependency of wind direction for the new design.

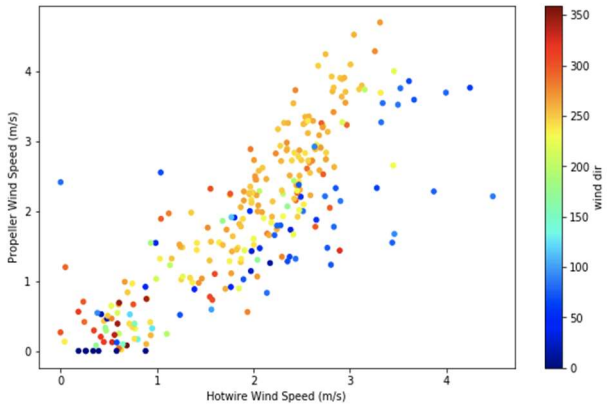

Figure 63: *Validation of the wind speed comparing the hot wire with the wind speed measured at the weather station. The colors represent the wind direction. Note how the estimates of the wind speed decline with wind directions are in the range 0-100 degrees.*

Another issue that was encountered with this sensor is its power requirements. The current prototype keeps the hotwire powered constantly, rather than powering it intermittently for doing the measurements. Measurements are done every minute and transmitted wirelessly. Because the supply power has to be >9V this requires an additional DC-DC converter which decreases the power efficiency of the system. The result is that the 3.5W solar power is not enough for maintaining the battery voltage which resulted in a limited dataset. We are currently investigating this and developing alternative power management strategies (power only to do the wind speed measurements), larger solar panels or alternative wind speed sensors. We are currently testing alternative solutions to obtain reliable wind speed measurements

Canopy Temperature

Measuring surface temperature in the critical step in this approach for calculating sensible heat and hence estimating ET. Infrared thermometry (IRT) has been used for decades as a common way to estimate crop water status and ET both with point and imaging sensors (Berni et al., 2009; Brenner et al., 2018; Hargreaves and Samani, 1985; Maes and Steppe, 2012; Smith et al., 1988). In essence, land surface temperature is also used in satellite-based methods for estimating crop ET (Allen et al., 2011; Bastiaanssen et al., 1998). Infrared thermometers measure the radiation emitted by the surface of vegetation in the long wave infrared part of the spectrum, normally in the spectral window of 8-14µm. Apogee IRT sensors (Apogee, Logan, UT, USA) have been commonly used successfully in previous research studies (Berni et al., 2009; Sepulcre-Cantó et al., 2006) but its high price and technical requirements (need for a datalogger to acquire the analog signal) makes its practical application quite limited. New infrared sensing technologies have enabled the development of commercial IRT sensors with accuracy well below 1K which have broader applications and much lower cost. There are sensors in different versions depending on the field of view (5, 10, 12, 35, 70 and 90 degrees). The CORDOVA IRT sensor has a 35º option and has been used in this development. The sensor provides a digital output of the object temperature as well as the sensor temperature. The temperature is already calibrated and compensated for changes in the sensor temperature as well as emissivity (default set to 1.0 and corrected afterwards). The sensor is factory

calibrated to the specifications in figure A10, which is ±0.5ºC for the normal range of operation in field conditions.

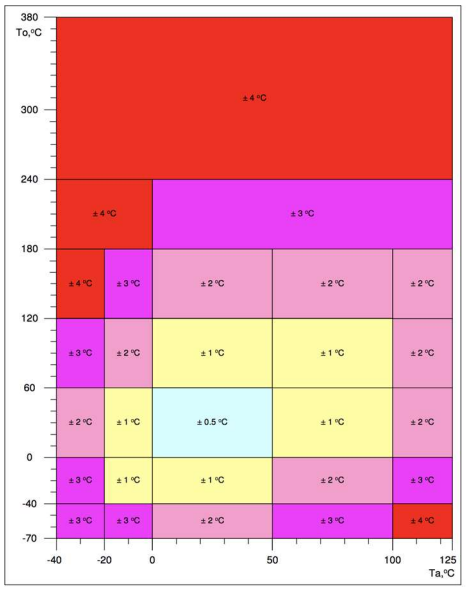

Figure 64: *Accuracy of the CORDOVA IRT sensor depending on the object and ambient temperature. For the normal range of operation in agricultural applications the accuracy is 0.5ºC.*

For the validation tests, the sensor was placed next to an Apogee model IRTS-P and looking to approximately the same patch of grass (Figure 65).

Figure 65: *Infrared thermometer (Melexis MLX90614) in an orange 3D printed housing installed next to an IRTS-P Apogee sensor.*

The validation results (Figure 66) show that the CORDOVA IRT sensor behaved almost exactly as the standard Apogee sensor with a r2=0.996, RMSE=0.61ºC and a Slope of 1.01.

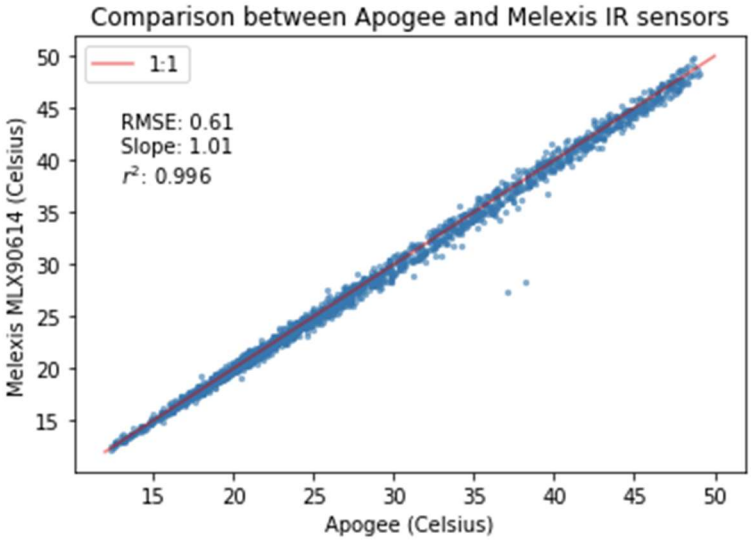

Figure 66: *Validation of the infrared temperature of the MLX90614 sensor compared with the Apogee IRTS-P sensor.*

Environmental protection and enclosures

It is critical to maintain the ingress protection and environmental protection of the sensors for different reasons.

1. Water, dust and insects can damage the sensors and electronics resulting in system failures and error in the measurements
2. Solar radiation can affect the temperature readings on the air temperature and canopy temperature sensors
3. Exposure to weather and in particular to UV light can damage plastic parts resulting in breakages and eventually loss of waterproof attributes

For this reason, they have been evaluating different alternatives for boxes and ingress protection mechanisms. In trying to keep the budget low, we have used standard gland nuts for passing through cables instead of using waterproof connectors. This has resulted in a total design failure (figure 67) as water can get into the enclosure as a result of changes in internal pressure. New prototypes are fitted with vent valves that thanks to a membrane allow air to get in and out but prevent water movement. Also, they are using IP67 (ingress protection against water) connectors instead of gland nuts. The system is powered with solar panels and backup batteries, which doesn't require replacing batteries and opening/closing the boxes. This will also result in increased reliability. Regarding the materials used for 3D printing protective elements for the sensors, we have tested different materials (PLA, ABS, HIPS, PETG) and found that PETG was the best material for outdoor deployment. After a deployment of +3 months in

the harsh summer of Cordoba, Spain, no apparent UV or weather damage was apparent on the PETG, while other materials showed color fade and became brittle.

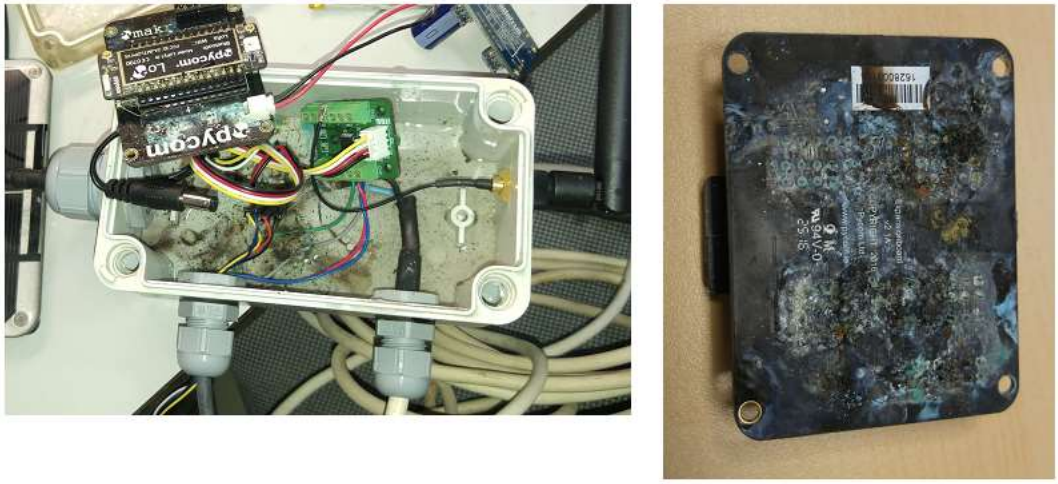

***Figure 67**: Water ingression in a IP67 box resulted in damaged electronics and total failure. Despite the use of outdoor rated gland nuts, this box was not suited with a vent valve that facilitated water sipping through the glen nuts with the changes of pressure.*

Microcontroller and communication protocols

They are using a microcontroller which includes wireless communication over WiFi, Bluetooth, LoRa and Sigfox. This board presents a more powerful alternative to the popular Arduino board but also incorporates all the wireless communications on a single board, which results in lower cost. The programming of the board is made with microPython which makes this board an innovative solution, both simple and powerful. A custom carrier board was designed to avoid any soldering and provide standard connectivity with the sensors and battery. Two options for long range wireless communications are available with this microcontroller: LoRaWAN and Sigfox. Both have similar range (around 10 km in line of sight), however, Sigfox relies on commercial providers to deploy base stations and coverage (similar to mobile phone operators). LoRaWAN, on the other hand, can be deployed by the user with regular routers that, once connected to the Internet can rely on the communications from the nodes to the server storage and visualization services. Each node is identified with a unique name as well as an encryption key that is unique for each device and server application. The encryption makes the communications secure and only the user with these keys can decode the content of the packages and therefore the measurements.

Base station

The base station consists of a LoRaWAN gateway (Laird Sentrius RG186 for Europe (868 MHz) or RG191 (915MHz) for the US and Oceania) that received the data from the nodes within the range of the base and forward the data to the Internet (figure 68). The router can be installed indoor or outdoor with a waterproof case and solar panels. In the indoor case, it just needs a Wifi or Ethernet internet connection and, depending on the location in the building, it may require an external antenna. For outdoor installation a mobile network router is also required. They are currently testing different alternatives for an integrated

solution (including solar power, batteries and 4G modem). Other LoRaWAN alternatives are also emerging very rapidly, including ruggedized units for outdoor deployment. However, their costs are still prohibitive (230€ for the indoor model versus 650€ for the IP67 outdoor unit).

Figure 68: *LoRaWAN gateway (Laird Sentrius RG186) used in the base stations. The long antenna receives the LoRaWAN data while the two smaller antennas are for the WiFi.*

Backend server and data storage

The LoRaWAN device communicates with the Gateway (base station) which relays the data to a server. For the CORDOVA system, we have selected The Things Network (TTN) (https://www.thethingsnetwork.org/), which is a collaborative LoRaWAN infrastructure where the users bring their own gateways and provide the services for managing the communications with the Cloud (figure 69). TTN doesn't provide any data storage or visualisation, it is just the messenger and the user needs to build the application. In this case, the messages are decoded and made available for our application to store and visualize them.

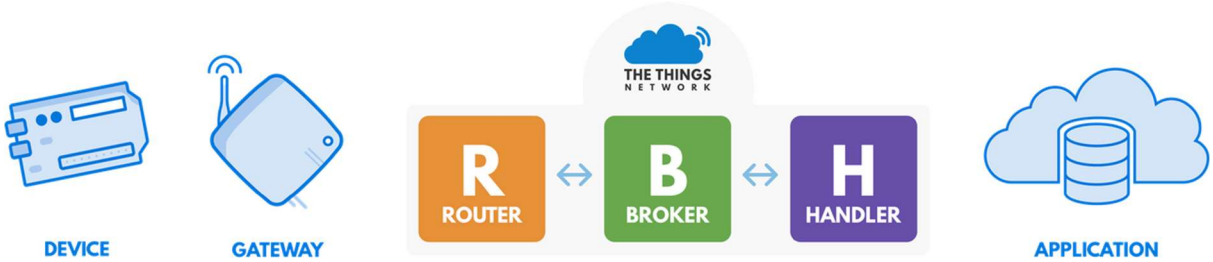

Figure 69: *The Things Network architecture.*